Institut für Erd- und Umweltwissenschaften
Mathematisch-Naturwissenschaftliche Fakultät
Universität Potsdam

Topographic evolution of the East African Plateau

A combined study on lava-flow modeling and paleo-topography

Henry Wichura

Kumulative Dissertation
zur Erlangung der Würde des akademischen Grades
Doktor der Naturwissenschaften (Dr. rer. nat.)

eingereicht an der Mathematisch-Naturwissenschaftlichen Fakultät
der Universität Potsdam

Potsdam, Juni 2010

Published online at the
Institutional Repository of the University of Potsdam:
URL http://opus.kobv.de/ubp/volltexte/2011/5236/
URN urn:nbn:de:kobv:517-opus-52363
http://nbn-resolving.org/urn:nbn:de:kobv:517-opus-52363

This thesis was carried out within the Graduate School GRK1364 *"Shaping Earth's Surface in a Variable Environment"*, a three years lasting series of interdisciplinary projects performed at the University of Potsdam. The Graduate School was initially launched by Prof. Manfred Strecker in 2006 and financed by the German Research Foundation (DFG), the federal state of Brandenburg, and the University of Potsdam.

The principal research theme of the Graduate School GRK1364 is the interaction between tectonics and climate in shaping the surface of Earth at different length and timescales. In addition, studying the impact of these processes on the biosphere is a central part of this effort. The regional basis for incorporated projects involves the India-Asia Collision Zone and the East African Rift System, both characterized by ongoing tectonics and the formation of pronounced relief contrasts in the Cenozoic.

Bring forth what is true,
Write it so it is clear,
And defend it to your last breath.

- Ludwig Boltzmann quoting Goethe's Faust

ABSTRACT

The East African Plateau provides a spectacular example of geodynamic plateau uplift, active continental rifting, and associated climatic forcing. It is an integral part of the East African Rift System and has an average elevation of approximately 1,000 m. Its location coincides with a negative Bouguer gravity anomaly with a semi-circular shape, closely related to a mantle plume, which influences the Cenozoic crustal development since its impingement in Eocene-Oligocene time.

The uplift of the East African Plateau, preceding volcanism, and rifting formed an important orographic barrier and tectonically controlled environment, which is profoundly influenced by climate driven processes. Its location within the equatorial realm supports recently proposed hypotheses, that topographic changes in this region must be considered as the dominant forcing factor influencing atmospheric circulation patterns and rainfall distribution. The uplift of this region has therefore often been associated with fundamental climatic and environmental changes in East Africa and adjacent regions. While the far-reaching influence of the plateau uplift is widely accepted, the timing and the magnitude of the uplift are ambiguous and are still subject to ongoing discussion. This dilemma stems from the lack of datable, geomorphically meaningful reference horizons that could record surface uplift.

In order to quantify the amount of plateau uplift and to find evidence for the existence of significant relief along the East African Plateau prior to rifting, I analyzed and modeled one of the longest terrestrial lava flows; the 300-km-long Yatta phonolite flow in Kenya. This lava flow is 13.5 Ma old and originated in the region that now corresponds to the eastern rift shoulders. The phonolitic flow utilized an old riverbed that once drained the eastern flank of the plateau. Due to differential erosion this lava flow now forms a positive relief above the parallel-flowing Athi River, which is mimicking the course of the paleo-river.

My approach is a lava-flow modeling, based on an improved composition and temperature dependent method to parameterize the flow of an arbitrary lava in a rectangular-shaped channel. The essential growth pattern is described by a one-dimensional model, in which Newtonian rheological flow advance is governed by the development of viscosity and/or velocity in the internal parts of the lava-flow front. Comparing assessments of different magma compositions reveal that length-dominated, channelized lava flows are characterized by high effusion rates, rapid emplacement under approximately isothermal conditions, and laminar flow. By integrating the Yatta lava flow dimensions and the covered paleo-topography (slope angle) into the model, I was able to determine the pre-rift topography of the East African Plateau.

The modeling results yield a pre-rift slope of at least 0.2°, suggesting that the lava flow must have originated at a minimum elevation of 1,400 m. Hence, high topography in the region of the present-day Kenya Rift must have existed by at least 13.5 Ma. This inferred mid-Miocene uplift coincides with the two-step expansion of grasslands, as well as important radiation and speciation events in tropical Africa.

Accordingly, the combination of my results regarding the Yatta lava flow emplacement history, its location, and its morphologic character, validates it as a suitable “paleo-tiltmeter” and has thus to be considered as an important topographic and volcanic feature for the topographic evolution in East Africa.

ZUSAMMENFASSUNG

Das Ostafrikanische Plateau ist ein eindrucksvolles Beispiel für aktive, kontinentale Grabenbildung, aber auch für geodynamische Hochebenenbildung mit weitreichendem klimatischen Einfluss auf die gesamte Region. Als integraler Bestandteil des Ostafrikanischen Grabensystems beläuft sich die mittlere Höhe des Plateaus auf durchschnittlich 1000 m ü.NN. Seine Lage korreliert gut mit der Präsenz einer halbkreisförmigen negativen Bouguer-Schwereanomalie, die an den Aufstieg eines Manteldiapirs im Untergrund gekoppelt ist. Dieser prägte die känozoische Krustenentwicklung seit seinem Aufstieg im Eozän-Oligozän.

Die Hebungsgeschichte und topographische Entwicklung des Hochlandes steht seither in enger Beziehung zum einsetzenden Vulkanismus, der Bildung erster Abschiebungssysteme und führte schließlich zur Entwicklung des heutigen Vollgrabensystems. Neueste Hypothesen lassen den Schluss zu, dass topographische Veränderungen als dominierende Einflussgrößen atmosphärischer Zirkulationsmuster sowie der regionalen Niederschlagsverbreitung anzusehen sind. Zusätzlich werden diese Prozesse durch die äquatoriale Lage des Ostafrikanischen Plateaus verstärkt und die Hebung dieser Region oft mit wichtigen Klima- und Umweltveränderungen in Ostafrika und angrenzende Gebiete in Verbindung gebracht. Während der weitreichende klimatische Einfluss des Hochlandes größtenteils akzeptiert ist, sind Zeitpunkt und Ausmaß seiner Heraushebung nicht eindeutig bestimmt und daher noch immer Grundlage bestehender Diskussionen. Diese Zwangslage hat ihre Ursache im Fehlen aussagekräftiger und datierbarer Referenzhorizonte.

Um den Hebungsbetrag zu quantifizieren und Beweise signifikanten Reliefs vor der Entwicklung des Grabensystems entlang des Ostafrikanischen Hochlandes zu erbringen, analysierte und modellierte ich einen der längsten terrestrischen Lavaströme. Dieser vor 13,5 Ma abgelagerte Yatta-Lavastrom hat mit 300 km Länge seinen Ursprung in der Region der heutigen östlichen Grabenschulter des zentralen Kenia-Rifts. Die phonolitische Lava ergoss sich entlang eines Flussbettes, das einst die östliche Flanke des Hochlandes entwässerte. Aufgrund unterschiedlicher Erosionspotentiale bildet der Lavastrom gegenwärtig ein positives Relief und befindet sich oberhalb des Athi Flusses, der parallel zum Paläofluß, und somit versetzt zu seinen früheren Verlauf, strömt.

Mein Ansatz der Lavastrom-Modellierung basiert auf einer Methode, die das Fließverhalten einer beliebigen Lava in Abhängigkeit von Temperatur und Magmenzusammensetzung in einem rechtwinkligen Kanal berechnet. Die wesentlichen Wachstumsmuster des Lavastroms sind durch ein eindimensionales Modell beschrieben, wobei Newtonsches Fließverhalten im Innern hinter der Lavastromfront von der zeitlichen Entwicklung der Viskosität und/oder der Fließgeschwindigkeit bestimmt wird. Vergleiche meiner Resultate mit verschiedenen Magmenzusammensetzungen zeigen, dass sich lange, kanalisierte Lavaströme mit hohen Ergussraten und schneller Platznahme bilden können. Dies geschieht unter annähernd isothermalen Bedingungen und erfordert laminares Fließen. Die Integration der Yatta-Lavastrom-Dimensionen und der bedeckten Paläotopographie (Neigungswinkel) in das Modell, erlaubte es mir die Topographie des Ostafrikanischen Hochlandes vor der Grabenbildung zu modellieren.

Das Ergebnis der Modellierung ergibt einen Neigungswinkel von mindestens 0,2° und impliziert, dass der Lavastrom seinen Ursprung in einer Höhe von mindestens 1400 m ü.NN gehabt haben muss. Somit existierte bereits vor 13,5 Ma hohe Topographie in der heutigen Region des zentralen Kenia-Rifts. Diese abgeleitete regionale Hebungsgeschichte im mittleren Miozän korreliert mit der zweistufigen Ausbreitung der Graslandschaften, sowie dem Aufkommen neuer Arten im tropischen Afrika.

Die Kombination aus Fließverhalten, Entstehungsort und morphologischer Eigenschaften macht den Yatta-Lavastrom zu einem "Paläoneigungsmesser" und wichtigen vulkanischen Untersuchungsobjekt für die topographische Entwicklung in Ostafrika.

CONTENTS

LIST OF FIGURES

LIST OF TABLES

ACKNOWLEDGEMENTS

This thesis would not have been completed and much more finalized without the help of numerous people - Thanks to all of you!

First of all I would like to thank my long-standing supervisors Prof. Dr. Romain Bousquet and Prof. Dr. Roland Oberhänsli for initiating this research project within the Graduate School GRK1364 and supporting me since my early days as a student in geology.

Romain Bousquet's inexhaustible abundance of new ideas was the source of several aspects of this study, and his support, open-mindedness, and perpetual readiness to discuss, provided the basic condition for efficient research. His positive attitude to all kind of things and his enthusiasm towards geodynamics were enormously motivating. Even in the hardest times, when problems appeared to be insurmountable, Romain still kept on saying: "Findet man eine Lösung", a french-accented phrase, which helped always to get through tough periods of this PhD. I will always remember our first year joint fieldwork in a very small car in Kenya.

From Roland Oberhänsli I learned how to look at geological structures and rocks in detail, even when you run up a mountain. His unpayable field experience, interdisciplinary interest, and knowledge about volcanism always encouraged me to follow my ideas. I profited a lot during fruitful discussions, constructive reviews of the manuscripts, and his always-friendly support during the last years.

This study benefited a lot from the contributions by Prof. Manfred Strecker, PhD. His profound knowledge in East African geology and its tectono-volcanic evolution were of great importance for the successful completion of this PhD thesis. His efficient work on numerous manuscripts significantly improved whatever I wrote and always within an incredible short time. This efficiency was extremely helpful during the last month while my thesis was rapidly developing. I will always remember the situation in a seminar when he pointed out the special geological situation of the Yatta Plateau and finally gave the ignition to develop my principal ideas of this thesis.

Dr. Martin Trauth brought the results of this thesis into a new light and always saw my work from an interdisciplinary point of view. He helped a lot to find aspects that supported my theory in many ways and shifted this project more into the center of the GRK1364 East African group.

I would like to thank Prof. Cynthia Ebinger, PhD from Rochester University (New York) and Prof. Dr. Sierd Cloetingh from the University of Amsterdam for accepting and reviewing my thesis without any hesitation.

I also would like to thank my colleague and friend Jannes Kinscher who accompanied me during the fieldwork along the Yatta Plateau in Kenya during the second year. He did a perfect job as scientific assistant and motivator. In particular, when times were hard and frustrating.

I had the great luck that Ernst Hauber and Joel Ruch did their PhD at the same time like me. With both I had stimulating discussions on the rheology and emplacement of lava flows and the interpretation of satellite imagery.

Antje Musiol performed XRF-analysis in cooperation with the geochemical laboratories at the GeoForschungsZentrum Potsdam (GFZ). Anne Jähkel was a great help during the sample preparation. As this was really the base for this thesis their help is greatly acknowledged.

Accordingly, I thank my office mates Dr. Paolo Ballato, Heiko Pingel, Dr. Angela Landgraf, Amaury Pourteau, Michael Krause, and Dr. Dirk Scherler for their collegiality.

I am grateful to Dr. Andreas Bergner for coordinating the Graduate School GRK1364 and keeping my head free to concentrate more on scientific and less administrative work. In this respect I thank all the PhD students of the GRK1364 for fruitful discussion, unprecedented team spirit, funny evenings in Potsdam's "Waschbar", and an unforgettable time during our two excursions to Kenya and the Indian Himalaya.

I thank kindly the German Research Foundation (DFG) for funding this project over the last three and a half years and giving me the opportunity to finish this thesis within the set timeframe.

Finally, I would like to express my deep gratitude for the encouragement and infinite support in so many ways to my family. And last but not least I thank Sarah for her understanding, patience, and love.

ORGANIZATION OF THE THESIS

This thesis is organized as a "cumulative thesis" and consists of a series of five chapters. Three of them (chapters 2-4) can be regarded as individual manuscripts to be published in international peer-reviewed scientific journals. Chapter 4 has already been published while the remaining chapters have been submitted. An outline of each of these chapters and the contributions of the individual co-authors is provided below.

CHAPTER 1

Introduction

This chapter presents the scope and aims addressed by this thesis, and briefly provides the general geological background.

CHAPTER 2

The middle Miocene East African Plateau: a pre-rift topographic model inferred from the emplacement of the Yatta lava flow, Kenya

Wichura, H., Bousquet, R., Oberhänsli, R., Strecker, M. R., Trauth, M. H.
submitted to: *Geological Society of London, Special Publications*

This chapter can be considered as an expanded version of the published manuscript presented in chapter 4 and is an invited submission to a Special Publication of the *Geological Society of London*, with the working title *"Out of Africa - a synopsis of 3.8 Ga of Earth History"*. It is devoted to the evidences and implications, which proofs that the East African Plateau acted as an important orographic barrier since at least the middle Miocene and therefore prior to the onset of continental rifting and the formation of the East African Rift System. Based on modeling the emplacement and the underlying topography (slope angle) of the mid-Miocene Yatta lava flow, a new approach for quantifying the elevation from where the flow originated was elaborated. Concurrently, the topographic level of the source area represents the elevation of the East African Plateau at that time. Furthermore, a qualitative discussion, integrating climatic and environmental proxy data and observations was carried out. This reveals that the existence of high topography in East Africa coincide with the two-step expansion of grassland and subsequent aridification in tropical Africa.

The first author carried out the fieldwork and was responsible for all sample preparations and geochemical analysis. Furthermore, he did the lava-flow modeling and wrote a first version of the manuscript including figures. The

second and third author (the thesis supervisors) essentially assisted the model development. The fourth and fifth author helped with the discussion and interpretation of the results and the preparation of the final version of the manuscript.

CHAPTER 3

Emplacement of the mid-Miocene Yatta lava flow, Kenya: Implications for modeling long, channeled lava flows

Wichura, H., Bousquet, R., Oberhänsli, R.

submitted to: *Journal of Volcanology and Geothermal Research*

In order to model the emplacement and present-day morphologic parameter of the length-dominated, channeled Yatta lava flow, this chapter focuses on the details of a lava-flow modeling technique and describes how this new approach was developed. The method combines well-constrained observations from the field and remote sensing with classical flow-advance calculations and state-of-the-art rheological modeling. Additionally, it integrates a temperature and composition-dependent viscosity model for natural anhydrous and hydrous silicate lavas.

The first author developed the model allowing the advance of length-dominated lava flows in a channel. Furthermore, he performed the entire fieldwork and sample selection for running the analytical viscosity model. He performed X-ray fluorescence analysis and employed a comparing lava-flow modeling analysis of different lava compositions. He wrote a first version of the manuscript including all figures and tables. The second and third author (thesis supervisors) provided discussions and help in finishing and improving the final version of the manuscript.

CHAPTER 4

Evidence for middle Miocene uplift of the East African Plateau

Wichura, H., Bousquet, R., Oberhänsli, R., Strecker, M. R., Trauth, M. H.

published 2010: *Geology*

This chapter can be regarded as a short version of the submitted manuscript in chapter 2. It is the first of three manuscripts that has been published. The contributions of each author are in accordance to chapter 2.

CHAPTER 5

Conclusion

This chapter presents the main conclusions of the combined results obtained from this thesis.

CHAPTER 1

Introduction

In the light of acceptance of the global tectonics concept, the East African Rift System (EARS) remains the archetypal continental extension zone and an analogue to the early stages of evolution of passive continental margins preceding oceanic opening (e.g., *Burke and Whiteman*, 1973; *Bosworth*, 1987; *Rosendahl*, 1987; *Courtillot et al.*, 1999; *Ebinger*, 2005). In this respect, active continental rifting is always accompanied by surface uplift and topographic changes, from the first crustal doming to the following volcanic accumulations, coeval graben formation, and finally surface rift-flank uplift (e.g., *Burke and Whiteman*, 1973; *Braun and Beaumont*, 1989; *Ebinger*, 1989; *Smith*, 1994).

The uplift history and topographic evolution of the EARS have undergone a revitalization in the past several years due to the increased availability of new techniques, including apatite fission-tracks thermochronology (e.g., *Wagner et al*. 1992; *Foster and Gleadow*, 1996; *Kohn et al.*, 2005; *Spiegel et al.*, 2007), digital topography and morphology analysis (e.g., *Chorowicz*, 2005; *Veldkamp et al.*, 2007; *Burke and Gunnel*, 2008; *Roberts and White*, 2010), lithospheric density modeling and geophysical gravity studies (e.g., *KRISP*, *1991*; *Nyblade and Brazier*, 2002; *Woldetinsae*, 2005; *Benoit et al.*, 2006), as well as quantification attempts of tectonically controlled uplift processes (e.g., *Smith*, 1994; *Spiegel et al*. 2007; *Pik et al*. 2008). In the realm of geodynamics, tectonics, and surface morphology, I have studied the cause of plateau uplift during the incipient stage of rifting and its response on spatiotemporal climatical and environmental variations in East Africa. Furthermore, I quantified the amount of plateau uplift by modeling a length-dominated lava flow on the eastern rim of the East African Plateau (EAP) and used it as a "paleo-tiltmeter".

The section of the EARS between 5°N and 10°S is characterized by three main topographic features: the classical graben structure of the Eastern branch; the highland region around the rift valley, known as the Kenya Dome; and the EAP comprising the Proterozoic Tanzania Craton and the adjacent western and eastern rift (*Maguire and Kalib Khan*, 1980).

Since their recognition, it was desirable to understand the geodynamic and tectonic mechanisms for their formation and to quantify the amount of the areally expansive EAP uplift during the Cenozoic. Pioneering studies revealed information on post-Cretaceous uplift obtained by the examination of paleo-erosion surfaces, lithologic contacts between Proterozoic basement rocks and great volumes of Cenozoic covering volcanic units, and plume-lithosphere interaction (*Dixey*, 1959; *King*, 1970; *Baker et al.*, 1972). These have been summarized by *Le Bas* (1971) as follows:

"It seems that the whole of Kenya, Uganda and Tanzania was first uplifted by 300 m, or more, in late Cretaceous times; a second period of uplift occurred in mid-Tertiary (pre-Miocene) times and this was followed by a third period in late Tertiary times (Pliocene), the latter two centered in southwest Kenya affecting a smaller (about 700 km diameter) area than the first... The combined uplift was about 1,500 m. The upwarp of the Western Rift in fact overlaps the third uplift."

However, this simple topographic history is incomplete due to the lack of unambiguous topographic and geomorphic reference horizons and clearly limits quantitative information about uplift across the entire EAP prior to rifting.

Accordingly, the aims of this study can be summed up in terms of the following four main scientific questions:

1. Is there geologic and geomorphic evidence for a large-scale uplifted area, which proofs the existence of high topography prior to the onset of rifting in East Africa? Thereby, a well-defined relative chronological

record based on the lithologic contacts between Proterozoic basement rocks and overlying Tertiary pre-syn-rift volcanic accumulations is of particular relevance for the reconstruction of the paleo-topography in the study area.

2. How much was the uplift? The quantification of surface uplift in East Africa is crucial as the build-up of high topography creates an orographic barrier for moisture bearing winds coming from the Indian Ocean in the east and the Congo basin in the west and must had a first order impact on the climatic and environmental evolution (*Sepulchre et al.*, 2006).

3. When did the build-up of high topography occur? Does the present topography reflect post-rift uplift due to geodynamic extension and post-rift relaxation or is it rather the surface expression of pre-syn-rift mantle plume impingement? While the first case suggests that the build-up of high topography should be younger than 7 Ma, the second case would imply surface uplift prior to 7 Ma. Therefore, the understanding of the topographic evolution and uplift history requires well-constrained time data. Such data are of particular importance regarding plateau-formation and its integration in the framework of existing hypotheses concerning the paleo-climatic and environmental evolution in East Africa.

4. What causes the uplift of plateau-type topography within a rifting setting? Examination of vertical movements provides constraints on the causal mechanism for the creation of the EAP and the formation of the EARS. These movements only refer to the surface of the Earth. However, it is important to understand how they relate to movements of boundaries within and between the underlying lithosphere and asthenosphere.

All these questions were addressed using a multidisciplinary and integrative approach that combines geomorphic and structural methods with lava-flow modeling and climatic proxy data. Therefore, the study required intense scientific cooperation with a multi-national team of specialists from the University of Potsdam, the University of Nairobi, the GeoForschungsZentrum Potsdam (GFZ), and the German Aerospace Center in Berlin (DLR).

The results of this thesis yield new findings regarding the topographic evolution of East Africa and its implication for climate and environmental changes. Furthermore, the thesis contributes to a better understanding of geodynamic processes that occur during progressive plume-lithosphere interaction and its surface expression.

CHAPTER 2

The middle Miocene East African Plateau: a pre-rift topographic model inferred from the emplacement of the Yatta lava flow, Kenya

Abstract

High topography in the realm of the rifted East African Plateau is commonly explained by two different mechanisms: (1) rift-flank uplift resulting from mechanical and/or isostatic relaxation, and (2) lithospheric uplift due to the impingement of a mantle plume. High topography in East Africa has far-reaching effects on atmospheric circulation systems and the amount and distribution of rainfall in this region. While the climatic and paleo-environmental influences of high topography in East Africa are widely accepted, the timing, the magnitude, and this spatiotemporal characteristic of changes in topography have remained unclear. This dilemma stems from the lack of datable, geomorphically meaningful reference horizons that could unambiguously record surface uplift. Here, we report on the formation of high topography in East Africa prior to Cenozoic rifting. We infer topographic uplift of the East African Plateau based on the emplacement characteristics of the ~300-km-long, and 13.5-m.y.-old Yatta phonolitic lava flow along a former river valley that drained high topography centered at the present-day rift. The lava flow followed an old riverbed that once routed runoff away from the eastern flank of the plateau. Using a compositional and temperature dependent viscosity model with subsequent cooling, and adjusting for the Yatta lava flow dimensions and the covered paleo-topography (slope angle), we use the flow as a "paleo-tiltmeter". Based on these observations and our modeling results, we

determine a paleo-slope of the Kenya Dome of at least 0.2° prior to rifting and deduce a minimum plateau elevation of 1,400 m. We propose that this high topography was caused by thermal expansion of the lithosphere interacting with a heat source generated by a mantle plume. Interestingly, the inferred middle Miocene uplift coincides with fundamental paleo-ecological changes, including the two-step expansion of grasslands in East Africa, as well as important radiation and speciation events in tropical Africa.

2.1 Introduction

Thermal and dynamic processes associated with mantle plumes and active continental rifting across East Africa have resulted in long-wavelength plateaus, pronounced regional topographic contrasts, and widespread geophysical anomalies in the different branches of the East African Rift System (EARS; e.g., *White and McKenzie*, 1989; *Prodehl et al.*, 1994; *Huerta et al.*, 2009). High plateau topography exists in Ethiopia and Kenya and reaches average elevations of 2,400 and 1,900 m, respectively. Both plateaus are traversed by Cenozoic rifts constituting the tectonically active EARS (Fig. 3-1). It has been suggested that the Eastern branch of the EARS propagated from north to south, accompanied by plateau-type volcanism at ~45 Ma in Ethiopia and ~8 Ma in Tanzania (*George et al.*, 1998), thus causing the distinct rift segments of Ethiopia, Kenya, and northern Tanzania. Separated from the Eastern branch by the Tanzania Craton, the Western branch of the EARS comprises a region of high topography extending from lakes Albert and Tanganyika southward to Lake Malawi, with isolated volcanism starting at about 12-10 Ma (e.g., *Ebinger*, 1989; Fig. 2-1). The extensional structures in both rift branches exploit pre-existing crustal anisotropies in Proterozoic mobile belts (e.g., *Ebinger*, 1989; *Hetzel and Strecker,* 1994; *Nyblade and Brazier*, 2002).

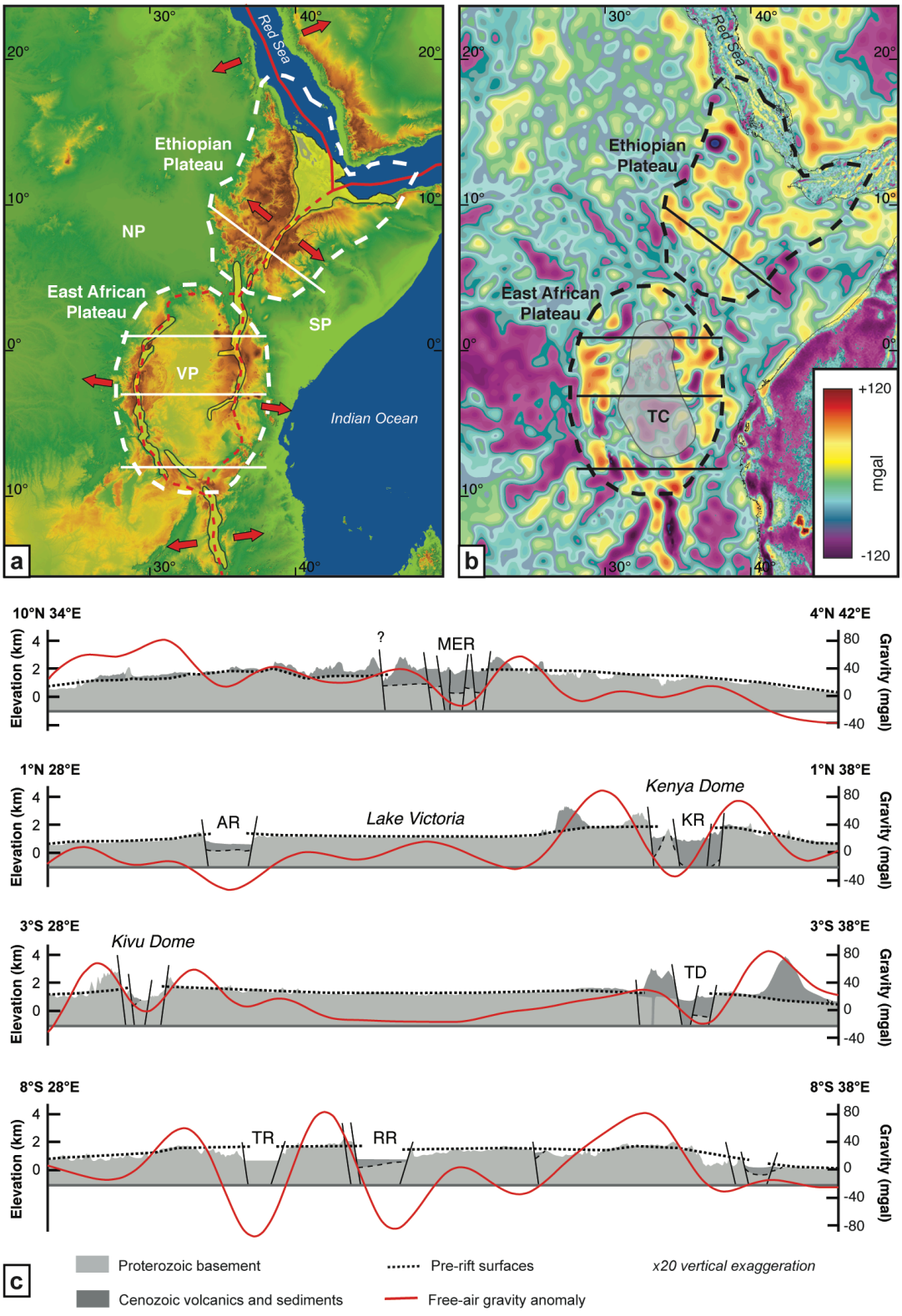
a
b
c
Red Sea
Ethiopian Plateau
East African Plateau
NP
SP
VP
TC
Indian Ocean
30°
40°
20°
10°
0°
+120
mgal
-120
10°N 34°E
4°N 42°E
MER
?
1°N 28°E
1°N 38°E
Kenya Dome
AR
Lake Victoria
KR
3°S 28°E
3°S 38°E
Kivu Dome
TD
8°S 28°E
8°S 38°E
TR
RR
Elevation (km)
Gravity (mgal)
Proterozoic basement
Cenozoic volcanics and sediments
Pre-rift surfaces
Free-air gravity anomaly
x20 vertical exaggeration

Figure 2-1. East African topography and free-air gravity anomalies. (a) Topography showing the main uplifted plateaus (white dashed lines) and the Eastern and Western branch of the East African Rift System (yellow areas). Red arrows display the main extension direction. Red lines mark the plate boundaries (solid) and developing plate boundaries (dashed) between the Nubian (NP), Somalian (SP), and Victoria Plate (VP). White lines denote the topographic profiles in Figure 2-1c. (b) Free-air gravity anomaly in East Africa for the same map section as in Figure 2-1a. Map is based on gravity anomaly grid of *Sandwell and Smith* (1997) and created with the gravity anomaly on-line map construction tool (*http://www.serg.unicam.it/Geo.html*). Gray area marks the extent of the Tanzania Craton (TC). Black lines denote free-air gravity anomaly profiles in Figure 2-1c. (c) Four east-west topographic and free-air gravity anomaly profiles from north to south. The topographic profiles (vertical exaggeration x20) integrate the potential pre-rift surface and contact between the Proterozoic basement and Cenozoic cover. MER - Main Ethiopian Rift; AR - Albert Rift; KR - Kenya Rift; TD - Tanzania Divergence; TR - Tanganyika Rift; RR - Rukwa Rift.

Spatially, high East African topography correlates with volcanism, extensional structures, long-wavelength negative gravity Bouguer anomalies, and reduced thickness of mantle lithosphere (e.g., *Achauer et al.*, 1994; *Class et al.*, 1994; *Smith*, 1994; *Simiyu and Keller*, 1997; *Fuchs et al.*, 1997; *Nyblade and Brazier*, 2002; Fig. 2-1). Radiometrically datable rocks and a wealth of geophysical information have thus made this region a premier location to investigate the relationship between potential mantle plume-induced plateau uplift, tectonic rift-flank development, and magmatic processes. Furthermore, Cenozoic uplift in East Africa has also formed an efficient orographic barrier to moisture-bearing winds from the Indian Ocean and the Congo basin, thus governing the distribution and amount of rainfall in East Africa and influencing the geomorphic process regime and environmental conditions (*Sepulchre et al.*, 2006; *Wichura et al.*, 2010).

Topographic uplift and related rift evolution in East Africa has been cast into two simplified end-member models: (1) late-stage uplift associated with major rift structures and regional-scale extensional detachments and mechanical relaxation and/or isostatic adjustment (e.g., Kenya Rift; *Bosworth*, 1987; *Ebinger et al.*, 1989; Fig. 2-2a), and (2) regional domal uplift followed by extensional processes associated with mantle-plume impingement on continental lithosphere (e.g., Ethiopian Plateau; *Braun and Beaumont*, 1989; *Burov and Cloetingh*, 2009; Fig. 2-2b).

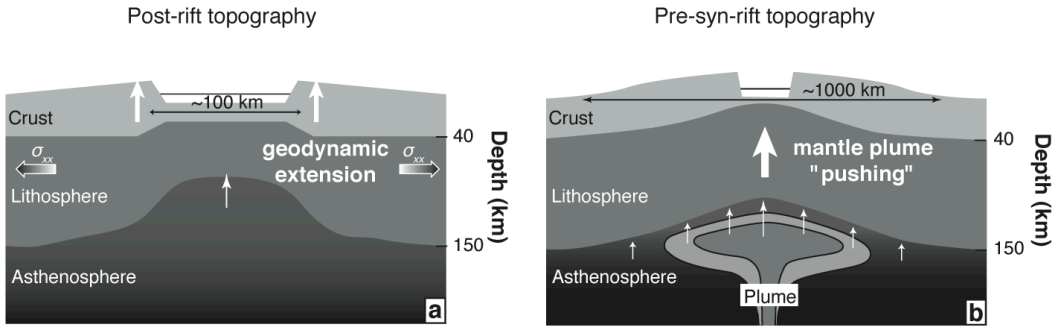

Figure 2-2. Sketch of plume-lithosphere interaction in a geodynamically active rift setting. (a) Conventional post-rift uplift model provide only rift shoulder uplift due to mechanical relaxation and/or isostatical adjustment at regional-scale. (b) Pre-syn-rift uplift model predicts large-scale uplifted dome provoked by mantle plume impingement on continental lithosphere.

For the Kenya Rift and neighboring regions it is not well known, however, which mechanisms, and in which order of events, rift processes have taken place.

Due to the lack of unambiguous topographic and geomorphic reference horizons, quantitative information about a pre-rift uplift across the Tanzania Craton and the adjacent two rift branches is limited. During the Cretaceous, East Africa acquired its identity as a continent-wide topographic feature of low mean elevation due to low tectonic activity, high sea levels, and a climate conducive to chemical weathering and downwearing reducing relief contrasts (*Burke and Gunnel*, 2008). For this reason, the Congo basin and regions to the northeast were covered by shallow-water Cretaceous marine strata that were related to the trans-Saharan seaway supporting the notion of low topography in East Africa (e.g., *Giresse*, 2005). *Smith* (1994) estimated <1,000 m of crustal uplift of an elongated pre-rift area, locally defined as the Kenya Dome, in early to middle Miocene time (Figs. 2-1c and 2-3). This term has also been used to describe the topography of the overall rift region, including phonolitic and basaltic plateau volcanics accumulated within and on the flanks of the Central Kenya Rift (e.g., *King*, 1978), thus making a rigorous assessment of topographic evolution difficult. Equally unclear is the topographic evolution of the amagmatic Kivu Dome in the Western branch (*Chorowicz*, 2005; Fig. 2-1c).

Apatite fission-track thermochronology has been used to attempt defining the timing of rift-related shoulder uplift from exhumation signals. However, due to the relatively high annealing temperature of apatite and slow geomorphic process rates, these studies only provided Cretaceous ages related to an earlier rifting event and thus preventing an assessment of Cenozoic uplift and exhumation of the East African Plateau (EAP) using this method (*Wagner et al.*, 1992; *Foster and Gleadow*, 1996). However, more temperature sensitive (U-Th)/He thermochronometry by *Spiegel et al.* (2007) suggests a rapid cooling episode in Kenya during late Neogene time that has been related to uplift and exhumation along the eastern and western flanks of the Kenya Rift. In contrast, sustained exhumation since the early Miocene has been reported for southern Ethiopia (*Pik et al.*, 2008).

Due to many ambiguities in the available geologic records (e.g., *King*, 1978; *Smith*, 1994) and only indirect indicators of uplift determined by thermochronology, we choose a different approach to determine the Cenozoic evolution of topography of the EAP using phonolitic flow characteristics on the eastern rift shoulder in Kenya. The Yatta lava flow may provide direct evidence for topography and relief conditions along the eastern flank of the EAP prior to rifting (*Wichura et al.*, 2010). The Yatta phonolites flowed away from higher topography centered in the region of the present-day rift, utilizing a river channel that formerly drained the plateau region toward the southeast. Based on these topographic and geomorphic conditions we posit that viscosity and slope angle of the flow may furnish important insights into the gradients for the emplacement of this lava flow, which ultimately provide information on the paleo-elevation of the source area.

2.2 The eastern flank of the EAP during the Miocene

Considering the total volume of effusive rocks (2.3×10^5 km^3) involved in the volcanic evolution of the Kenya Rift (e.g., *Williams*, 1982; *Hay et al.*, 1995), the

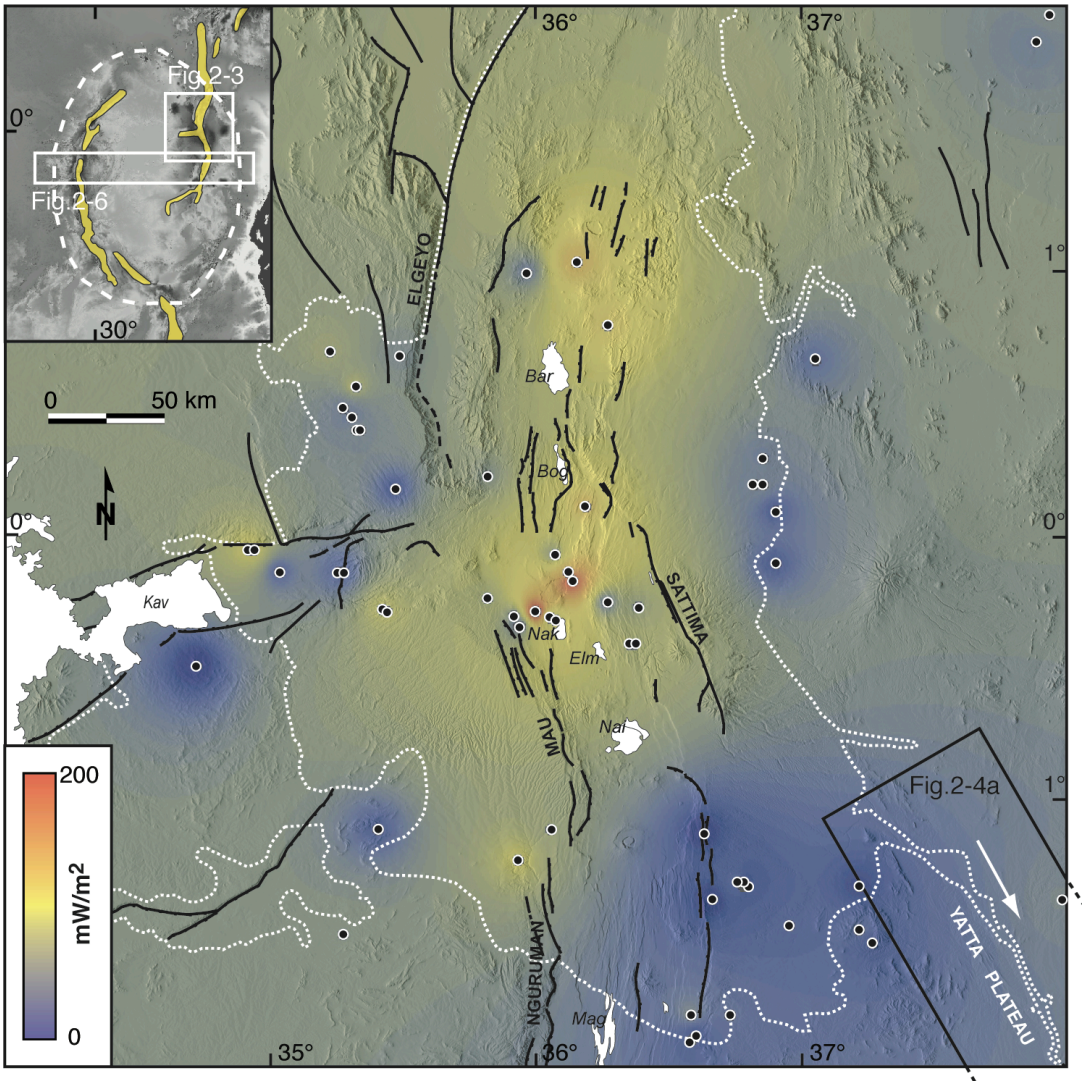

Figure 2-3. Recent heat flow in the Central Kenya Rift. East African Plateau inbox shows map section of Figure 2-3 and topographic swath profile rectangle used for Figure 2-6. Heat flow map is compiled from 62 heat flow measurements (black dots) taken from the global heat flow database of the International Heat Flow Commission (*http://www.heatflow.und.edu/index2.html*) and *Wheildon et al.* (1994). Data points were inverse distance weighted with a d-value of 12. White areas show present rift lakes in Central Kenya. Black lines display major escarpments and normal faults. Volcanic extent of the Miocene plateau volcanism is shown by white dotted line. Black outlines show the northwestern part of the Yatta Plateau (Fig. 2-4a). Flow direction of the Yatta lava flow is from NW to SE (white arrow). Bar - Lake Baringo; Bog - Lake Bogoria; Kav - Kavirondo Golf; Nak - Lake Nakuru; Elm - Lake Elmenteita; Nai - Lake Naivasha; Mag - Lake Magadi.

plateau phonolites represent the product of the largest phase of volcanism with estimates of 4.0-5.0 x 10^4 km^3 (*Lippard*, 1973) erupted between middle and late Miocene time (*Smith*, 1994). The greatest amount of phonolites erupted between 13 and 11 Ma (*Smith*, 1994), as suggested by their isotopic ages and spatial extent (e.g., *Baker and Wohlenberg*, 1971; Fig. 2-3). *Lippard* (1973) reported on individual flows with thicknesses ranging from a few tens of meters to as much as 270 m, emplaced over relatively short periods of time. However, one of the most prominent and spectacular flows is the 13.51-m.y.-old Yatta lava flow (*Fairburn*, 1963; *Veldkamp et al.*, 2007), which was emplaced prior to the formation of the oldest rift structures in northern Kenya. The Yatta phonolites constitute one of the longest lava flows on Earth, which flowed southeastward along a paleo-valley. Although the location of the volcanic center of the Yatta phonolites must have been centered in the present-day rift region, the exact source however has not been unambiguously identified (e.g., *Williams and Chapman*, 1986). *Smith* (1994) inferred the eruptive center to have been in the vicinity of Sattima Fault, which bounds the Central Kenya Rift on the east.

2.3 Yatta lava flow characteristics

The Yatta lava flow was channelized for a distance of at least ~300 km (length *L*) from northwest to southeast into the Tsavo plains (e.g., *Walsh*, 1963; *Fujita*, 1977; *Wichura et al.*, 2010). Due to differential erosion this lava flow now constitutes positive relief and stands tall above the Athi River (*Fujita*, 1977), which is parallel to the flow, mimicking the course of the paleo-river (Figs. 2-4a and b).

The Yatta lava flow dimensions have been derived using satellite imagery (SRTM and LANDSAT) and field observations including GPS support and geomorphic mapping (Fig. 2-4a). The observable thickness of the Yatta Plateau phonolites from the basement contact to the flow-top remnants is between 12

and 25 m (Fig. 2-4b). The maximum width is between 8 km in the northwestern, and 1 km in the remote southeastern part. A compilation of 30 (every 10 km) topographic SW-NE profiles yielded estimations of the average width of the flow, the altitude of the upper flow surface, and the slope angle (Fig. 2-4c). The remnant average width is estimated to be 3 km; along the eroded top of the flow exists an average elevation difference of 2.8 m/km. This

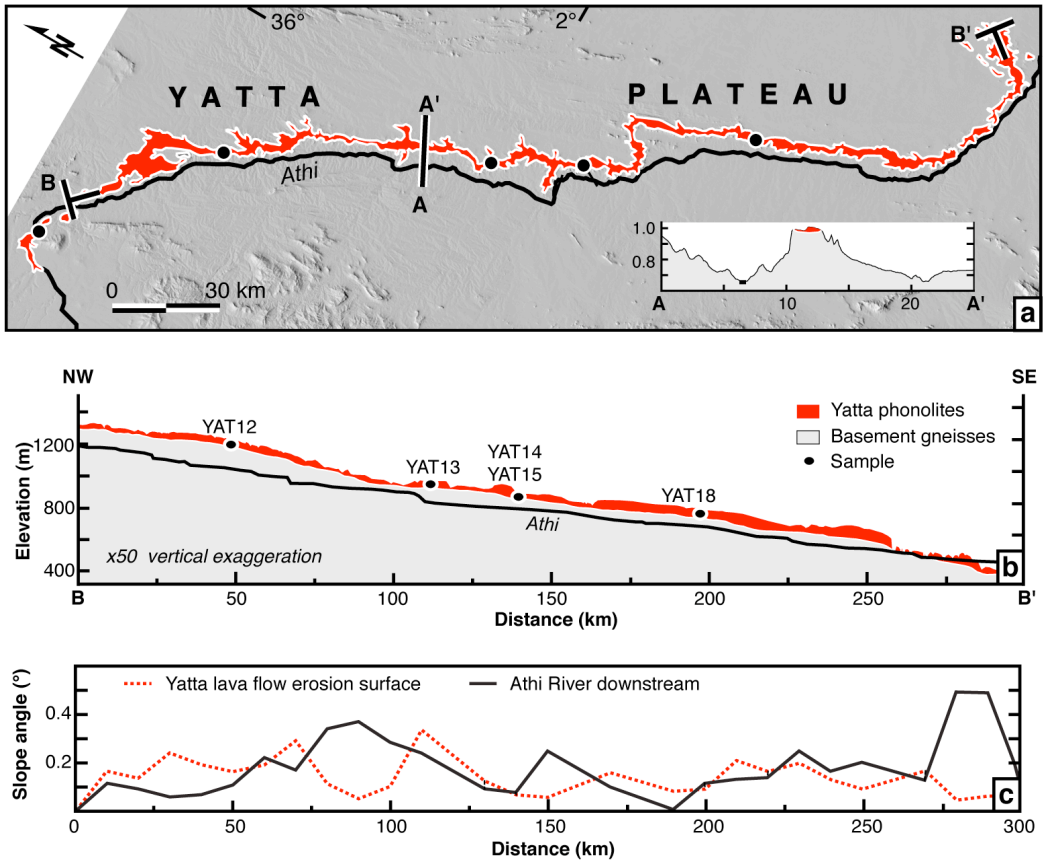

Figure 2-4. The Yatta Plateau morphology. (a) SRTM-image highlighting the Yatta lava flow and the Athi River coursing parallel to the flow. North is 60° anticlockwise rotated. Black dots mark sample locations. A-A' and B-B' denote the geological cross sections of the Yatta lava flow perpendicular to the flow direction (Fig. 2-4a) and along the central flow top (Fig. 2-4b), respectively. Labeling of cross section A-A' is distance in km (x-axis) and elevation in km (y-axis). (b) Geological cross sections constructed along the Yatta lava flow and present Athi River downstream. Black circles mark the location of phonolitic samples, which were used to calculate viscosities by applying the model by *Hui and Zhang* (2007). (c) Recent slope angle distribution corresponding to the erosion surface of the Yatta lava flow and the Athi River relative to the lava flow distance. Slope angles were measured every 10 km. SRTM - Satellite Radar Topographic Mission.

Table 2-1. X-ray fluorescence major element chemistry for eight samples from the Yatta lava flow. YAT_{mean} is a synthetic composition representing the average of all displayed samples. Latitude and longitude localities for these samples are also displayed. Major oxides in wt%.

Sample	YAT12-4	YAT12-5	YAT13-1	YAT13-2	YAT14-2	YAT15-1	YAT15-2	YAT18-2	YAT_{mean}
Longitude	37°39.34'E	37°39.81'E	37°57.59'E	37°57.86'E	37°58.36'E	38°05.03'E	38'05.29'E	38°21.44'E	
Latitude	1°22.16'S	1°22.58'S	1°58.50'S	1°58.34'S	1°58.76'S	2°10.90'S	2°11.46'S	2°31.36'S	
SiO_2	54.60	54.80	54.30	53.50	55.20	54.30	54.30	54.80	54.48
TiO_2	0.80	0.83	0.81	0.81	0.80	0.82	0.82	0.82	0.81
Al_2O_3	19.00	19.10	19.10	19.20	19.00	18.90	19.00	18.60	18.99
FeO^T	5.49	5.72	5.60	5.90	5.53	5.63	5.54	5.56	5.62
MnO	0.25	0.27	0.25	0.45	0.25	0.25	0.23	0.24	0.27
MgO	0.90	0.86	0.80	0.81	0.88	0.81	0.89	0.80	0.84
CaO	2.16	1.44	1.45	1.74	1.33	1.45	1.83	2.04	1.68
Na_2O	7.33	7.57	8.06	6.51	7.42	8.25	6.43	6.43	7.25
K_2O	4.92	5.59	5.39	5.67	5.60	5.29	6.33	5.48	5.53
P_2O_5	0.27	0.29	0.26	0.28	0.27	0.28	0.32	0.29	0.28
H_2O	3.88	2.89	3.51	4.78	3.28	3.48	3.79	4.27	3.74
Total	99.60	99.36	99.53	99.65	99.56	99.46	99.48	99.33	99.50

corresponds to the average slope angle of 0.16° along the bottom of the paleo-valley, as determined from erosional cuts, which is in good agreement with the early estimate by *Saggerson* (1963). As the Yatta lava flow is very narrow compared to its length and the distinguishing ratio of maximal width to maximal length (W_m/L_m) is 0.028, it appears that this flow comprises a single major flow (*Walsh*, 1963), namely S-type following the classification of *Kilburn and Lopes* (1991). Indeed, our field observations and assessments by earlier workers (e.g., *Saggerson*, 1963; *Fujita*, 1977) clearly show that the lava flow is neither the result of multiple volcanic eruptions nor fissure eruptions along its axis.

Previous studies on the Columbia River basalt in the western U.S.A., the Deccan Volcanic Province in India, and the island of Hawaii led to the conclusion that the formation of length-dominated lava flows is related to the efficient delivery of lava through well-developed tube systems (e.g., *Self et al.*, 1996; *Bondre et al.*, 2004; *Harris and Rowland*, 2009). The efficiency of lava tubes in transferring turbulent-flowing lava over long distances and in minimizing (isothermal) cooling is well known and has previously been discussed in detail (e.g., *Keszthelyi*, 1995). However, the features associated with this particular flow formation are generally easily discernible and include collapse pits,

longitudinal cracks along the roof, and secondary vents, as they have been observed in analogous flows on the moon, Mars, and Venus (*Sakimoto et al.*, 1997; *Calvari and Pinkerton*, 1999). Additionally, porphyric rock texture due to turbulent flow and coated spatter fragments generated by constantly degassing and inclined grooves on the internal wall remnants are characteristic for many lava tubes (*Calvari and Pinkerton*, 1999). All these tube-fed characteristics do not apply to the Yatta phonolites.

For a detailed analysis of flow dynamics and the influence of chemical composition on the final dimension of the Yatta lava flow and its style of emplacement, we examined five different localities with well-preserved flow sections (Table 2-1). Fortunately, the Yatta Plateau encompasses several fault-related erosion cuts perpendicular to the paleo-flow direction, which provides access to the internal part of the flow. Here, we observed evidence for laminar flow indicated by aligned feldspars parallel to the flow direction, both along flow rims and in the interior. As turbulent flow does not allow crystallization of aligned phenocrysts (e.g., *Bryan*, 1983; *Smith*, 2002) and evidence for tube-fed flow is not recognized, we consequently interpret the Yatta lava flow as a giant, channelized surface flow.

Locally, pillow lavas at the contact between the phonolites and the basement rocks suggest the presence of water during emplacement. Interestingly, despite all the different features suggesting emplacement in a paleo-drainage system, no fluvial sediments were observed in the contact zone between the flow and the basement rocks. This phenomenon, however, may be explained by the thermal erosion effect of flowing lava (e.g., *Greeley et al.*, 1998).

2.4 Basic assumptions

Lava flows can be either considered to behave as a Bingham or Newtonian fluid, which are rheologically characterized by plastic or dynamic viscosities (e.g., *Griffith*, 2000), respectively, depending on the initial yield strength supporting a fluid to flow. The flow advance is mainly controlled by the

rheological conditions in its rear frontal zone (RFZ) - that part of a flow between its convex-curved outer front and its established channel structure upstream (*Lopes and Kilburn*, 1990; *Kilburn and Lopes*, 1991). This zone is assumed to be characterized by isotropic and non-fractionated conditions and uniform density (e.g., *Lopes and Kilburn*, 1990; *Tallarico and Dragoni*, 1999). Due to low deformation rates in the RFZ (*Lopes and Kilburn*, 1990), we follow the approach by *Tallarico and Dragoni* (1999) and assume the lava to be an approximately isothermal Newtonian liquid flowing in a rectangular channel. Accordingly, this channel simulates a model-based shape of the Athi river paleo-valley, which was occupied by the Yatta lava flow along an inferred constant slope angle β. The solution for viscous flow in a channel with a width W and thickness H can be obtained from the solution for a filled rectangular conduit having the same width and double thickness (e.g., *White*, 1991). The channel dimensions are compatible with the average Athi paleo-valley width (3 km) and channel margins (lava-flow thickness 12-25 m) over the entire length (290 km). Clearly, downstream variations of width or slope can hydraulically affect the velocity field; in this case the one-dimensional model is an approximation at a single cross section, thus assuming laminar flow in flow direction (*Tallarico and Dragoni*, 1999). Furthermore, we regard the lava flow from its eruption temperature near the vent, where lava has not yet developed significant yield strength and thus can be treated as a Newtonian liquid (*Pinkerton and Stevenson*, 1992; *Dragoni and Tallarico*, 1994). It is important to note that we keep this assumption of Newtonian flow along the entire length and with consequent cooling, because it is not yet known at which temperatures lava flows change to Bingham rheology.

2.5 Modeling lava-flow emplacement

Basaltic lava flows reach distances in excess of 150 km along slope angles <0.1° (*Self et al.*, 1996). Since viscosities of phonolites are higher compared to basalts,

we tested the hypothesis if phonolitic lava could reach a distance of ~300 km along a slope of 0.16°. For this simulation we developed a one-dimensional empirical model. The model relies on the viscosity equation by *Hui and Zhang* (2007):

$$\log\eta = A + \frac{B}{T} + \exp\left(C + \frac{D}{T}\right) \tag{2-1}$$

This equation simulates viscosity η as a function of temperature T, chemical composition, and water content of the lava. A, B, C, and D are linear functions of X_i (mole fractions of oxide component i) (*Hui and Zhang*, 2007). The mole fraction for water is integrated in D and combined with an internal temperature dependence of the hydrous component (*Hui and Zhang*, 2007). The 2σ deviation of this fit is 0.61 $\log\eta$ units (*Hui and Zhang*, 2007). As input data we took information from eight standard X-ray fluorescence analyzed samples from the Yatta Plateau (Table 2-1). Fresh hand-specimens were collected on five different outcrops along the general flow trend (Figs. 2-4a and b). Furthermore, we added one synthetic sample YAT_{mean} to capture the full chemical range of phonolites related to the Yatta Plateau eruptions. This sample is an averaged mixture of oxide components of all Yatta samples (Table 2-1).

Starting from the eruption temperature typical for phonolitic magmas (T_0=870 °C; *Ablay et al.*, 1995) we defined a stepwise (n) cooling process with ΔT=10 °C. The gradually increasing viscosity of the lava during cooling corresponds to the stepwise decreasing rear frontal velocity v_n following Jeffreys' equation (*Jeffreys*, 1925), expressed by:

$$v_n(T_n, X_i) = \frac{H^2 g \rho \sin\beta}{a\eta_n(T_n, X_i)}, \tag{2-2}$$

where β is the slope angle, g is the gravity constant (9.81 m/s^2), ρ is the rock density (phonolite 2.4 x 10^3 kg/m^3), H is the mean lava-flow thickness, a is 3 as

suggested by *Booth and Self* (1973) for channels that are wide relative to their depth, and η_n is the viscosity, computed stepwise from the model by *Hui and Zhang* (2007). Furthermore, we defined the simulation to finish, when no flow advance can be recognized. This happens when cooling forces the velocity to fall below 0.01 m/s.

In order to evaluate the time for the rear frontal zone (RFZ) of the Yatta lava flow to reach its final position, we used estimates of effusion rates *F*, the flux of lava expressed by the volume of effused material per unit of time, approximately given by:

$$F = WH\overline{V}\,, \tag{2-3}$$

where *W* is the mean width, *H* the mean thickness, and *V*-bar is the mean velocity of the RFZ (the sum of all v_n divided by *n* cooling steps). Furthermore, we assume a constant production rate of material at the vent. Estimates of the emplacement time (t_{em}) were obtained using the Graetz model, an empirical conduction-limited cooling model (*Pinkerton and Sparks*, 1976), in which lava-flow cooling is compared to the heat loss of a hot fluid moving through a cool conduit. The heat advection within the flow along its length is described by the dimensionless Graetz (G_Z) number (*Carrasco-Núñez*, 1997) and is given by:

$$G_Z = \frac{H^2\overline{V}}{kL}, \tag{2-4}$$

where *k* is the thermal diffusivity (phonolite 3.5 x 10^{-7} m^2/s; *Martin and White*, 2002), and *L* is the lava-flow length. It has been empirically determined that lava flows come to rest before G_Z falls to about 300 (*Carrasco-Núñez*, 1997). Hence, the emplacement time (t_{em}) can be considered as:

$$t_{em} = \frac{L}{\overline{V}}, \tag{2-5}$$

so that the equation can be rewritten as:

$$t_{em} = \frac{H^2}{G_Z k} \tag{2-6}$$

Finally, we modeled the lava flow in two ways: (1) pre-defining a fixed thickness and calculating how far the lava can flow, and (2) assuming the present lava-flow length, estimating the required mean thickness, to compute the mean frontal velocity and effusion rate, simultaneously. In addition, in both simulations we calculated the mean thickness and length as a function of the underlying topography (*Wichura et al.*, 2010).

2.6 Modeling results

During the advance of long, channelized lava flows from the vent to the attainment of their final morphology, simultaneous viscosity changes are essentially temperature controlled. Therefore, the viscosity equation (2-1) is well suited to be applied to our model, integrating a composition dependency and a validation over the full range of temperatures considered (600-870 °C). Starting from the eruption temperature the model computed viscosities for five selected Yatta samples (YAT12-5, YAT14-2, YAT15-2, YAT18-2, YAT_{mean}; Table 2-1 and Fig. 2-5a) according to *n* temperature steps. As the number of cooling steps increases the trend toward higher viscosities is maintained for all samples with varying degrees (Fig. 2-5a), the model predicts the highest viscosities between 6.2 x 10^3 and 1.3 x 10^7 Pa s for the composition with the lowest water content (2.89 wt%; YAT12-5). We also calculated the lowest viscosities ranging from 2.6 x 10^3 to 3.4 x 10^6 Pa s for the sample with the highest water content (4.27 wt%; YAT18-2). Viscosities for sample YAT15-2 and YAT_{mean} overlap over the entire temperature range from 3.6 x 10^3 to 6.0 x 10^6 Pa s (Fig. 2-5a).

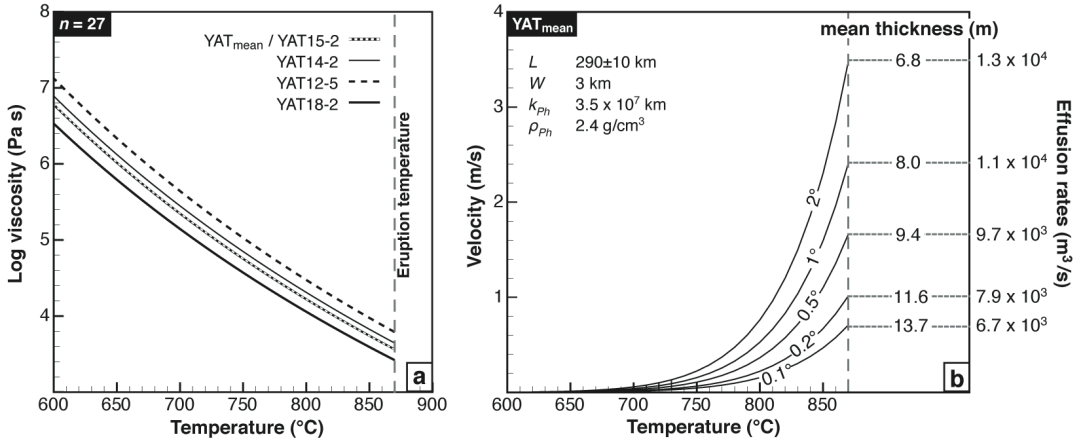

Figure 2-5. Emplacement of the Yatta lava flow. (a) Viscosities as a function of temperature and composition of four phonolitic samples from the Yatta lava flow. Sample compilation is added by one synthetic composition considered as representative for all studied samples (YAT_{mean}). All viscosities were stepwise (ΔT=10 °C) calculated with the *Hui and Zhang* (2007) model starting from the eruption temperature T_0=870 °C (*Ablay et al.,* 1995). 2σ for calculated viscosities is 0.61 logη units. (b) Rear frontal velocity profiles of sample YAT_{mean} as a function of temperature, mean thickness, slope angle, and effusion rate. Every profile represents the parameter fixing the conditions (slope angle, mean thickness, and effusion rate) under which the recent Yatta lava flow dimension can be achieved. *L* - lava-flow length; *W* - lava-flow width; k_{ph} - thermal diffusivity for phonolite; ρ_{ph} - density for phonolite.

The development of the rear frontal velocity for the sample YAT_{mean} is shown in Figure 2-5b, determining the constraints (mean thickness, slope angle, and effusion rates) under which a theoretical lava flow reaches the morphological parameters of the Yatta lava flow, specifically the length of 290±10 km. According to slope angles between 2 and 0.5° the rear frontal velocities at the eruption temperature range from 3.5 to 1.7 m/s, respectively. Constant slope angles in the range of 0.1 and 0.2° are more realistic with respect to the slope angle of 0.16° estimated for the Yatta lava flow. For that range the mean frontal velocities at the vent were calculated between 0.7 and 1.0 m/s. The stepwise calculated flow advance in the channel comes to a halt at temperatures between 620 °C for a slope angle of 2°, and 670 °C for a slope angle of 0.1°.

Modeling small active lava flows on different volcano types has shown that the shape and roughness of the channel used by the lava are of great importance (*Del Negro et al.*, 2007). Sensitivity tests of our model, however,

suggest that topographic disturbances along the course of the river valley do not significantly influence the model result, particularly when dealing with high effusion rates between 6.7 x 10^3 to 1.3 x 10^4 m^3/s (Fig. 2-5b). We found that the most important parameters controlling lava-flow length are water content of the lavas, viscosity change with ongoing cooling, and lava-flow thickness (*Wichura et al.*, 2010).

Our simulation of the Yatta lava flow suggests that sustained flow may occur at slope angles of at least 0.18 to 0.20°, with an estimated uncertainty of 15% (*Wichura et al.*, 2010). Under these circumstances and a lava-flow thickness of 12±3 m, the lava-flow front must have been able to reach the eastern Tsavo plains over a distance of ~300 km. For comparable thicknesses and the present-day slope of 0.16° the flow simulation yields a maximal flow length of ~260 km, which is 13% shorter than the Yatta lava flow. It is important to note that the slope angles we calculated are minimum values.

In this respect, the applicability of the model is limited because of two crucial facts observed on the Yatta lava flow. First, the source of the lava flow is not well known. Hence, it is possible that the Yatta lava flow may have been even longer than the 290±10 km used in our model. Therefore, the simulation would either predict a higher mean flow thickness or flow with a slope angle >0.2°. The latter scenario is more likely, because the thickness depends not just on the slope, but also on mass loss to levees, volume loss (or gain) by degassing or inflation, and rheological changes during transport (e.g., *Baloga et al.*, 2001). Second, the flow direction is NW-SE and therefore rotated by 60° northward with respect to the slope of the East African Plateau (EAP) in this area. The projection of the lava flow onto an east-west profile along the same inclined plane yields a slope angle of up to 0.38° (Fig. 2-6).

Using the calculated slope angle of 0.18-0.20° across the EAP, and assuming a virtually flat top of the uplifted region and a uniform uplift at both flanks of the plateau, the phonolites would have originated in a plateau setting with a maximum elevation of 1,400 m (Fig. 2-6). This supports our initial hypothesis

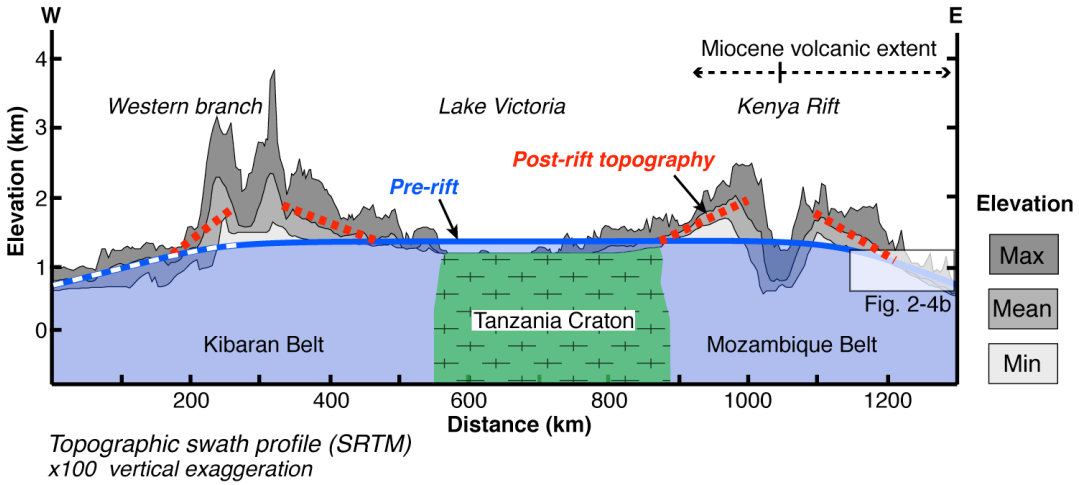

Figure 2-6. Middle Miocene East African Plateau derived from slope angle modeling on the eastern flank. The pre-rift topographic model uses a slope angle of 0.2°, which yields a flat plateau 1,400 m high and 1,300 km wide across the Tanzania Craton and adjacent Proterozoic belts (Kibaran and Mozambique). The dotted line represents the pre-rift topography of the western flank assuming that the East African Plateau rose uniformly at both flanks (e.g. *Ebinger*, 1989). Different grey areas display the modern topography across the center of the East African Plateau (1° x 12° topographic swath profile extracted from SRTM data; see also inbox in Fig. 2-3). Thick red-dashed lines mark the portion of syn- and post-rift uplift. White box shows the location of the profile shown in Figure 2-4b. E-W arrows display the Miocene volcanic extent from the Central Kenya Rift axis. SRTM - Satellite Radar Topographic Mission.

of an areally expansive, high pre-rift topography prior to 13.5 Ma that comprised a region at least 1,300 km in diameter in the present-day EAP region (*Wichura et al.*, 2010; Fig. 2-6). This assessment is also in line with earlier interpretations by *Le Bas* (1971) and *Burke* (1996). The lower slope angle measured today on the eastern rim of the EAP may thus may be related to crustal bending during limited uplift of the rift shoulders.

2.7 Linkages between tectonics, topography, climate, and evolution

Our results provide important new insights into the East African topographic evolution prior to rifting and ensuing environmental change. Today, the East African Plateau (EAP) constitutes an important topographic feature that

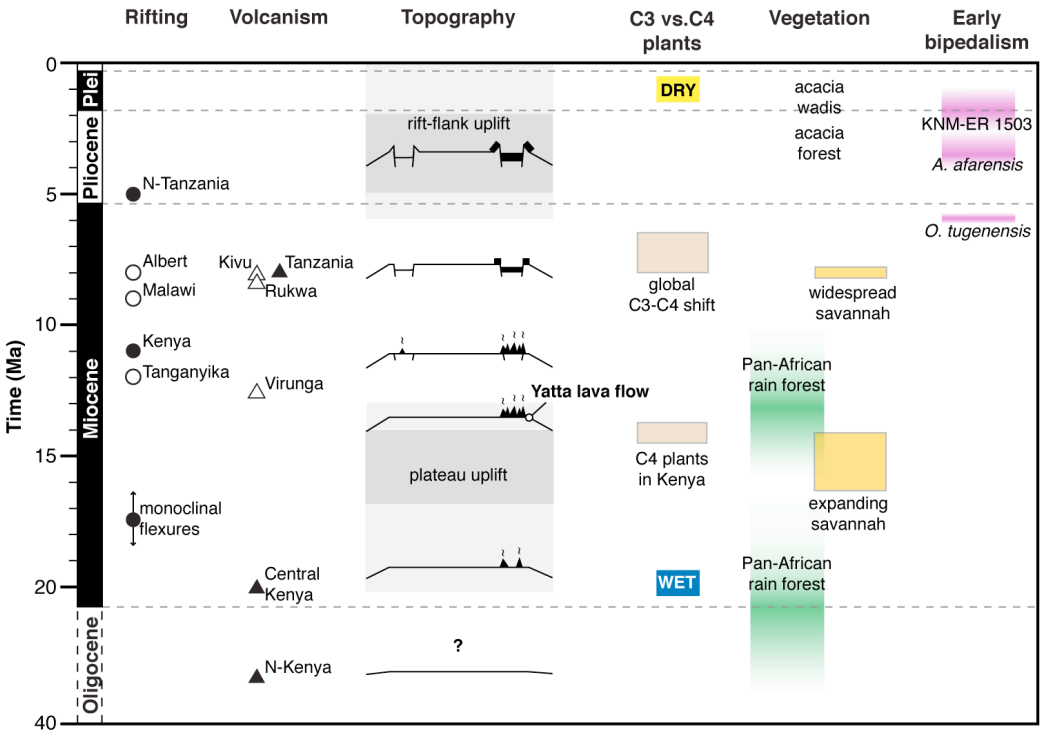

Figure 2-7. Cenozoic uplift chronology, vegetation changes, and early hominids evolution in East Africa. Middle Miocene uplift correlates with major climatic and environmental shifts. Data compilation as follows: onset of volcanic activity (triangle) and rifting (circle) in the Eastern (filled) and Western branch (empty) of the East African Rift System (*Baker and Wohlenberg*, 1971; *Cohen et al.*, 1993; *Chorowicz*, 2005), Pliocene rift-flank uplift (*Ebinger et al.*, 1993; *Spiegel et al.*, 2007), K-Ar age of the Yatta lava flow (*Veldkamp et al.*, 2007), pollen and carbon isotopes (*Retallack et al.*, 1990; *Kingston et al.*, 1994; *Cerling et al.*, 1997; *Jacobs*, 2004), Pan-African rainforest expansion-isolation phases (*Couvreur et al.*, 2008), and early hominids bipedalism (*Richmond and Jungers*, 2008).

influences the distribution and amount of rainfall associated with the African-Indian monsoon and westerly moisture sources at continental-scale (*Sepulchre al.*, 2006; *Roberts and White*, 2010). Exacerbated by the additional effects of rift-shoulder uplift and the construction of volcanoes adjacent to the rift flanks (*Shakleton*, 1945), the uplift of the EAP has consequently impacted the drainage system in East Africa. In combination, the long-wavelength uplift, the build-up of volcanic edifices, and the rifting process have helped compartmentalize the EAP into semi-independent basins. Indeed, the Eastern branch of the East African Rift System comprises a patchwork of closely spaced humid and arid sedimentary environments in the vicinity of the Equator (*Sepulchre et al.*, 2006; *Bergner et al.*, 2009), which have repeatedly changed their characteristics during

episodes of climatic change (*Trauth et al.*, 2003, *Trauth et al.*, 2005; *Garcin et al.*, 2009). Many of these basins hold lakes ranging from freshwater to alkaline in character, and these changes must have impacted paleo-environmental conditions and evolutionary patterns in a fundamental way. For example, the middle Miocene uplift of the EAP documented in our study correlates with an early expansion of C4 plants in East Africa at ~14 Ma (*Kingston et al.*, 1994; *Morgan et al.*, 1994; Fig. 2-7). In addition, *Retallack et al.* (1990) reported a change from grassy woodland to wooded grassland, based on fossil soils and grasses analyzed at the Miocene mammal fossil locality at Fort Ternan, western Kenya. *Jacobs* (2004) studied a grass-dominated savannah biome that began expanding in the middle Miocene (16 Ma), and became widespread during the late Miocene (~8 Ma), as documented by pollen and carbon isotopes from both West and East Africa (Fig. 2-7).

Taken together, the history of paleo-vegetation development in East Africa suggests a two-step evolution toward more pronounced dry conditions at the expense of rainforests at 16-14 Ma, and the expansion of grasslands at 8-7 Ma (*Jacobs*, 2004; Fig. 2-7). Based on our analysis, the first step toward increasingly arid conditions may have been linked with incipient uplift of the East African and Ethiopian plateaus prior to 13.5 and 20 Ma (*Pik et al.*, 2008), respectively. In contrast, the second shift towards a dominance of grassland vegetation may have taken place in response to the global decrease in pCO_2 (*Cerling et al.*, 1997; *Ségalen et al.*, 2007), possibly severed by the additional topographic effects of rifting, rift shoulder uplift, and volcanism.

The middle Miocene uplift of the East African and Ethiopian plateaus and coeval environmental changes also impacted radiation and speciation. For example, molecular phylogenetic studies have been performed on the evolutionary history of Pan-African lineages of the rainforest restricted plant family *Annonaceae*. The Pan-African clade of *Annonaceae* unravels a pattern in diversification of rainforest restricted trees occurring in West/Central and East African rain forests and provide strong evidence for diachronous origins (*Couvreur et al.*, 2008). Successive connection-isolation events between the

Guineo-Congolian rainforest and East Africa at ~16 Ma and ~8 Ma (*Couvreur et al.*, 2008; Fig. 2-7) temporally correlate with our interpretation of two-tiered environmental change due to plateau uplift prior to 13.5 Ma and global pCO_2 changes in late Miocene time (Fig. 2-7).

2.8 Model for East African Plateau uplift

Although poorly constrained, the evolution of the oldest major erosion surface in East Africa falls into the age range between 53 and 24 Ma and is attributed to the Africa Surface (*Burke and Gunnel*, 2008). This surface can be viewed as a basal reference surface, which was successively uplifted, and finally became an integral part of the East African Plateau (EAP). Arguments in support of such a surface in East Africa are (1) Miocene volcanic flows (e.g., Yatta Plateau) and lake deposits in the Kavirondo Gulf of Lake Victoria covering this erosional surface sculpted into basement rocks; (2) the volcanic rocks related to the regions encompassing Mount Elgon (20-22 Ma; *Walker et al.*, 1969) and Lake Turkana (18-16 Ma; *Joubert*, 1966) in western and northern Kenya, respectively, overlie an erosion surface in basement rocks (*Morley et al.*, 1992); and (3) paleo-drainage reconstructions by *King et al*. (1972) and *King* (1978) suggest that the Kenya Rift had developed along an ancient drainage divide, possibly uplifted during the Paleogene (*Smith*, 1994). Vestiges of the basement-cut erosion surface exist in form of broad interfluves or wide plateaus, such as the surface comprising the region across the Serengeti Plains at an elevation of 1,500 m (*Burke and Gunnel*, 2008).

In an active geodynamic setting, such as the East African Rift System (EARS), which has been affected by buoyant asthenospheric material and high heat flow since ~45 Ma (*Ebinger and Sleep*, 1998; Fig. 2-3), large temporal and spatial variations of geothermal gradients are to be expected when the disparate onset of volcanism and extensional faulting are taken into account. Therefore, the quantification of lithospheric warping due to a mantle anomaly and cones-

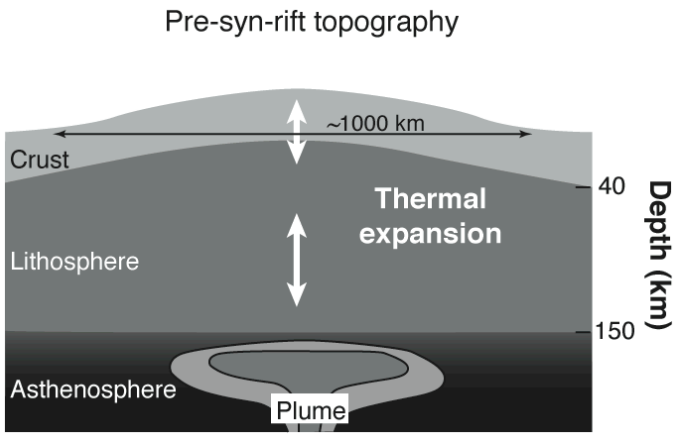

Figure 2-8. Thermal dilatation model for pre-rift plateau. The heating of a mantle plume affecting the East African lithosphere is inducing a volume change of the lithosphere and allowing a large-scale uplift of the East African Plateau.

quently uplift and deformation of geomorphic reference horizons is complex and depends on several parameters. While dimension, temperature, and density differences constitute main controlling factors between the plume, the surrounding asthenosphere, and the overlying lithosphere (e.g., *White and McKenzie*, 1989; *Moore et al.*, 1999), the mantle/crust strength ratio ("coupled crust-mantle" model) and the Moho temperature can also fundamentally influence the configuration of a domal uplift, rift segments, and the ensuing topographic response (*Gueydan et al.*, 2008). In this regard inherited crustal anisotropies could induce an asymmetric structure as observed in the East African Rift (e.g., *Smith and Mosley*, 1993; *Hetzel and Strecker*, 1994; *Tommasi and Vauchez*, 2001). However, based on the fact that the mantle plume below the Tanzania Craton not only give rise to the observed volcanism in the adjacent rifts but is also significantly interacting with the lithosphere and generate lithospheric uplift across the EAP (*Nyblade et al.*, 2000), *Koehn et al.* (2008) proposed that a component of thermal uplift is probably realistic and would add to the complexity of the rift system. As inferred from our study, the evolution of the EAP pre-rift topography reached an elevation of 1,400 m, represents a change of 1% thermal induced lithospheric expansion, and can be

interpreted as a large-scale surface expression caused by lithosphere-plume interactions (Fig. 2-8). While coeval regional-scale lithospheric folding (*Burov and Cloetingh*, 2009) may have triggered the reactivation of pre-existing Proterozoic structures straddling the Tanzania Craton, initial monoclinal flexures developed in the middle Miocene and fundamentally influenced the rifting process in East Africa.

2.9 Conclusion

Using a modeling approach involving the channelized and length-dominated phonolitic Yatta lava flow on the eastern Kenya Rift shoulder during its emplacement in middle Miocene time, we determine that this lava flow moved on a paleo-topography with a slope angle of 0.18-0.2°, originating at an elevation with a maximum elevation of 1,400 m. We conclude that this elevation corresponds to the middle Miocene elevation of the East African Plateau (EAP) in Kenya, which integrated a Paleogene erosion surface sculpted into basement rocks, dynamically uplifted due to plume-lithosphere interactions. Furthermore, topographic changes (in the order of 1,000 m) clearly affect moisture transport and spatial rainfall patterns and amounts. For this reason it is most likely that the uplift of the EAP and the formation of pronounced paleo-topography by middle Miocene time had a first-order impact on the evolution of the East African tropical climate. The timing of uplift is consistent with hydrologically induced vegetation shifts, such as the two-step expansion of grasslands at ~16 and ~8 Ma. In addition, the evolution of topography coincides with important radiation and speciation events.

Acknowledgements

This work was conducted in the Graduate School GRK1364 *Shaping Earth's Surface in a Variable Environment* funded by the German Research Foundation

(DFG), co-financed by the federal state of Brandenburg and the University of Potsdam. We thank the Government of Kenya (Research Permits MOST 13/001/30C 59/10) and the University of Nairobi for research permits and support.

CHAPTER 3

Emplacement of the mid-Miocene Yatta lava flow, Kenya: Implications for modeling long, channeled lava flows

Abstract

The emplacement of the 13.51-m.y.-old Yatta lava flow in Kenya has been investigated using evidence from field observations combined with a novel method of modeling length-dominated lava flows along channels. The Yatta lava erupted as an individual flow from a single vent on the eastern rim of the present-day East African Plateau during the extensive volcanism that occurred in mid-Miocene times. It then followed an old river valley for nearly 300 km, thus forming one of the longest phonolitic lava flows on Earth. For our modeling we combined a composition and temperature dependent viscosity equation with empirical cooling and morphological relationships. By using an average channel width and the known length of the Yatta lava flow but varying the mean thickness and underlying topography we have improved flow rate calculations for the internal part of the lava, close to the front of the lava flow. Within this zone the lava's motion was treated as steady, uniform, and laminar, following a stepwise cooling from the eruption temperature to the temperature at the cessation of flow. Comparison of eight different compositions ranging from basaltic to rhyolitic has revealed that the length-dominated Yatta lava flow emplacement was rapid (~15 days), approximately isothermal (cooling at 0.71 °C/km), and the result of high effusion rates (~7,900 m^3/s). This study shows that morphology of a lava flow, and in particular its length, is not a simple function of rheological properties and effusion rate, but is also affected by many other parameters. Small changes in H_2O compounds in the lava chemistry can affect melt viscosity significantly and thus lava flow morphology.

Therefore H_2O content, together with slope angle and the mean lava flow thickness, ultimately control the length of a lava flow within a channel.

3.1 Introduction

Numerous attempts have been made to understand the evolution of long (>150 km) channeled lava flows and the mechanisms that affect their propagation and distribution, both on Earth and on other planets of the solar system. Whether relying on empirical models (e.g., *Kilburn and Lopes*, 1991), laboratory experiments (e.g., *Hulme*, 1974; *Gregg and Fink*, 1996), or three-dimensional numerical simulations (e.g., *Miyamoto and Sasaki*, 1997; *Harris and Rowland*, 2001; *Del Negro et al.*, 2007), most of these studies have been based on comparisons between emplacement patterns and intra-flow structures, as well as textural and morphological data, either recorded from field observations or retrieved from final flow shapes by satellite imagery. Each of these approaches has been widely used to identify the major factors controlling the style of emplacement.

Understanding the relationships between final flow dimensions, lava rheology (e.g., viscosity) (e.g., *Hulme*, 1974; *Griffith*, 2000), composition (*Reidel*, 1998), effusion rate (e.g., *Walker*, 1973; *Wadge*, 1978; *Gregg and Fink*, 1996; *Harris and Rowland*, 2009), and the underlying topography (*Hulme*, 1974; *Miyamoto and Sasaki*, 1998; *Glaze and Baloga*, 2007) is critical for developing monitored forecasting for lava flows and for assessing the hazard potential from terrestrial effusive eruptions. For these reasons, the relationship between eruption conditions and lava morphology has become one of the most important fields of study in volcanology.

It is difficult to simultaneously control the large number of interdependent factors affecting lava flows (e.g., *Hulme*, 1974; *Wadge*, 1978; *Wilson and Head*, 1981; *Crisp and Baloga*, 1990; *Dragoni*, 1993; *Pinkerton and Wilson*, 1994). Because of this limitation, a majority of existing models are empirical in nature

and require many assumptions, which have generally resulted in over-simplifications in the models. *Gregg and Fink* (1996) specifically criticized the existing models for failing to take into account the relationships between viscosity, chemical composition, and cooling, stating that the results achieved to date are therefore only partly satisfactory. Nevertheless, empirical formulations can be very helpful in understanding the internal and external dynamics of lava flows in order to establish new correlations, as the most promising evidence comes from empirical analysis of flow dimensions (*Kilburn and Lopes*, 1991). The use of empirical models therefore remains appropriate and adequate, and may potentially give rise to new numerical models.

This study has combined different analytical lava flow models to quantify the effects of viscosity, cooling, chemical composition, effusion rate, and slope angle on long, channeled lava flows. Our subject area is the Yatta Plateau in Kenya, which lies to the east of the East African Plateau and has a length of 290 km, forming one of the Earth's most extensive phonolitic lava flows. Detailed studies of outcrops and stratigraphic relationships in erosional cuts into the lava flow, together with fluid dynamic analyses for different chemical compositions, have provided insights into emplacement variations and yielded information on flow advance that may be applied to other long, terrestrial lava flows or their planetary counterparts.

3.2 Regional setting

3.2.1 Yatta lava flow evolution

The total volume of effusive magma involved in the volcanic evolution of the Kenya Rift has been estimated to be 230,000 km^3 (e.g., *Williams*, 1982). The plateau phonolites represent the largest phase of volcanism with an estimated volume of 40,000-50,000 km^3 (*Lippard*, 1973) erupted between the middle and late Miocene (*Smith*, 1994; Fig. 3-1a). The largest volume of

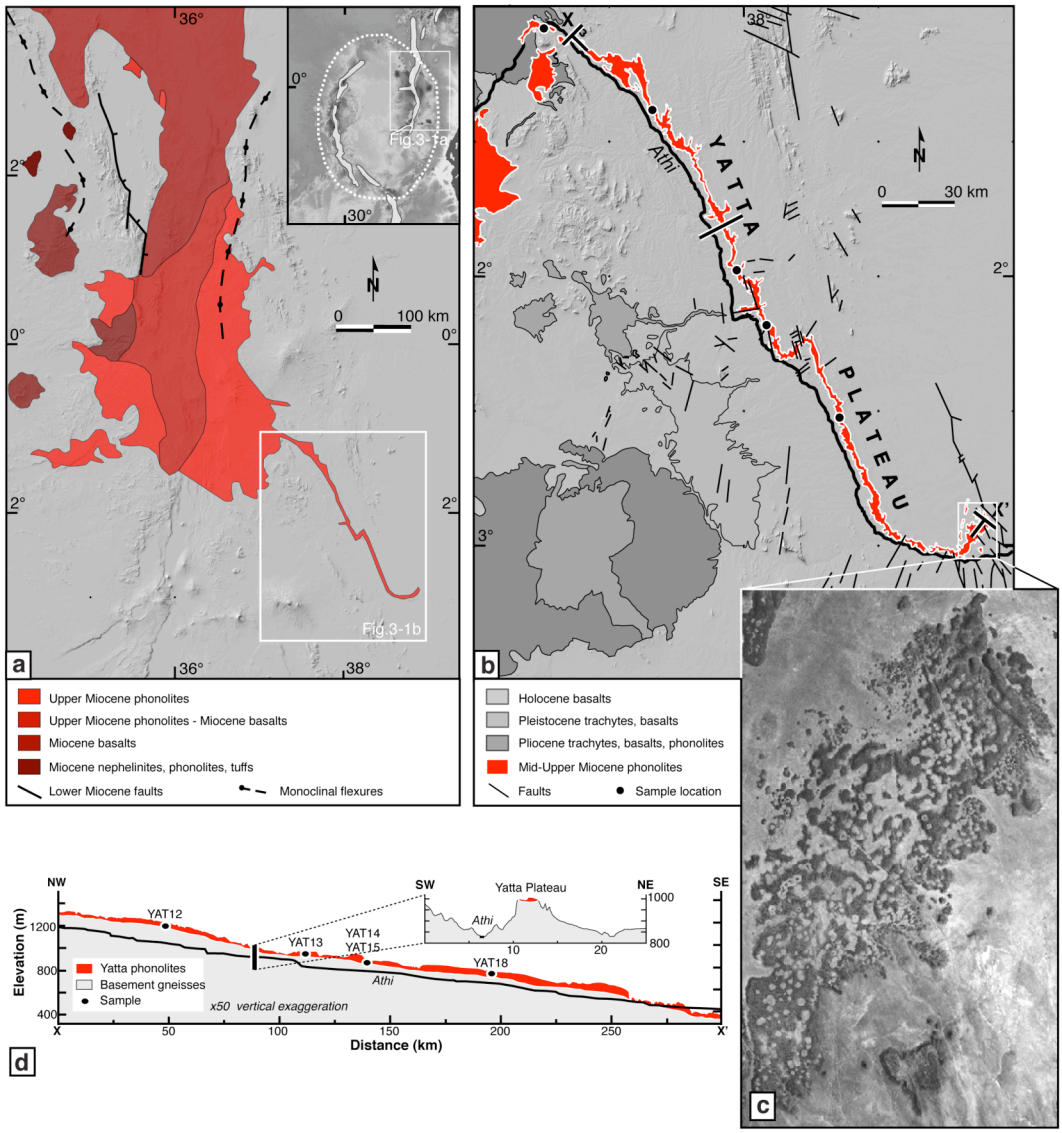

Figure 3-1. Geological setting and lava-flow characteristics. (a) Inset: overview map displaying topography of the present-day East African Plateau (white dashed line) and Cenozoic rifts (gray areas). Main geological map showing Miocene volcanism and faulting in Kenya set on present-day topography of Central Kenya (modified after Baker and Wohlenberg, 1971). White box outlines the Yatta Plateau geological map shown in Figure 3-1b. (b) Geological map showing the track of the Yatta lava flow, together with topographic features and lithologies corresponding to volcanic activity since the mid-Miocene. Small white box outlines the area of Figure 3-1c covering the end of the lava flow. The black lines designated X and X' denote the geological cross sections of the Yatta lava flow (Fig. 3-1d). (c) LANDSAT image showing phreatic structures in the area of flow stagnation. (d) Geological cross sections along the Yatta lava flow and present-day Athi River. Black circles mark the locations of phonolite samples collected (Table 3-1).

estimated volume of 40,000-50,000 km^3 (*Lippard*, 1973) erupted between the middle and late Miocene (*Smith*, 1994; Fig. 3-1a). The largest volume of phonolites appears to have erupted between 13 and 11 Ma (*Smith*, 1994), as indicated by their isotopic ages and broad spatial extent (e.g., *Baker and Wohlenberg*, 1971). *Lippard* (1973) reported individual flows with thicknesses ranging from a few tens of meters to as much as 270 m, emplaced over relatively short periods of time. One of the most prominent and spectacular flows attributed to the mid-Miocene plateau phonolites in Kenya is the Yatta lava flow. Its emplacement occurred at 13.51 Ma, as determined by K-Ar geochronology (*Veldkamp et al.*, 2007), which means that it was emplaced prior to the onset of rifting in Central Kenya between 10 and 8 Ma (e.g., *Smith*, 1994; *Chorowicz*, 2005).

The volcanic center of the Yatta phonolites is difficult to identify and remains speculative (*Williams and Chapman*, 1986). *Smith* (1994) inferred that the eruption was centered in the vicinity of the Sattima Fault. However, a volcanic source in the center of the region that now corresponds to the Kenya Rift is considered more likely as this would have made possible low-viscosity effusions with extensive overspill on the western and eastern margins of the present-day rift (*Lippard*, 1973). This plateau-type volcanism and the formation of a fluvial system that drained away from the plateau region to the Indian Ocean could thus have facilitated the formation of one of the longest phonolitic lava flows on Earth (Fig. 3-1b). Paleo-valleys and minor late Miocene faulting observed and recorded along the Yatta Plateau may represent the reactivation of ruptures in the crystalline Mozambique belt, related to the Azwa shear zone (*Chorowicz*, 2005). In addition, the eruption centers of Quaternary basalt flows are aligned along NNE-SSW trends and may similarly reflect pre-existing zones of crustal weakness, reactivated during the evolution of the Kenya Rift (*Pohl and Horkel*, 1980). Numerous phreatic structures visible on LANDSAT images suggest that the Yatta lava flow may have terminated in a lacustrine environment (Fig. 3-1c).

3.2.2 Yatta lava flow characteristics

The Yatta phonolitic flow followed an old riverbed that once conveyed runoff away from the eastern rim of the East African Plateau, and appears to have flowed along this channel for 290 km in a south-easterly direction to the Tsavo plains (e.g., *Walsh*, 1963; *Fujita*, 1977; *Wichura et al.*, 2010). Because of differential erosion, this lava flow now has a positive relief that stands above the parallel-flowing Athi River (*Fujita*, 1977), and mimics the course of the paleo-river (Figs. 3-1b and c).

The dimensions of the Yatta lava flow have been derived from satellite imagery (SRTM and LANDSAT) and field observations (Figs. 3-1 and 3-2). The observed thickness of the Yatta phonolites, from the basement contact to the flow-top remnants, ranges from 12 to 25 m (Fig. 3-2a). The maximum width ranges from 8 km in the northwest to 1 km in the far southeast. A compilation of 30 SW-NE topographic profiles (at ~10 km intervals along the flow) yielded estimates of the average flow width and slope angle. The average width of the flow remnant is estimated to be 3 km and along the eroded top of the flow there is an average gradient of 2.8 m/km. This correlates well with the average slope angle of 0.16° along the base of the paleo-valley, as determined from erosional cuts, and is also in good agreement with an earlier estimate by *Saggerson* (1963). Since the Yatta Plateau is very narrow in relation to its length and the ratio of maximal width to maximal length (W_m/L_m) is 0.028, it appears to be comprised of a single major flow (*Walsh*, 1963), namely S-type following the classification of *Kilburn and Lopes* (1991). Our field observations, as well as assessments by earlier workers (e.g., *Saggerson*, 1963; *Fujita*, 1977), also confirm that the Yatta lava flow did not result from either multiple volcanic eruptions or fissure eruptions along its axis.

Previous studies on the Columbia River Basalt (CRB) in the western U.S.A., the Deccan Volcanic Province (DVP) in India, and the island of Hawaii, have led to the conclusion that length-dominated lava flows are formed by the

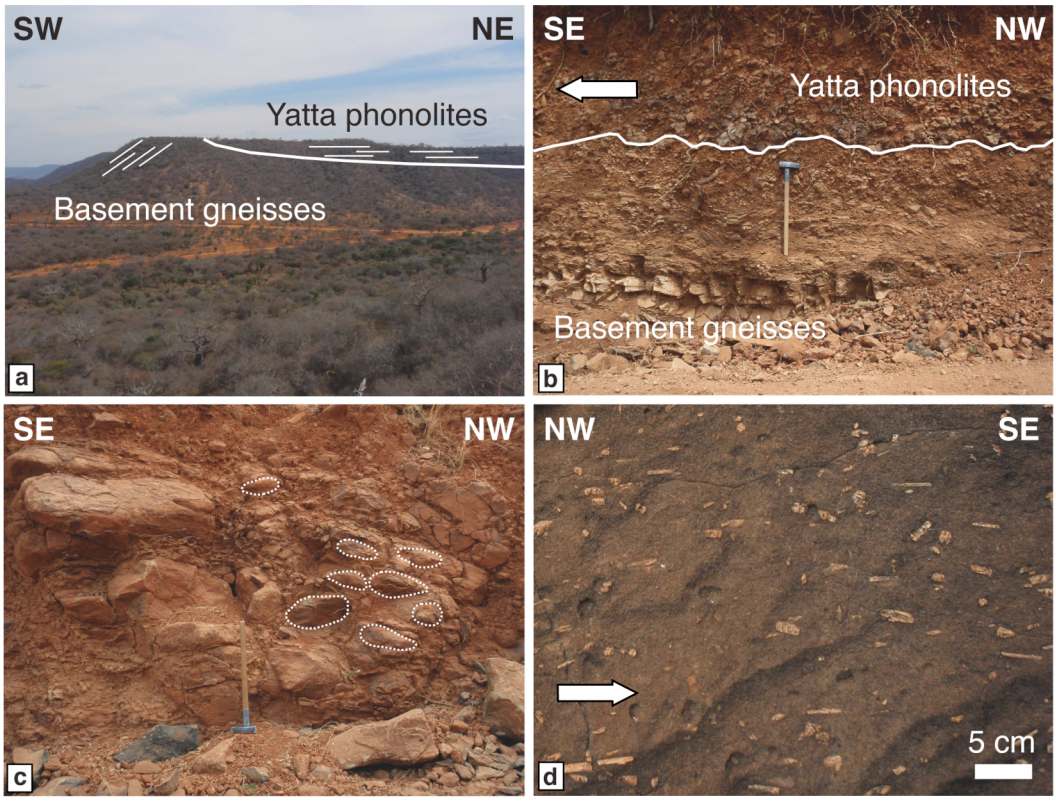

Figure 3-2. On-site field observations. (a) Photograph showing one of the erosion cuts and the paleo-valley occupied by the phonolites overlying a gneissic basement. (b) Outcrop showing contact between Yatta phonolites and basement gneisses (hammer for scale). (c) Phonolitic pillow lavas indicating the presence of water during emplacement in places (hammer for scale). (d) Detailed photograph of a typical Yatta phonolite showing aligned phenocrysts of anorthoclase, indicative of laminar flow. Direction of flow is indicated by the white arrow.

efficient delivery of lava through well-developed tube systems (e.g., *Self et al.*, 1996; *Bondre et al.*, 2004; *Harris and Rowland*, 2009). The efficiency of lava tubes in conveying turbulent-flowing lava over long distances and in minimizing (isothermal) cooling is well established and has been discussed in detail by *Keszthelyi* (1995), *Keszthelyi and Self* (1998), *Kauhikaua et al.* (1998), etc. The features associated with this particular type of flow are generally, however, easily discernable and include collapse pits, longitudinal cracks along the roof, and secondary vents, as have even been observed in analogous flows on the moon, Mars, and Venus (e.g., *Sakimoto et al.*, 1997; *Calvari and Pinkerton*, 1999). Porphyric rock textures due to turbulent flow, coated spatter fragments

generated by constant degassing, and inclined grooves on the internal wall remnants are also characteristic of many lava tubes (*Calvari and Pinkerton*, 1999), but no such features are evident in the Yatta phonolites.

For a detailed analysis of flow dynamics and the influence of chemical composition on the style of emplacement and final dimensions of the Yatta lava flow, we examined five separate localities with well-preserved flow sections (Table 3-1). The Yatta Plateau contains several fault-related erosional cuts perpendicular to the paleo-flow direction that provide access to the internal part of the flow (Fig. 3-2a). In these sections we observed evidence for laminar flow, in the form of feldspars aligned parallel to the flow direction in both the margins of the flow and its interior (Fig. 3-2d). Since turbulent flow would not allow the crystallization of aligned phenocrysts (e.g., *Bryan*, 1983; *Smith*, 2002) and no evidence for tube-fed flow has been identified, we interpret the Yatta lava flow to have been a channeled surface flow.

Fresh hand-specimens were collected from the above-mentioned sections, within the general trend of the flow (Figs. 3-1b and d; Table 3-1). The phonolites are fine-grained holocrystalline rocks with large white phenocrysts that are predominantly anorthoclase (up to 5 cm) and rarely nepheline (<1 cm), embedded in a grey-black aphanitic matrix (Fig. 3-2d). Where degassing vesicles are present they are filled with calcite and zeolites. Thin sections reveal that the main components of the holocrystalline matrix are flow-aligned feldspar prisms, nepheline, and zoned aegirine, accompanied by dark red-brown cossyrite, strongly pleochroic kataphorite, and minor iron ore (*Saggerson*, 1963).

Locally developed pillow lavas at the contact between the phonolites and the basement rocks suggest the presence of water during emplacement (Fig. 3-2c). It is interesting to note that despite all the different features suggesting emplacement in a paleo-drainage system, no fluvial sediments have been observed in the contact zone between the lava flow and the basement rocks. This phenomenon, however, may be explained by the thermal erosion effect of flowing lava (e.g., *Greeley et al.*, 1998).

Table 3-1. X-ray fluorescence major element chemistry for eight samples from the Yatta lava flow and seven further samples from different volcanic localities, with their bulk rock compositions taken from the literature. Major oxides in wt%.

Rock	Phonolite hydrous								
Locality	Yatta Plateau (KEN)								
Group									1
Sample	YAT12-4	YAT12-5	YAT13-1	YAT13-2	YAT14-2	YAT15-1	YAT15-2	YAT18-2	YAT_mean
Longitude	37°39.34'E	37°39.81'E	37°57.59'E	37°57.86'E	37°58.36'E	38°05.03'E	38'05.29'E	38°21.44'E	
Latitude	1°22.16'S	1°22.58'S	1°58.50'S	1°58.34'S	1°58.76'S	2°10.90'S	2°11.46'S	2°31.36'S	
SiO_2	54.60	54.80	54.30	53.50	55.20	54.30	54.30	54.80	54.48
TiO_2	0.80	0.83	0.81	0.81	0.80	0.82	0.82	0.82	0.81
Al_2O_3	19.00	19.10	19.10	19.20	19.00	18.90	19.00	18.60	18.99
FeO^T	5.49	5.72	5.60	5.90	5.53	5.63	5.54	5.56	5.62
MnO	0.25	0.27	0.25	0.45	0.25	0.25	0.23	0.24	0.27
MgO	0.90	0.86	0.80	0.81	0.88	0.81	0.89	0.80	0.84
CaO	2.16	1.44	1.45	1.74	1.33	1.45	1.83	2.04	1.68
Na_2O	7.33	7.57	8.06	6.51	7.42	8.25	6.43	6.43	7.25
K_2O	4.92	5.59	5.39	5.67	5.60	5.29	6.33	5.48	5.53
P_2O_5	0.27	0.29	0.26	0.28	0.27	0.28	0.32	0.29	0.28
H_2O	3.88	2.89	3.51	4.78	3.28	3.48	3.79	4.27	3.74
Total	99.60	99.36	99.53	99.65	99.56	99.46	99.48	99.33	99.50

Rock	Phonolite[1] hydrous	Phonolite[2] anhydrous	Basalt[3] anhydrous	Basaltic Andesite[4] hydrous	Andesite[5] anhydrous	Rhyolite[6] hydrous	Rhyolite[7] anhydrous
Locality	Vesuvius (ITA)	Teide (TEN)	Kilauea (HAW)	Mascota (MEX)	Unzen (JAP)	Waiti (NZ)	Ben Lomond
Group	1	2	1	1	2	2	2
Sample	V_1631_W	Td_ph	1921	MAS304	AndU0	OVCs7	BL6
SiO_2	53.52	60.46	50.01	52.66	56.65	75.22	77.48
TiO_2	0.60	0.56	2.60	1.00	1.01	0.25	0.17
Al_2O_3	19.84	18.81	12.56	17.40	17.41	13.53	12.20
FeO^T	4.80	3.31	10.79	6.62	8.16	1.81	1.30
MnO	0.14	0.20	0.24	0.12	0.13	0.08	0.05
MgO	1.76	0.36	9.39	5.14	4.30	0.38	0.17
CaO	6.76	0.67	10.88	8.07	7.38	1.63	1.14
Na_2O	4.66	9.76	2.33	4.32	3.23	4.17	3.90
K_2O	7.91	5.45	0.48	1.71	1.56	2.89	3.60
P_2O_5	0.00	0.06	0.00	0.42	0.00	0.04	0.00
H_2O	3.32	0.00	0.00	1.01	0.00	0.79	0.00
Total	103.31	99.64	99.28	98.47	99.83	100.79	100.01

[1] *Romano et al*., (2003); [2] *Giordano et al*. (2000); [3] *Kushiro et al*., (1976); [4] *Lange and Carmichael*, (1990); [5] *Liebske et al.*, (2003)
[6] *Stevenson et al*. (1994); [7] *Stevenson et al*., (1998)

3.3 Methodology and basic assumptions

3.3.1 Rheology

Lava flows behave as either Bingham or Newtonian fluids, which are rheologically characterized by plastic or dynamic viscosities, respectively (e.g., *Griffith*, 2000), depending on the initial yield strength required for fluidization. The rate of flow advance is largely controlled by the rheological conditions in the rear frontal zone (RFZ; Fig. 3-3) - that part of a flow between its convex-curved outer front and its established channel structure upstream (*Lopes and Kilburn*, 1990; *Kilburn and Lopes*, 1991). This zone is assumed to be characterized by isotropic, non-fractionated conditions and a uniform density (e.g., *Lopes and Kilburn*, 1990; *Tallarico and Dragoni*, 1999). Because of the low deformation rates in the RFZ (*Lopes and Kilburn*, 1990), we have followed the approach by *Tallarico and Dragoni* (1999) and assumed that the behavior of the lava approximated that of an isothermal Newtonian liquid, flowing in a channel with a rectangular cross section. This channel simulates a model-based shape of the Athi paleo-valley, which was occupied by the Yatta lava flow along an inferred constant slope angle β (Fig. 3-3, after *Tallarico and Dragoni*, 1999).

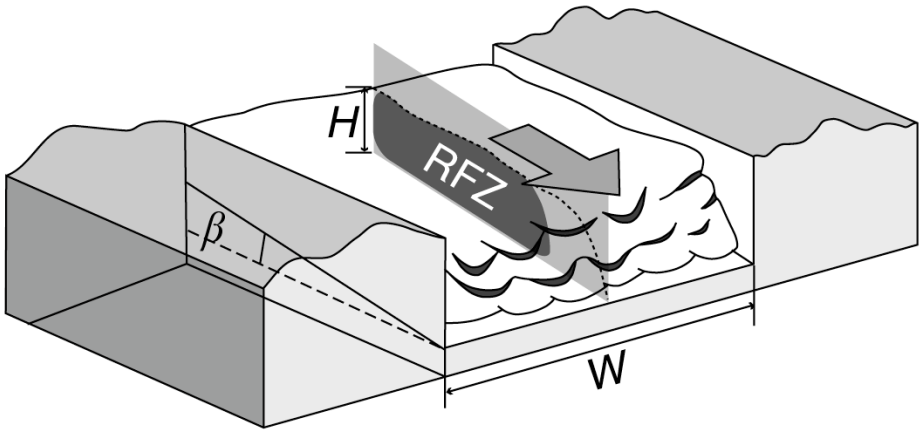

Figure 3-3. Rear frontal zone (RFZ) in the simulated lava-flow channel, showing relevant parameters used for modeling. Arrow indicates flow direction (modified after *Tallarico and Dragoni*, 1999).

Table 3-2. Morphological data for the Yatta lava flow, various rock properties, and physical and empirical constants used to calculate rheologic parameters with equations (3-1 to 3-7).

Parameter	SI-unit	Value	Reference
Yatta lava flow			
Length (L)	m	290000	SRTM and ASTER images
Width (W)	m	3000	averaged over L
Phonolite			
Density (ρ_{Ph})	kg/m^3	2400	*Martin and White* (2002)
Thermal diffusivity (k_{Ph})	m^2/s	3.5 x 10^{-7}	*Martin and White* (2002)
Eruption temperature ($T_{n=0}$)	°C	870	*Ablay* (1995)
Basalt			
Density (ρ_{Bl})	kg/m^3	2700	*Hoskuldsson and Sparks* (1997)
Thermal diffusivity (k_{Bl})	m^2/s	8.3 x 10^{-7}	*Hoskuldsson and Sparks* (1997)
Eruption temperature ($T_{n=0}$)	°C	1150	*Williams and McBirney* (1979)
*Andesite**			
Density (ρ_{An})	kg/m^3	2600	*Couch et al*. (2001)
Thermal diffusivity (k_{An})	m^2/s	8.0 x 10^{-7}	*Couch et al*. (2001)
Eruption temperature ($T_{n=0}$)	°C	900	estimated Magma temperature
Rhyolite			
Density (ρ_{Rv})	kg/m^3	2200	*Couch et al*. (2001)
Thermal diffusivity (k_{Rv})	m^2/s	7.5 x 10^{-7}	*Couch et al*. (2001)
Eruption temperature ($T_{n=0}$)	°C	850	overestimated Magma temperature
Constants			
Gravity (g)	m/s^2	9.81	
Graetz number (G_z)	dimensionless	300	
a	dimensionless	3	*Booth and Self* (1973)

*the same material properties have been used for basaltic andesites

The solution for viscous flow in a channel with a width W and a thickness H can be obtained from modeling a rectangular conduit filled to the same width but with a double thickness (e.g., *White*, 1991). The channel dimensions used in our model were the average Athi paleo-valley width (3 km) and lava thickness (12-25 m) over its entire 290 km length (Table 3-2). Downstream variations in width or slope angle can clearly affect the hydraulics of the velocity field; in this case the one-dimensional model is an approximation at a single cross section, thus assuming laminar flow along the flow axis (*Tallarico and Dragoni*, 1999) (Fig. 3-3). Furthermore, we considered the lava flow from its eruption temperature close to the vent, where the lava had not yet developed a significant yield strength and thus could be treated as a Newtonian liquid (*Pinkerton and Stevenson*, 1992; *Dragoni and Tallarico*, 1994). We retained this

assumption of Newtonian flow along the entire length of the flow, despite the subsequent cooling, because it is not yet known at which temperatures the flow laws would have changed to Bingham rheology.

3.3.2 Viscosity

The viscosity of a lava is one of the major factors controlling lava-flow morphology (*Glaze and Baloga*, 2006; *Riker et al.*, 2009). After lava effuses from a vent, it cools. In response to this cooling and consequent crystallization, the viscosity increases and the velocity decreases. Degassing may also affect lava viscosity significantly because decreasing volatile (especially water) content can increase melt viscosity. However, because the rheology and cooling are too complex to be modeled accurately, most of the previous analytical studies on lava flows have regarded the viscosity as constant and modeled the lava separately as either a Bingham or a Newtonian liquid.

In our research we have applied the empirical viscosity equation from *Hui and Zhang* (2007), which allows the calculation of viscosity for anhydrous and hydrous natural silicate melts over a wide temperature range, such as during magma chamber processes and volcanic eruptions. This equation, in its most simplified form, is given by:

$$\log \eta = A + \frac{B}{T} + \exp\left(C + \frac{D}{T}\right), \tag{3-1}$$

where η is the viscosity, T is the temperature in K, and A, B, C, and D are linear functions comprising the mole fractions of oxides and another term related to H_2O (*Hui and Zhang*, 2007). The mole fraction for water is integrated in D and combined with an internal temperature dependence. The 2σ deviation of this fit is 0.61 $\log\eta$ units. The original publication by *Hui and Zhang* (2007) provides a general description of viscosity, including the parameters A, B, C, and D, and its 37 statistically significant fitting parameters (see Appendix).

3.3.3 Composition

The dependence of viscosity on chemical composition has been extensively studied as a control on the internal and external mobilities of lavas, both from a theoretical point of view and from numerous laboratory measurements (e.g., *Bottinga and Weill*, 1972; *Persikov*, 1998; *Whittington et al.*, 2000; *Giordano and Dingwell*, 2003; *Liebske et al.*, 2003; *Hui and Zhang*, 2007). Variations in the SiO_2 content in particular may play an important role in the viscosity of melt because Si-O bonds promote high degrees of polymerization, which reduces lava mobility (*Hulme and Fiedler*, 1977; *Carrasco-Núñez*, 1997). Whereas crystallization may cause an increased bulk viscosity (*Marsh*, 1981), the water content may contribute to a reduction in the degree of polymerization of the melt by breaking Si-O-Si bridges (*Carrasco-Núñez*, 1997). This effect of water content can be lost during degassing processes. A direct correlation between these dependencies is not clear for the Yatta lava flow, partly because its composition and water content are homogenous along the entire flow length, so that the variation of major elements is very limited (Table 3-1). We therefore created a synthetic sample (YAT_{mean}) to represent the full chemical range of phonolites related to the Yatta Plateau eruptions, and used it for subsequent calculations and comparisons. This sample is an averaged of the oxide components of all Yatta samples (Table 3-1).

Inspired by the idea that the integration of different lava compositions into our model may help to derive large-scale terrestrial lava morphologies from their compositions, or conversely to estimate lava compositions from final lava-flow dimensions on other planets of the solar system, we extended our studies to include other compositions for the sake of comparison. For this purpose we took bulk compositions from six different volcanic sites covering the range of hydrous and anhydrous terrestrial lava types with varying silica content: phonolite (Vesuvius and Teide), basalt (Kilauea), basaltic andesite (Mascota), andesite (Unzen), and rhyolite (Waiti) (Table 3-1), and an additional bulk rock

composition taken to be representative of an anhydrous rhyolite (Ben Lomond dome; *Stevenson et al.*, 1998).

3.3.4 Velocity and cooling

As mentioned in the rheology section, we have modeled the lava-flow advance from the vent to the achievement of its final form. To achieve this we defined a stepwise (n) cooling process with ΔT=10 °C, starting from the eruption temperature for the particular lava composition under consideration. The eruption temperatures of magmas are difficult to measure, but eruption temperatures ($T_{n=0}$) of various lavas, based on laboratory measurements and limited field observations, are shown in Table 3-2. The viscosity of a given flow may increase markedly with subsequent crystallization as the lava cools. This gradual increase in viscosity η of a lava during the cooling process corresponds to the stepwise decrease in rear frontal velocity v_n following Jeffreys' equation (*Jeffreys*, 1925), expressed by:

$$v_n\left(T_n, X_i\right) = \frac{H^2 g \rho \sin\beta}{a\eta_n\left(T_n, X_i\right)}, \tag{3-2}$$

where H is the mean lava-flow thickness, g is the gravitational acceleration on Earth, ρ is the rock density, β is the slope angle of the underlying topography, a is 3 as suggested by *Booth and Self* (1973) for channels that are wide relative to their depth, and η_n is the viscosity computed with equation (3-1), and X_i are mole fractions of oxide component i. We computed the rear frontal velocity for each cooling step n and designed the simulation to finish when no further flow advance could be recognized, i.e. when cooling forced the velocity to drop below 0.01 m/s. The corresponding temperature for that step (index n=x) was the final cooling temperature ($T_{n=x}$) that was used to quantify cooling rates by the ratio of $\Delta T_{0\text{-}x}/L$, where $\Delta T_{0\text{-}x}$ is the difference between $T_{n=0}$ and $T_{n=x}$.

3.3.5 Effusion rate and emplacement time

In order to evaluate the time taken by the RFZ of the Yatta lava flow to reach its final position, we used an estimate of the effusion rate F (the flux of lava expressed by the volume of effused material per unit of time), given approximately by:

$$F = WH\overline{V}, \tag{3-3}$$

where W is the mean flow width, H is the mean flow thickness, and V-bar is the mean velocity of the RFZ (the sum of all v_n divided by n cooling steps). We also assumed a constant production rate of the material at the vent. Estimates of the emplacement time (t_{em}) were obtained using the Graetz model, an empirical conduction-limited cooling model in which lava-flow cooling is compared to the heat loss of a hot fluid moving through a cool conduit (*Pinkerton and Sparks*, 1976; *Hulme and Fiedler*, 1977; *Carrasco-Núñez*, 1997). The heat advection within the flow along its length is described by the dimensionless Graetz number (G_Z) and given by:

$$G_Z = \frac{H^2\overline{V}}{kL}, \tag{3-4}$$

where k is the thermal diffusivity, and L is the length of the lava flow (*Carrasco-Núñez*, 1997). It has been empirically determined that lava flows come to rest before G_Z falls to about 300 (*Carrasco-Núñez*, 1997). Solving equation (3-3) for velocity gives an effusion rate, which is exclusively dependent on morphological parameters and the thermal properties of the rock (*Carrasco-Núñez*, 1997):

$$F = \frac{G_Z WLk}{H} \tag{3-5}$$

Hence, the emplacement time t_{em} can be expressed as:

$$t_{em} = \frac{L}{\overline{V}} \tag{3-6}$$

Solving equation (3-6) for *V*-bar and substituting in equation (3-4) then allows the formula for the emplacement time to be rewritten as:

$$t_{em} = \frac{H^2}{G_Z k} \tag{3-7}$$

Since the Graetz number model assumes a continuous, steady state eruption, the emplacement time generally tends to be underestimated, as has been pointed out by *Carrasco-Núñez* (1997).

Finally, we modeled the lava flow in two ways, by (1) predefining a fixed thickness and calculating how far the lava would flow, and (2) assuming the present lava-flow length and estimating the required mean thickness, in order to simultaneously compute the mean frontal velocity and the effusion rate. In addition, we calculated the mean thickness and length in both simulations, as a function of the underlying topography (*Wichura et al.*, 2010).

3.4 Results

3.4.1 Viscosity development with cooling

The fact that the viscosity of silicate melts depends on both temperature and chemical composition always raises the question of whether the melt has an Arrhenian or non-Arrhenian behavior (*Hui and Zhang*, 2007). Whereas the Arrhenian equation fits quite well for narrow temperatures ranges and viscosities of between 0.1 and 10^4 Pa s, non-Arrhenian empirical formulations are better able to describe viscosity variations for larger temperature ranges. As we follow the advance of large-scale lava flows from their vents to their final

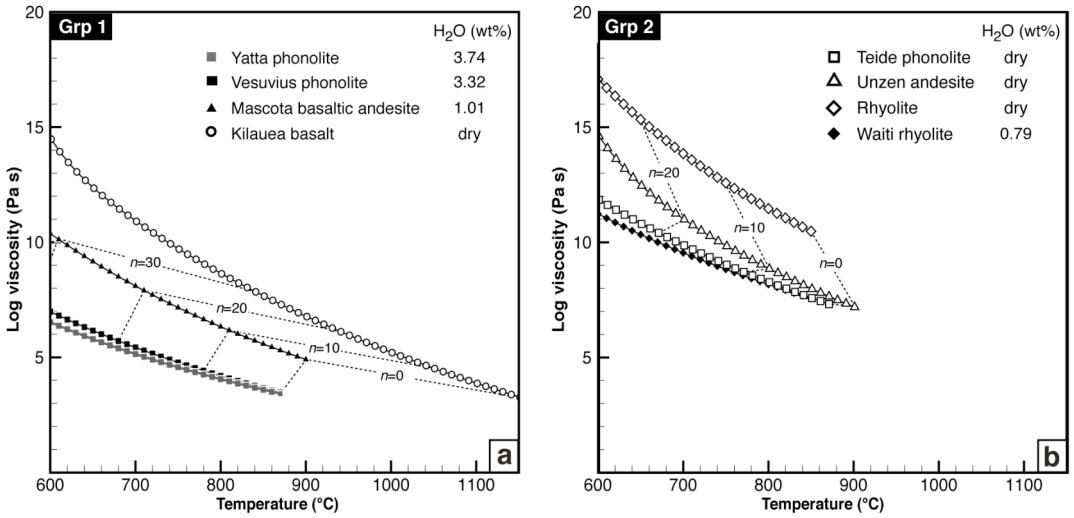

Figure 3-4. Viscosities as a function of temperature and composition, calculated with the *Hui and Zhang* (2007) model, for the low-viscosity Group 1 (a) and high-viscosity Group 2 (b). Cooling steps are represented by *n*, where *n*=0 is representative of the eruption temperature (Table 3-2). Symbols indicate different lava compositions (hydrous: filled; anhydrous: un-filled). 2σ for calculated viscosities is 0.61 logη units.

extent, the viscosity changes that we encounter are basically temperature controlled. The viscosity as shown in equation (3-1) therefore appears well suited for application in our model, integrating a compositional dependency and valid over the full temperature range under consideration (600-1,150 °C).

Starting from the eruption temperature (Table 3-2), equation (3-1) gives viscosities for each of the chemical compositions investigated (Table 3-1) for each of *n* temperature steps. Hydrated phonolites from the Yatta lava flow and from Vesuvius have viscosities generated with equation (3-1) of 3.6 x 10^3-6.0 x 10^6 Pa s and 2.9 x 10^3-9.7 x 10^6 Pa s, respectively, for the cooling interval between 870 °C and 600 °C (*n*=27). Similarly, for an anhydrous basalt from Kilauea using the same number of steps but starting from a higher eruption temperature of 1,150 °C, the model generates viscosities in the range of 1.9 x 10^3-1.3 x 10^7 Pa s (Fig. 3-4a). Higher initial and final viscosities of 8.1 x 10^4 Pa s at 900 °C and 2.4 x 10^8 Pa s at 600 °C were calculated for a hydrated basaltic andesite from Mascota. Figure 3-4a shows that all viscosity values calculated for these compositions are low because of their low silica and/or water content (except for the Kilauea basalt).

In contrast, dry chemical compositions within the same temperature range are generally more viscous than their hydrous equivalents. For example, at 870 °C, an anhydrous phonolite from Teide has a viscosity that is 5 orders of magnitude higher (2.1×10^7-7.4×10^{11} Pa s) than the phonolites from the Yatta Plateau and Vesuvius. Modeled viscosities for rhyolites show a similar range of lower viscosities for hydrous lavas (Fig. 3-4b). While the viscous evolution for a hydrated rhyolite from Waiti is similar to that for a dry phonolite, with a viscosity ranging between 3.7×10^7 Pa s at 850 °C and 1.8×10^{11} Pa s at 600 °C, an anhydrous rhyolite shows the highest viscosity values of all compositions studied, ranging from 3.1×10^{10} to 1.2×10^{17} Pa s for an identical cooling path (850 to 600 °C; Fig. 3-4b). Interestingly, a dry andesite at 900 °C shows a viscosity of 1.6×10^7 Pa s, which is comparable with the values that were calculated for a dry phonolite (Fig. 3-4b). The negative slope of this graph, however, increases more rapidly and finally reaches a value of 4.1×10^{14} Pa s at 600 °C, which is of the same order of magnitude as a dry rhyolite at 670 °C (Fig. 3-4b).

Taken together, Figure 3-4 clearly shows that when the number of cooling steps increases the trend to higher viscosities is maintained (to varying degrees) for all bulk compositions.

3.4.2 Velocity of the RFZ and cooling rates

As a lava cools, the viscosity eventually becomes so high that it cannot generate any further advance in the RFZ and the lava flow comes to a halt. In our model the temperature at which this occurs is different for each chemical composition, and is dependent on both the mean lava-flow thickness and the underlying slope angle.

Figure 3-5 shows velocity profiles for the RFZ in lava flows of different compositions as cooling proceeds, indicating the constraints (mean thickness, slope angle, and bulk composition) under which these theoretical lava flows

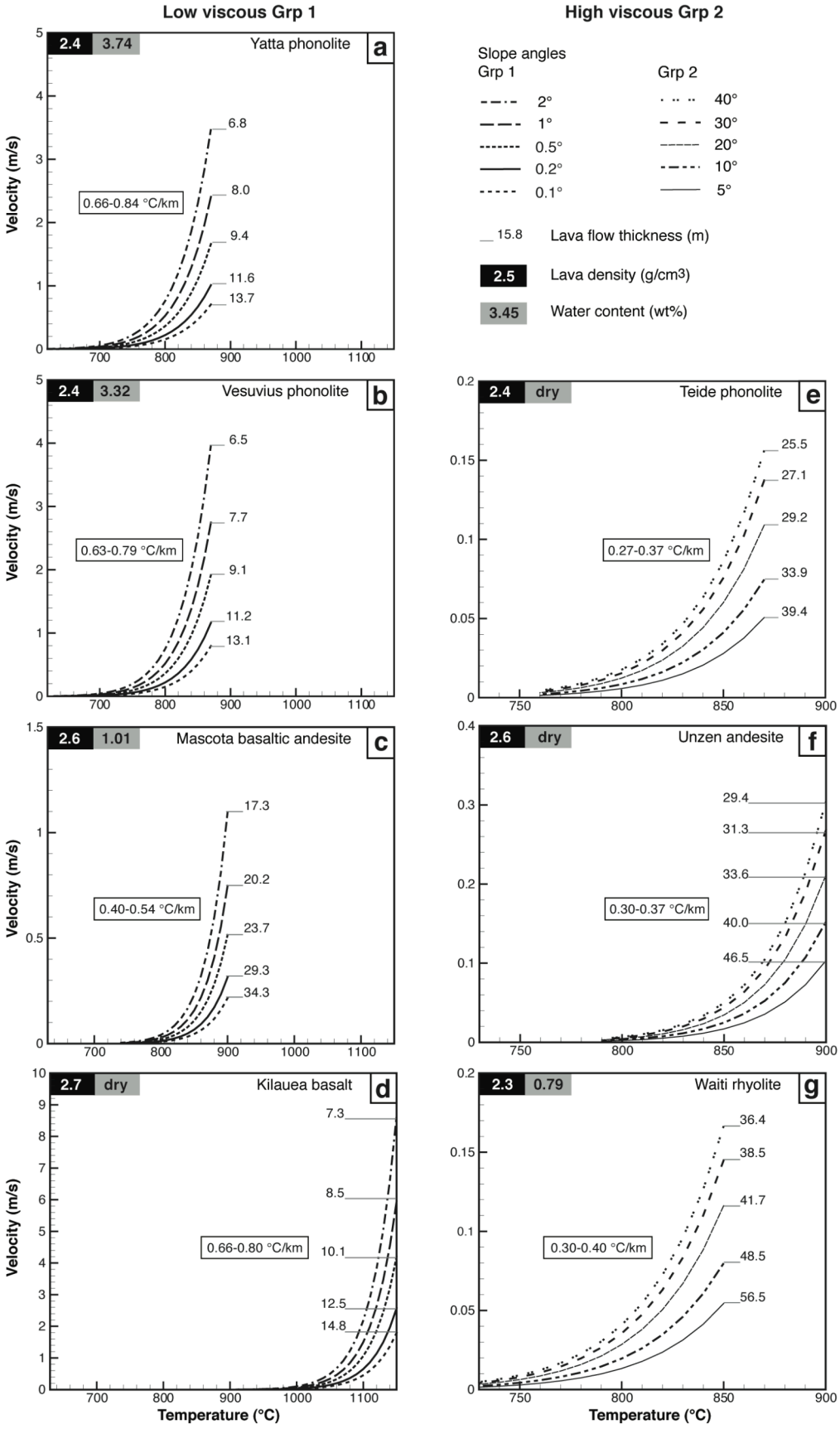
Low viscous Grp 1
High viscous Grp 2
Slope angles
Grp 1
Grp 2
2°
1°
0.5°
0.2°
0.1°
40°
30°
20°
10°
5°
15.8 Lava flow thickness (m)
2.5 Lava density (g/cm3)
3.45 Water content (wt%)
2.4 3.74 Yatta phonolite a
0.66-0.84 °C/km
6.8
8.0
9.4
11.6
13.7
2.4 3.32 Vesuvius phonolite b
0.63-0.79 °C/km
6.5
7.7
9.1
11.2
13.1
2.6 1.01 Mascota basaltic andesite c
0.40-0.54 °C/km
17.3
20.2
23.7
29.3
34.3
2.7 dry Kilauea basalt d
0.66-0.80 °C/km
7.3
8.5
10.1
12.5
14.8
2.4 dry Teide phonolite e
0.27-0.37 °C/km
25.5
27.1
29.2
33.9
39.4
2.6 dry Unzen andesite f
0.30-0.37 °C/km
29.4
31.3
33.6
40.0
46.5
2.3 0.79 Waiti rhyolite g
0.30-0.40 °C/km
36.4
38.5
41.7
48.5
56.5
Velocity (m/s)
Temperature (°C)

Figure 3-5. Rear frontal velocity profiles as a function of temperature, mean thickness, slope angle, and chemical composition for low-viscosity Group 1 (a-d; left panel) and high-viscosity Group 2 (e-g; right panel). Different slope angles are indicated by different styles of line. White boxes label ranges of cooling rates according to the composition. Every profile represents the parameter determining the conditions under which the Yatta lava flow dimensions can be achieved.

would reach the morphological parameters of the Yatta lava flow, in particular the length of 290±10 km. The modeling revealed that the differences in chemical character, and hence in viscosity, of the studied compositions had an enormous effect on the rear frontal velocity development as well as on the emplacement time. We therefore split the samples into two groups. Group 1 consisted of hydrated phonolite, basaltic andesite, and basalt and was characterized by low viscosity, short emplacement times (of the order of days), and very gentle slopes (0.1-2°). Group 2 included dry phonolite, andesite, and rhyolite, which required higher viscosities, longer emplacement times (of the order of months), and steeper topographic slope angles (5-40°) in order to attain the final dimensions of the Yatta lava flow.

However, modeling a mean lava-flow thickness of between ~6 and 8 m (for β=2°) and between ~13 and 15 m (for β=0.1°) for Group 1, produced differences in the velocity profiles for hydrated phonolites and anhydrous basalt (Fig. 3-5). For hydrous phonolites we calculated velocities of 0.7-3.5 m/s at their eruption temperature and a final temperature for cessation of flow of 630-670 °C (Figs. 3-5a and b). The calculated initial velocity for the basalts was generally higher (1.8-8.6 m/s) and their flow ceased at 910-950 °C (Fig. 5d). The initial propagation velocity for the hydrated basaltic andesite was computed to be 0.2-1.1 m/s for a mean thickness of ~17-35 m, with the cessation of flow occurring at a temperature of 740-780 °C (Fig. 3-5c).

The velocities for Group 2 were consistently lower and the corresponding calculated thicknesses (~25-36 m for β=40° and ~39-57 m for β=5°) were higher than for Group 1, regardless of whether the composition was anhydrous phonolitic, andesitic or hydrous rhyolitic (Fig. 3-5). Furthermore, the initial velocities at temperatures between 850 and 950 °C were modeled markedly

lower (of the order of ~0.1-0.3 m/s) and the cessation of flow occurred at temperatures up to 90 °C higher than for the low-viscosity group (Fig. 3-5). Due to the high viscosities of the anhydrous rhyolite from the Ben Lomond dome, it was not possible to calculate a velocity development for this composition.

Estimated cooling rates for the low-viscosity Group 1 ranged between 0.40 and 0.84 °C/km, compared to between 0.27 and 0.40 °C/km for the high-viscosity Group 2 (Fig. 3-5).

3.4.3 Effusion rates and mean thickness

For a better understanding of the flow development of the Yatta plateau phonolites and the other compositions investigated, it was important to know how distinct lava flows formed and how the effusion rate affects the length of channeled flows. We calculated the effusion rates for each lava composition from equation (3-5) and used these figures to model the maximal flow length for each lava type. Because equation (3-5) is comprised solely of geometrical constants (width, length, and mean thickness), the empirical G_Z number, and the thermal rock properties (thermal diffusivity; Table 3-2), we calculated the effusion rates as a function of the mean thickness. The mean thicknesses have been mentioned in the previous section, where they were related to different slope angles (Figs. 3-5 and 3-6). Their required estimates again derive basically from the simultaneously employed mean frontal velocity calculations of equation (3-2) and the effusion rate calculations of equation (3-5). The effusion rates, mean thicknesses, and corresponding slope angles considered indicated the conditions under which theoretical lava flows would reach the final dimensions of the Yatta lava flow (Figs. 3-7 and 3-8). Calculated effusion rates ranged between 1,100 and 3,600 m^3/s for the Teide phonolite, and between 14,500 and 29,900 m^3/s for the Kilauea basalt (Fig. 3-6). Our data showed that greater mean lava-flow thicknesses require lower effusion rates and more gentle underlying topography to attain the required flow dimensions.

Our data fit lava compositions according to the thermal diffusivities used for

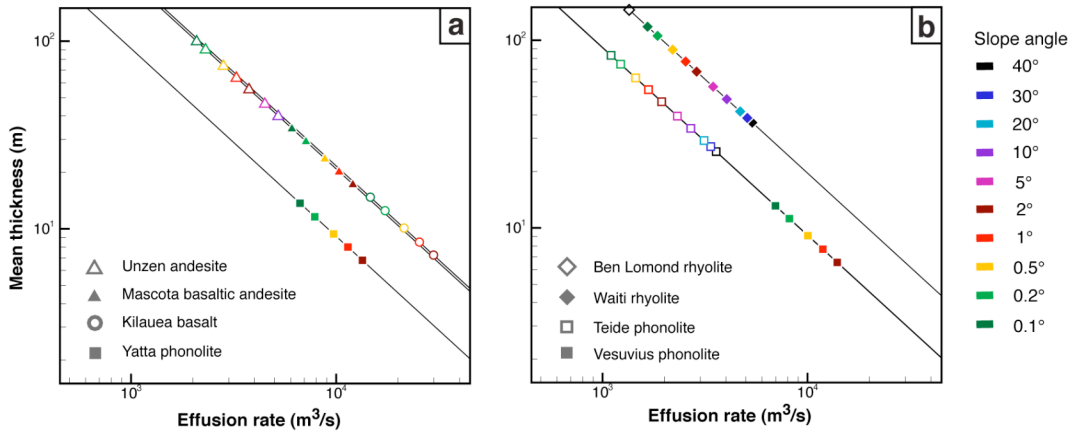

Figure 3-6. Mean thickness as a function of effusion rates and chemical compositions. Displayed mean thicknesses represent the conditions under which the Yatta lava flow dimensions can be achieved (Figs. 3-5 and 3-7). Different fitting lines correspond to different assumed diffusivities (Table 3-2). Hydrous lava compositions are represented by filled symbols, anhydrous lava compositions by un-filled symbols.

the model (Table 3-2). In this respect phonolites, andesites/basaltic andesites, and rhyolites plot on fitting lines corresponding to their thermal properties regardless of their origins and compositions (Fig. 3-6). However, effusion rates show a correlation with the water content: the lower the H_2O component, the lower the calculated effusion rate. For example, whereas the effusion rates for an anhydrous Teide phonolite lay between 1,100 and 3,600 m^3/s (for slope angles of between 0.1 and 40°), calculations for the hydrous Yatta phonolite (3.74 wt% H_2O and reduced thickness of 6.8-13.8 m; Table 3-1 and Fig. 3-6) yielded effusion rates of between 6,700 and 13,400 m^3/s (for slope angles between 0.1 and 2°; Fig. 3-6).

3.4.4 Emplacement time and maximal length

One of the main questions to be addressed by the modeling was how long it would take to emplace a lava flow of a given dimension down a gentle slope. Since our model was designed to have three degrees of freedom (viscosity, thickness, and slope angle) - see equation (3-2) - we first tested the maximum varying the slope angles for the different compositions with a fixed mean

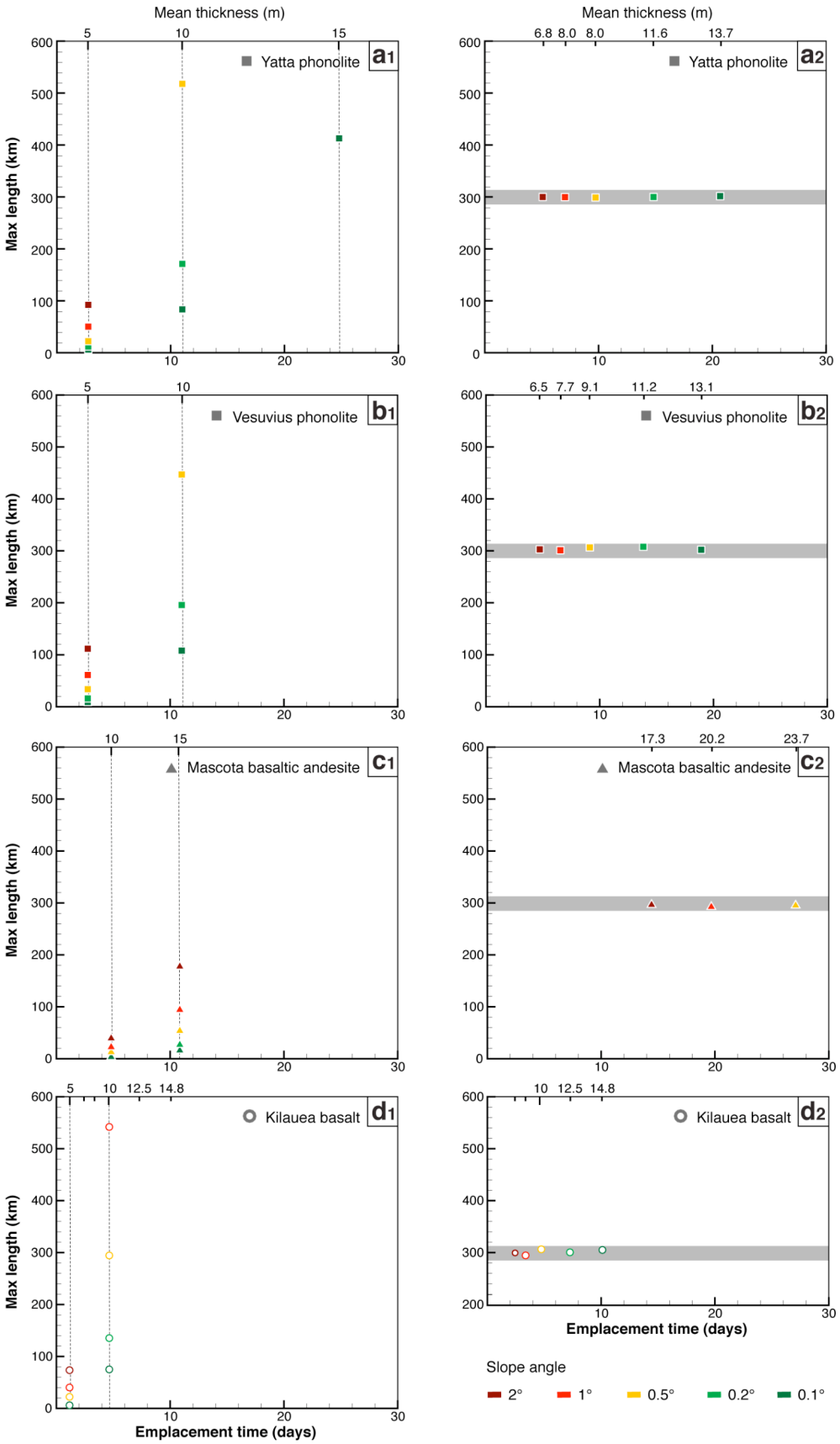
Mean thickness (m)
Yatta phonolite
a1
a2
Vesuvius phonolite
b1
b2
Mascota basaltic andesite
c1
c2
Kilauea basalt
d1
d2
Max length (km)
Emplacement time (days)
Slope angle
2°
1°
0.5°
0.2°
0.1°

Figure 3-7. Maximal lava-flow length as a function of emplacement time, mean thickness, slope angle, and chemical composition for low-viscosity Group 1. Dashed vertical lines indicating emplacement time calculated with a predefined fixed mean thickness (5, 10, and 15 m) and the corresponding maximal lava-flow length (a_1-d_1; left panel). Horizontal gray bar displays the present-day Yatta lava flow length (290±10 km; a_2-d_2; right panel). Plotted symbols on that bar correspond to the modeled thickness and emplacement time for the respective color-coded slope angles. As in all previous figures, symbols for hydrous lava compositions are filled and those for anhydrous compositions are un-filled.

thickness (5 m, 10 m, and 15 m). The emplacement time is equal to those described in equations (3-6) and (3-7) and therefore will always be the same for each particular mean thickness (Fig. 3-7). As an example we compared the results for the hydrated Yatta phonolite with those for the dry Kilauea basalt within Group 1.

The emplacement time for the phonolite (represented by the vertical data points in Figure 7) was ~2.5 and ~25 days for mean thicknesses of 5 m and 15 m, respectively (Figs. 3-7a_1 and b_1), while for the basalt it was lower, at ~1 day and ~4.5 days for mean thicknesses of 5 m and 10 m, respectively (Fig. 7d_1). This internal form of fixed parameter reduces the degrees of freedom to one (the slope angle) and renders calculation of the potential maximum flow length possible. Specifically, for a 10 m thick phonolitic lava flow we computed a length of between ~86 km (β=0.1°) and ~645 km (β=1°; Figs. 3-7a_1 and b_1). Although the rheological properties of a basaltic lava should allow much longer flows, the maximum length for a basaltic lava flow with the same thickness (10 m) and variation of slope angle (0.1-1°) is between ~75 and ~541 km, and therefore shorter than for the phonolitic flow (Fig. 3-7d_1). As an experiment we added 0.5 wt% H_2O to the original anhydrous basaltic composition. Between 1,150 and 1,050 °C (n=10) this small change in water content reduced the viscosity by about two orders of magnitude (1.9×10^2-2.6×10^3 Pa s) and generated a rear frontal velocity at the vent of v_0=8.3 m/s (for β=0.1°).

Calculation of emplacement time and maximum length within the group of higher viscosities is more difficult because assuming the same mean thicknesses of between 5 and 15 m requires higher slope angles (between 5° and 40°) for

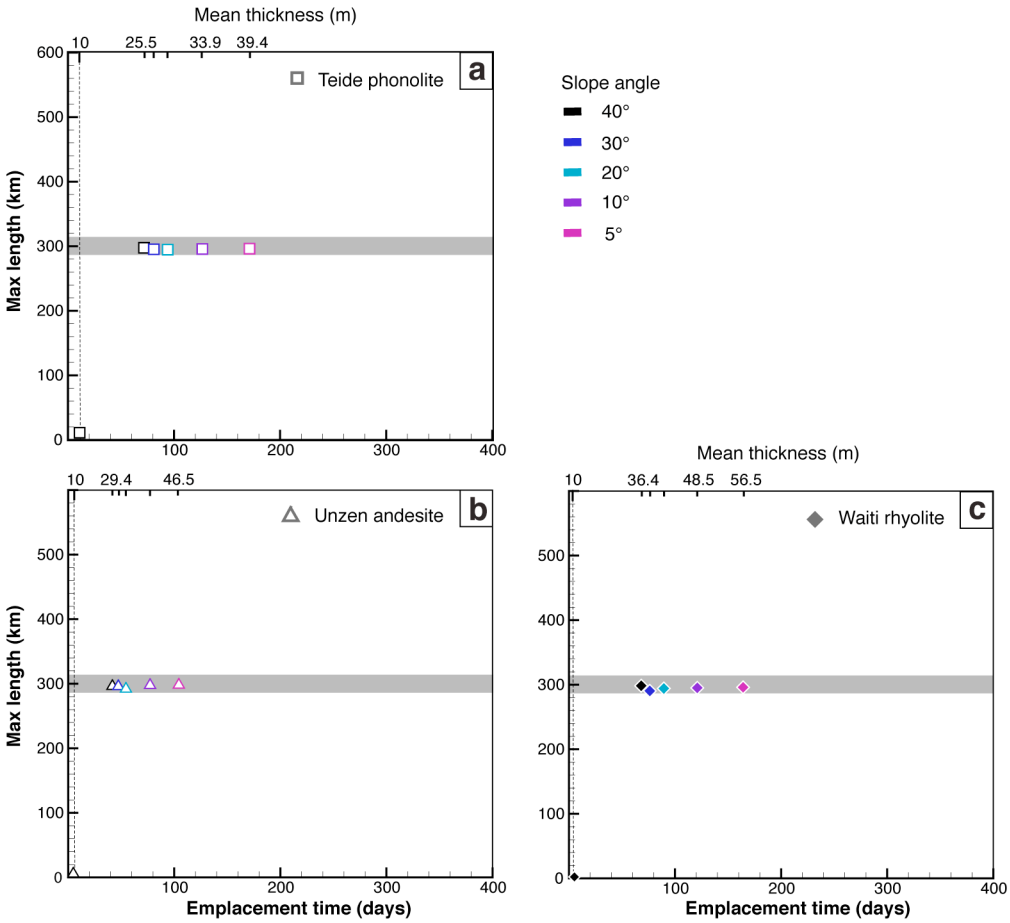

Figure 3-8. Maximal lava-flow length as a function of emplacement time, mean thickness, slope angle, and chemical composition for high-viscosity Group 2 (according to Fig. 3-7). Dashed vertical lines indicating emplacement time calculated with a predefined fixed mean thickness (5, 10, and 15 m) and the corresponding maximal lava-flow length. Horizontal gray bar displays the present-day Yatta lava flow length (290±10 km). Plotted symbols on that bar correspond to the modeled thickness and emplacement time for the respective color-coded slope angles. As in all previous figures symbols for hydrous lava compositions are filled and those for anhydrous compositions are un-filled.

these compositions to flow. For example, our calculations indicated that a 10 m thick anhydrous phonolite will, in ~11 days, flow between 3 km (for β=5°) and 11 km (for β=40°); and a hydrated rhyolite will flow between 0.75 and 3.5 km in ~5 days with the same slope angles.

In a second test, we considered the actual Yatta lava flow length of 290±10 km as a fixed dimension and calculated the required mean thickness of the lava flow. The values are displayed in Figures 3-7 and 3-8 where they are represented by the horizontal fitted data points. In these calculations, the

emplacement times for the Yatta phonolites ranged from ~5 to ~21 days (Fig. 3-7a_2) and for the anhydrous basalts from ~2.5 to ~10 days (Fig. 3-7d_2), assuming slope angles of between 0.1° and 2°, respectively. In contrast, calculations for Group 2 lavas to be able to match the morphological parameters of the present-day Yatta Plateau, calculations require a greater emplacement time, significantly thicker flows (at least 25 m), and a higher topographic slope angle (≥5°). As an example, the anhydrous andesitic lava flow would require between 42 and 105 days for emplacement (Fig. 3-8b), and the hydrous rhyolite would require between 68 and 164 days (Fig. 3-8c).

3.5 Discussion

Long, channeled terrestrial or planetary lava flows (e.g., the CRB) are traditionally considered to have been emplaced rapidly (within a matter of days) when low-viscosity lava is erupted at high effusion rates (*Shaw and Swanson*, 1970; *Hulme*, 1974; *Reidel*, 1998; *Miyamoto and Sasaki*, 1998). *Rowland and Walker* (1990) proposed that a continuous chilled crust cannot develop at effusion rates >10 m^3/s and *Harris and Rowland* (2001) quantified accompanying cooling rates at between 1 and 100 °C/km. Therefore, the lava flows that were studied should not have developed surface crusts (e.g., tubes) and turbulent flow would not have occurred (*Reidel*, 1998). However, recent detailed field studies and measurements on Kilauea have revealed lower effusion rates and have also shown that inflation of lava flows after emplacement can result in reactivation and continued isothermal lengthening of turbulent flows by the formation of insulating lava tubes (*Self et al*. 1996). In this case emplacement time could range from a few years to tens or hundreds of years (*Reidel*, 1998), and cooling rates of 0.35-1.8 °C/km (*Keszthelyi*, 1995; *Clague et al*., 1999) would allow thermally efficient lavas to advance farther before cooling forced eventual stagnation (*Harris and Rowland*, 2001). We therefore have a classic two end-member case. However, in both cases the

rheological properties and cooling mechanism were consistently calculated separately, and neither took into account variations in viscosity with cooling nor variations in chemical compositions. Possible explanations may lie in the discrepancies between measured or calculated rheologies and bulk flow viscosities measured in the field through application of the frequently used Jeffreys' equation (*Jeffreys*, 1925), which often result in overestimation of lava viscosities and the resulting underestimation of implied velocities (e.g., *Crisp et al.*, 1994). They may also be related to the fact that long lava flows were exclusively attributed to low viscous basaltic compositions. We therefore modified Jeffreys' equation by integrating the temperature and composition-dependent viscosity model of *Hui and Zhang* (2007), which then allows simultaneous calculation of cooling and flow advance for different lava types.

Reconstructions of underlying topography during the mid-Miocene emplacement of the Yatta lava flow have yielded a paleo-slope angle of at least 0.18-0.2° and is therefore slightly higher than presently observed (*Wichura et al.*, 2010). On this basis and using estimates of viscosity, mean frontal velocity, cooling and effusion rate, emplacement time, and mean thickness, the following points can be made concerning the emplacement style of the Yatta lava flow:

1. Calculated viscosities for the Yatta phonolites range from 3.6×10^3 Pa s at the vent to 7.5×10^6 Pa s at its final position after flowing for 297 km.

2. During cooling (at 0.71 °C/km) the velocity of the RFZ slowed from 1.01 m/s at 870 °C to the cessation of flow at 660 °C.

3. Using a minimum mean thickness of 11.6 m and average effusion rates of 7,875 m^3/s, the minimum time taken for the RFZ to reach stagnation would have been ~15 days.

Our model therefore predicts high effusion rates under conditions of laminar flow during a rapid and approximately isothermal emplacement of the 290 km long channeled phonolitic lava flow. This appears to contradict the two models mentioned earlier in this section, although it fits some aspects of both, in particular the low cooling rates of tube-fed flows and the high effusion rates of channeled surface flows. *Harris and Rowland* (2001) proposed that to increase channel length without increasing channel depth, the rate of heat loss must be reduced. However, we believe that if effusion rates are high enough (and reach a certain threshold that limits the influence of surface contact), they may act as a driving force for approximately isothermal, non-turbulent flow that could result in the formation of long, channeled lava flows such as the Yatta lava flow in Kenya, or flows on other planets that exhibit similar characteristics. This interpretation is supported by a small but crucial overlap in cooling rates between both end-member models (*Keszthelyi*, 1995; *Clague et al.*, 1999, *Harris and Rowland*, 2001). Furthermore, comparing various studies on long terrestrial lava flows (CRB and DVP) reveals that there is only a limited comparability with the Yatta Plateau, for the following reasons:

a. The Yatta lava flow has a volume of ~25 km^3, whereas the volumes of individual lava flows associated with the CRB or DVP effusions are of the order of 100-1,000 km^3 (e.g., *Self et al.*, 1996; *Reidel*, 1998; *Bondre and Duraiswami*, 2004). They each therefore represent at least 300% more erupted volcanic material than is contained in the Yatta lava flow.
b. The model that we have employed is very sensitive to the mean lava-flow thickness as it is the only parameter (to the power of two) that affects both velocity and cooling. While local thicknesses of between 0.3 and 30 cm for lobate flows, and between 10 and 50 m for CRB sheet flows (e.g., *Tolan et al.*, 1989; *Self et al.*, 1996; *Reidel*, 1998) are indeed comparable to the thickness of the Yatta lava flow, when considering these multiple lava flows as a whole their average thicknesses are more than double than that of the Yatta Plateau lava. A higher mean

thickness implies a higher volume of effused volcanic material, which would result in a lava flow capable of propagating much farther than the length indicated by the morphology of the Yatta lava flow. We therefore believe that the existing models of lava flows with similar flow-lengths cannot be easily adapted to the Yatta Plateau.

c. Some studies have correlated silica content with rheologic parameters (e.g., *Hulme*, 1976; *Hulme and Fiedler*, 1977; *Carrasco-Núñez*, 1997), but none has integrated a complete set of bulk rock compositions into viscosity calculations and used it to model the advance of lava flows over >150 km, for compositions other than basaltic. We believe that the composition and, in particular the water content, has a very large effect on the viscosity (*Giordano and Dingwell*, 2003; *Romano et al.*, 2003; *Giordano et al.*, 2004; *Hui and Zhang*, 2007) and the rheologic behavior of a lava. It may be the major factor affecting the development of long lava flows, not only on Earth but also on other planets. The effects that small amounts of a hydrous component have on viscosity are described by a power law (*Giordano et al.*, 2004, pp. 49-61). By adding 0.5 wt% H_2O to the Kilauea basalt our simulation shows that a 10 m thick lava flowing over a Yatta Plateau type morphology would reach a length of 540 km. This distance has been calculated for a slope angle of 0.1°, corresponding to the gentle CRB slope (*Self et al.*, 1996), and is therefore in good agreement with their longest flows, e.g., the 500 km long Ginkgo flow (*Ho and Cashman*, 1997).

3.6 Conclusion

We have presented a new model of lava flow for the emplacement of the mid-Miocene Yatta Plateau in Kenya, based on an improved, composition and temperature dependent, method to model the flow of lava along a channel with a rectangular cross section. The essential growth pattern is described by a one-dimensional model in which Newtonian rheological flow advance is governed

by the development of viscosity and/or velocity in the lava interior, close to the flow front. The modeling of long, channeled lava flows is difficult because each individual parameter has the potential to substantially change the length of lava flow. Of particular importance are the H_2O content, the mean thickness, and the slope angle. The emplacement style of a phonolitic lava flow with low viscosity shows some correlations with two earlier end-member models. It is therefore tempting to speculate that our approach may provide a missing link between both models and thus represent a new method for assessing length-dominated lava flows characterized by high effusion rates, laminar flow, and rapid emplacement under approximately isothermal conditions. Although further refinement of the model may be required, its agreement with the actual observations for the Yatta lava flow may mean that it is possible to predict the physical properties and compositions of existing terrestrial, as well as planetary, long lava flows that show similar morphologies.

Acknowledgements

This research has been conducted within the University of Potsdam's Graduate School GRK1364 (*Shaping Earth's Surface in a Variable Environment*), funded by the German Research Foundation (DFG), and co-financed by the federal state of Brandenburg and the University of Potsdam. The authors are grateful to the Government of Kenya for research permits (Research Permits MOST 13/001/30C 59/10) and the University of Nairobi for their support. We would also like to thank the members of the DFG Graduate School GRK1364 for fruitful discussions and Ed Manning for proofreading the manuscript.

CHAPTER 4

Evidence for middle Miocene uplift of the East African Plateau

Abstract

Cenozoic uplift of the East African Plateau (EAP) has been associated with fundamental climatic and environmental changes in East Africa and adjacent regions. While this influence is widely accepted, the timing and the magnitude of plateau uplift have remained unclear. This uncertainty stems from the lack of datable, geomorphically meaningful reference horizons that could record surface uplift. Here, we document the existence of significant relief along the EAP prior to rifting, as inferred from modeling the emplacement history of one of the longest terrestrial lava flows, the ~300-km-long Yatta phonolite flow in Kenya. This 13.5 Ma lava flow originated on the present-day eastern Kenya Rift flank, and utilized a riverbed that once routed runoff from the eastern rim of the plateau. Combining an empirical viscosity model with subsequent cooling and using the Yatta lava flow geometry and underlying paleo-topography (slope angle), we found that the pre-rift slope was at least 0.2°, suggesting that the lava flow originated at a minimum elevation of 1,400 m. Hence, high paleo-topography in the Kenya Rift region must have existed by at least 13.5 Ma. We infer from this that middle Miocene uplift occurred, which coincides with the two-step expansion of grasslands, as well as important radiation and speciation events in tropical Africa.

4.1 Introduction

Uplift of the Cenozoic EAP, subsequent volcanism, and faulting are important hallmarks of the geodynamic evolution of the African continent that have

influenced one of the largest magmatic rifts on Earth. Located over an areally extensive mantle anomaly (e.g., *Simiyu and Keller*, 1997) and at an average elevation of ~1,000 m (Fig. 4-1), this region forms an orographic barrier to moisture-bearing winds and thus influences the distribution and amount of rainfall in East Africa (e.g., *Sepulchre et al.*, 2006). Uplift of this region has often been cited as a pre-requisite for generating the differential stresses necessary for extensional faulting (e.g., *Strecker et al.*, 1990; *Le Gall et al.*, 2008). However, reliable paleo-altimetry data for this region is virtually non-existent. Although the existence of an areally expansive plateau in East Africa has been mentioned in many studies (e.g., *Ebinger and Sleep,* 1998; *Pik et al.*, 2008), opinions diverge over the mechanistic links between topography and rifting, as well as over the timing and magnitude of plateau uplift. *Smith* (1994) postulated that the available geological and geophysical evidence supported the presence of limited topography (<1,000 m) prior to early to middle Miocene volcanism in the Kenya Rift, and attributed this pre-rift topography to the Kenya Dome. Determining paleo-altimetry more rigorously has been hampered by the lack of suitable reference horizons. Recently, studies employing apatite (U-Th)/He thermochronology on the present-day rift shoulders have suggested that uplift-related erosional exhumation may have started at ~6 Ma in Kenya (*Spiegel et al.*, 2007) and at ~20 Ma in Ethiopia (*Pik et al.*, 2008). However, these studies provide information on only the onset of localized basement exhumation, and not on the spatiotemporal characteristics of surface uplift. In contrast, the Yatta lava flow of Kenya may provide direct evidence for topographic conditions along the eastern flank of the EAP prior to rifting. This lava flowed away from the present-day rift by utilizing a river channel that formerly drained the early plateau region. Thus, viscosity and slope angle modeling of this lava flow may provide the necessary gradients for lava flow, and ultimately indicate the elevation of the area where the lava flow originated.

4.2 Geological setting

Geodynamic and magmatic activity in the East African Rift System initiated between 45 and 35 Ma by the buoyancy and melt generation of an asthenospheric plume beneath the present EAP (*Ebinger et al.*, 1993; Fig. 4-1). This resulted in widespread phonolites, basalts, and trachytes erupting over Proterozoic basement rocks since 20 Ma (e.g., *Smith*, 1994). The oldest recognizable rift structures are the east-facing Elgeyo, Mau, and Nguruman escarpments (e.g., *Baker and Wohlenberg*, 1971), which postdate the most voluminous period of plateau-phonolite volcanism between 13 and 11 Ma (*Smith*, 1994).

The Yatta lava flow is the most prominent manifestation of the major phonolitic eruption at 13.51 Ma (*Veldkamp et al.*, 2007; Fig. 4-1). Likely, it originated in a region that now corresponds to the eastern Kenya Rift flank and flowed ~300 km through the ancient Athi River valley toward the southeast. In contrast to other areally important volcanics, the Yatta Plateau flow was channelized and is regarded as one of the longest lava flows on Earth (Fig. 4-1).

Subsequent downwearing of the basement rocks confining the flow and the low erodibility of the phonolites have caused relief inversion and thus formed the Yatta Plateau (Fig. 4-2). Early estimates of the slope of the Yatta lava flow based on field mapping and simple topographic considerations suggested a minimum slope angle of 0.16° (*Saggerson*, 1963; Fig. 4-2).

However, this estimate involves large uncertainties, because it assumed that the East African topography was developed during a single rift-flank uplift phase in Pliocene time (*Spiegel et al.*, 2007), ignoring the possibility of an earlier plateau uplift associated with the buoyant East African mantle plume.

The presently observable thickness of the Yatta Plateau phonolites from the basement contact to flow-top remnants is 12-25 m (Fig. 4-2). Pronounced and consistent northwest-southeast alignment of feldspar phenocrysts is parallel to the direction of flow and supports the inference that flow was laminar.

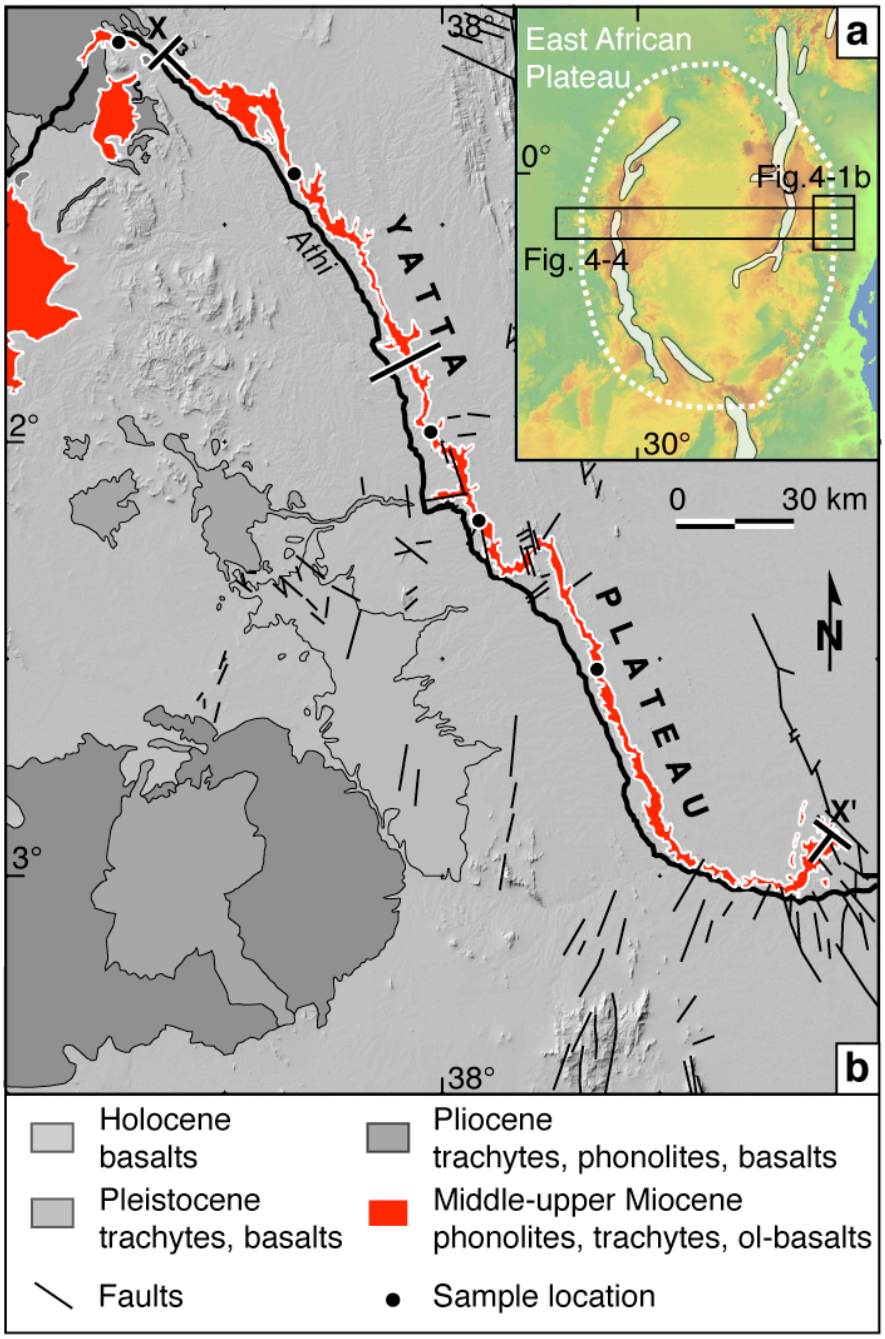

Figure 4-1. Location and geological setting. (a) Overview map showing topography of the current East African Plateau (white dashed line) and Cenozoic rifts (gray areas). White boxes are linked to the geological overview map in Figure 4-1b and to the topographic swath profile shown in Figure 4-4. (b) Principal geological map shows topographic features and lithologies corresponding to volcanic activity since the middle Miocene on the eastern rim of the East African Plateau. X–X' and the black line denote the geological cross sections of the Yatta lava flow (see Fig. 4-2). ol-basalts - olivine basalts.

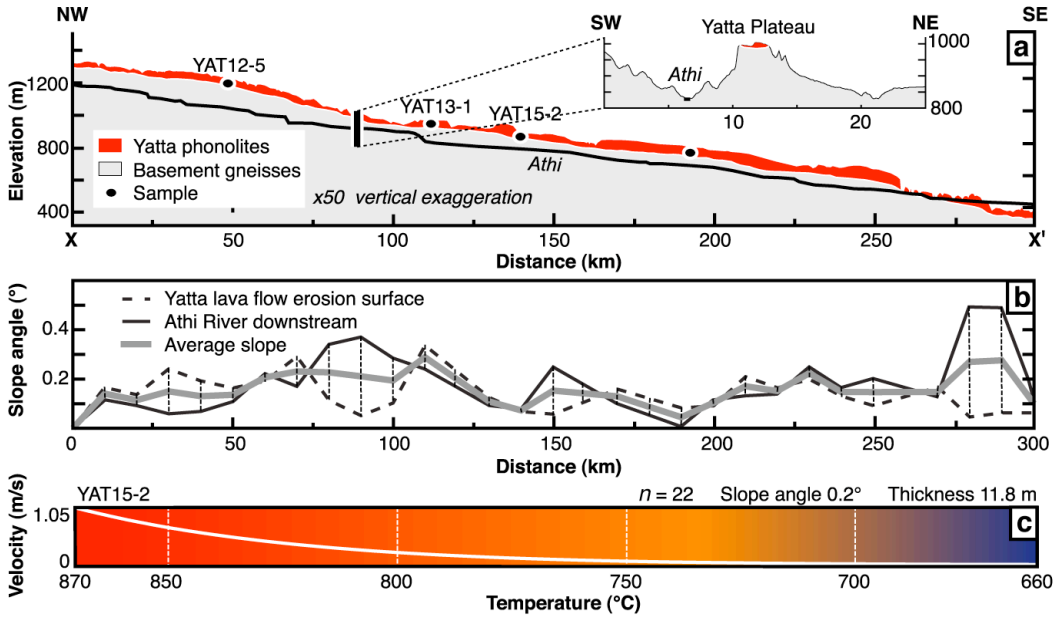

Figure 4-2. Yatta lava flow cross section, recent slope angle distribution, and lava-flow velocity. (a) Geological cross sections constructed along the Yatta lava flow and present Athi River downstream. Black circles mark the location of phonolitic samples, which are considered to be representative of the Yatta lava flow chemical composition and were used to calculate viscosities by applying the model by *Hui and Zhang* (2007). (b) Recent slope angle distribution corresponding to the erosion surface of the Yatta lava flow and the Athi River relative to the lava flow distance. The "moving" average slope angle is displayed by the thicker gray line and calculated every 10 km between the lava-flow erosion surface slope and the Athi River downstream. (c) Decreasing lava-flow velocities with proceeding cooling steps *n* and a constant slope angle of 0.2°, here calculated for sample YAT15-2. X-axis is parallel to the lava-flow length.

Evidence for tube-fed flow has never been described in the literature, nor has been observed by us. Pillow lavas at the contact between the phonolites and the basement suggest the local presence of water during emplacement.

The Yatta Plateau consists of one single flow and is not the result of multiple, superposed volcanic flows. By using satellite imagery and field observations in erosional cuts, we derived the lava-flow geometry, in particular the lava-flow length L (300 km), width W, and present slope (Fig. 4-2). The width of the flow is between 8 km in the northwest and 1 km in the remote southeast part. The average elevation difference along the eroded flow top is 2.8 m/km. This corresponds to the present-day average slope angle of 0.16° along the bottom of the paleo-valley, as inferred from four different erosional cuts and in good agreement with the estimate by *Saggerson* (1963; Fig. 4-2).

Because viscous flow in a channel with a defined width and thickness can be determined from the solution for a filled rectangular conduit having the same width and double thickness (e.g., *White*, 1991), we derived a simple topographic model for lava-flow emplacement. This model assumes an average flow width of 3 km and a constant slope angle. Significant downstream variations of the width or slope can hydraulically affect lava velocity. The model is thus an approximation at a single cross section with laminar flow assumed in the flow direction (*Tallarico and Dragoni*, 1999). Using these geometric parameters and rheological assumptions, we modeled the lava flow along its entire length and determined the minimum slope angle required at the time of eruption to permit flow of phonolitic lava over 300 km.

4.3 Approach, methods, and results

The recognition of very long, channelized Martian and lunar lava flows and the extensive areal distribution of the Columbia River basalts in the western U.S.A. promoted attempts to relate lava-flow lengths to certain rheological properties of lavas (e.g., *Hulme and Fielder*, 1976; *Reidel*, 1998; *Harris et al.*, 2007), an approach that inspired this study. To test the hypothesis that the present slope angle of 0.16° was required for such a long lava flow, we developed a one-dimensional empirical model. The model relies on the viscosity equation by *Hui and Zhang* (2007):

$$\log \eta = A + \frac{B}{T} + \exp\left(C + \frac{D}{T}\right) \tag{4-1}$$

This equation simulates viscosity η as a function of temperature T, chemical composition, and water content of the lava. A, B, C, and D are linear functions of X_i (mole fractions of oxide component i) except for H_2O (*Hui and Zhang*, 2007). The mole fraction for water is integrated in D and combined with an internal temperature dependence of the hydrous component (*Hui and Zhang*,

2007). The 2σ deviation of this fit is 0.61 logη units (*Hui and Zhang*, 2007). In a first experimental run, we assumed a stepwise (n) cooling process with ΔT=10 °C, starting at an initial eruption temperature of 870 °C, which is typical for phonolitic magmas (*Ablay et al.*, 1995; Fig. 4-2). The chemical composition of our modeled lava flow is based on the chemistry of five samples collected at five sites along the flow (Fig. 4-1). The gradually increasing viscosity of the lava during cooling corresponds to the stepwise decreasing lava flow velocity v_n following Jeffreys' law (*Jeffreys*, 1925):

$$v_n(T_n, X_i) = \frac{H^2 g \rho \sin\beta}{a\eta_n(T_n, X_i)}, \tag{4-2}$$

where β is the slope angle, g is the gravity constant (9.81 m/s^2), ρ is the rock density (phonolite 2.4 x 10^3 kg/m^3), H is the lava-flow thickness, and η_n is the viscosity, stepwise computed with the *Hui and Zhang* model (2007) (Fig. 4-2). Employment of this equation is valid, as we model the lava velocity in the rear frontal zone (RFZ), the part of a flow between its convex-curved front and its established channel structure upstream. This zone is characterized by approximately Newtonian rheology, isotropic and non-fractionated conditions, and uniform density (*Lopes and Kilburn*, 1990). Estimates of the emplacement time (t_{em}) were obtained using the Graetz model, an empirical conduction-limited cooling model (e.g., *Pinkerton and Sparks*, 1976), in which lava-flow cooling is compared to the heat loss of a hot fluid moving through a cool conduit. Heat advection within the flow along its length is described by the dimensionless Graetz number (G_Z) (*Pinkerton and Sparks*, 1976):

$$G_Z = \frac{H^2 \overline{V}}{kL}, \tag{4-3}$$

where V-bar is the mean velocity of the RFZ (the sum of all v_n divided by n cooling steps), k is the thermal diffusivity (phonolite 3.5 x 10^{-7} m^2/s; *Martin and*

White, 2002), and L is the lava-flow length. It has been empirically determined that lava flows come to rest before G_Z falls to ~300 (*Hulme and Fielder*, 1976). Hence, the emplacement time (t_{em}) can be considered as:

$$t_{em} = \frac{L}{\overline{V}}, \tag{4-4}$$

which can be rewritten as:

$$t_{em} = \frac{H^2}{G_Z k} \tag{4-5}$$

Finally, we modeled the lava flow in two ways: (1) keeping the thickness constant and estimating how far the lava can flow, and (2) assuming the present lava-flow length and computing the required thickness (Fig. 4-3). In both simulations, we calculated thickness and length as a function of the underlying topography. Modeling small active lava flows on different volcano types showed that the shape and roughness of the channel used by the lava are of great importance (*Del Negro et al.*, 2007). Sensitivity tests of our model, however, suggest that topographic disturbances along the course of the river valley do not significantly influence the model result. We found that the most important parameters controlling lava-flow length are volumetric flow rates at the vent, viscosity change with ongoing cooling, and lava-flow thickness.

Our simulation suggests that protracted flow may occur at a slope angle of at least 0.18-0.20° with an estimated uncertainty of 15% (Fig. 4-3). With this slope angle and a lava-flow thickness of 12-15 m, the lava-flow front must have been able to reach the eastern Tsavo plains over a distance of ~300 km. Because flow was to the southeast and therefore 60° northward rotated relative to the slope of the EAP in this area, our calculated slope angles are minimum values. Projection of the lava flow onto an east-west profile (Fig. 4-4) along the same inclined plane yields a slope angle of 0.35-0.38°.

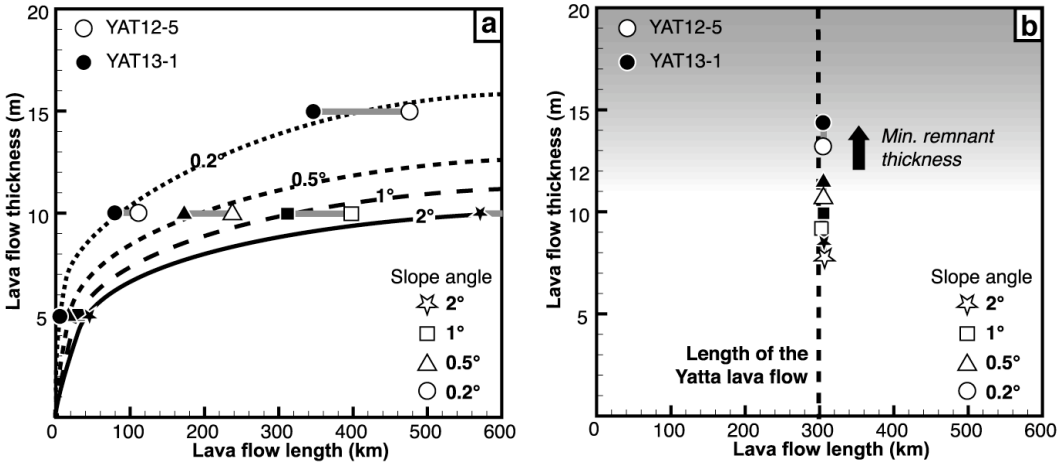

Figure 4-3. Yatta lava flow thickness vs. length. (a) Maximum lava-flow length with a fixed thickness as a function of slope angle. Influence of the chemical composition is indicated by different data points, which connect two representative samples displayed by the filled (YAT13-1) and empty (YAT12-5) symbols. (b) Maximum lava-flow thickness with a fixed length (300 km) as a function of different slope angles and chemical composition. Black arrow represents minimum remnant thickness.

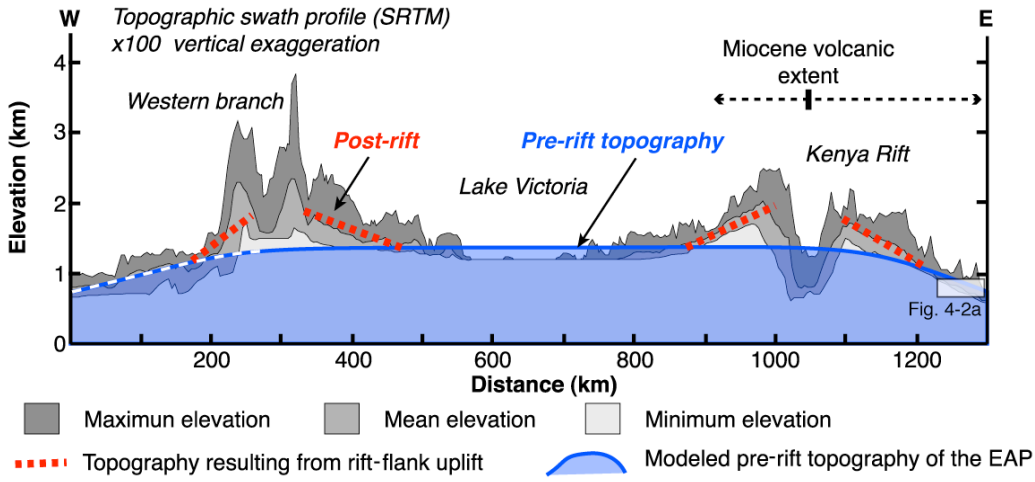

Figure 4-4. Middle Miocene East African Plateau derived from slope angle modeling on the eastern rim. The pre-rift topographic model uses a slope angle of 0.2°, which yields a flat plateau 1,400 m high and 1,300 km wide. Different gray areas display the modern topography across the center of the East African Plateau (1° x 12° topographic swath profile extracted from SRTM data). Thick red-dashed lines mark the portion of syn- and post-rift uplift. White box shows the location of the profile shown in Figure 4-2a. E-W arrows display the Miocene volcanic extent from the Central Kenya Rift axis. EAP - East African Plateau; SRTM - Shuttle Radar Topography Mission.

Using the calculated slope angle of 0.18-0.20° across the EAP, and assuming a virtually flat top of the uplifted region, the plateau phonolites would have originated in a plateau setting at a maximum elevation of 1,400 m (Fig. 4-4). This supports our initial hypothesis of expansive, high pre-rift topography at least 1,300 km in diameter prior to 13.5 Ma in the present-day EAP region (Fig. 4-4). This uplifted area may have been the surface expression of mantle plume-lithospheric interactions (*Burov and Cloetingh*, 2009).

4.4 Discussion

Our results give insights into East African topographic evolution and ensuing environmental change. Today, topography of the EAP influences the distribution and amount of rainfall associated with the African-Indian monsoon and westerly moisture sources at a continental-scale. Exacerbated by additional effects of rift shoulder uplift and the construction of volcanic edifices adjacent to the rift, uplift of the EAP has resulted in pronounced topographic changes and modifications in the drainage system in East Africa. This created a patchwork of closely spaced humid and arid sedimentary environments (*Sepulchre et al.*, 2006), which must have impacted paleo-environmental conditions. Indeed, middle Miocene uplift of the EAP correlates with a number of changes, including an early expansion of C4 plants in East Africa at ~14 Ma (*Kingston et al.*, 1994; *Morgan et al.*, 1994), a change from grassy woodland to wooded grassland in fossil soils and grasses based on Miocene mammal fossils in western Kenya (*Retallack et al.*, 1990), and expansion of a grass-dominated savannah biome that started in the middle Miocene (16 Ma), and became widespread in the late Miocene (~8 Ma) (*Jacobs*, 2004; Fig. 4-5).

Paleo-vegetation development in East Africa suggests a two-step evolution toward more pronounced dry conditions at the expense of rainforests at 16-14 Ma, and the expansion of grasslands at 8-7 Ma (Fig. 4-5).

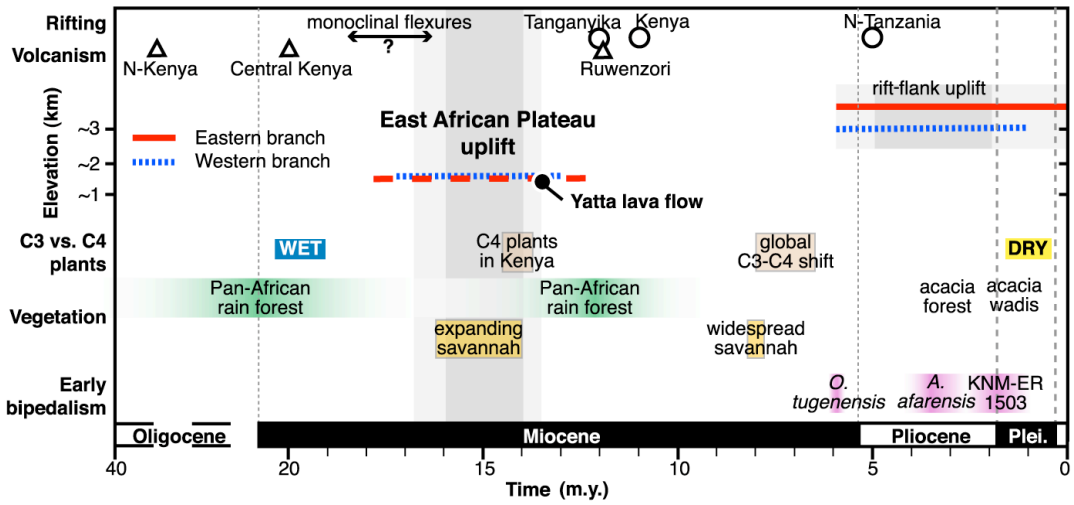

Figure 4-5. Cenozoic uplift chronology, vegetation changes, and early hominids evolution in East Africa. Middle Miocene uplift correlates with major climatic and environmental shifts. Data compilation as follows: onset of important volcanic activity (triangle) and rifting (circle) (*Baker and Wohlenberg*, 1971; *Cohen et al.*, 1993; *Chorowicz*, 2005), Pliocene rift-flank uplift (*Ebinger et al.*, 1993; *Spiegel et al.*, 2007), K-Ar age of the Yatta lava flow (*Veldkamp et al.*, 2007), pollen and carbon isotopes (*Retallack et al.*, 1990; *Kingston et al.*, 1994; *Cerling et al.*, 1997; *Jacobs*, 2004), Pan-African rain forest expansion-isolation phases (*Couvreur et al.*, 2008), and early hominids bipedalism (*Richmond and Jungers*, 2008).

Based on our analysis, the first step toward more arid conditions may have been linked to uplift of the East African and Ethiopian plateaus prior to 13.5 and 20 Ma (*Pik et al.*, 2008), respectively. In contrast, the second shift toward increasing grassland vegetation may have been a response to the global decrease in pCO_2 (e.g., *Cerling et al.*, 1997) combined with the topographic effects of rifting and volcanism.

Middle Miocene uplift of the East African and Ethiopian plateaus and coeval environmental changes also influenced radiation and speciation. For example, molecular phylogenetic studies on the evolutionary history of rainforest restricted Pan-African lineages of *Annonaceae* plants demonstrate that they have significantly different temporal origins (*Couvreur et al.*, 2008). Successive connection-isolation events between the Guineo-Congolian rainforest and East Africa at ~16 Ma and ~8 Ma (*Couvreur et al.*, 2008) (Fig. 4-5) correlate temporally with our interpretation of a two-tiered environmental change due to plateau uplift prior to 13.5 Ma and global pCO_2 changes in late

Miocene time (Fig. 4-5). The mid-Miocene uplift of the EAP is thus consistent with documented shifts in existing vegetation mosaics in East Africa and may have ultimately affected hominids evolution.

Acknowledgements

This work was conducted under the auspices of the Graduate School GRK1364 *Shaping Earth's Surface in a Variable Environment*, funded by the DFG. We thank the Government of Kenya and the University of Nairobi for research permits and support. We also thank the members of the GRK1364 for fruitful discussions and inspiration, and Taylor Schildgen for rewording the manuscript.

CHAPTER 5

Conclusions

In order to find evidence and test the hypothesis that high topography existed in East Africa prior to the formation of rifting segments, I investigated the emplacement of the Yatta lava flow in Kenya. Two coincidences prior to its formation made this lava flow a well-suitable "paleo-tiltmeter" that can be used to quantify the vent elevation on the East African Plateau. Firstly, a river drained the early plateau region to the southeast, incising a valley into the Proterozoic basement, and forming a type of geomorphologic casting mold for the Yatta lava flow. Secondly, the onset of plateau-type volcanism facilitated the phonolitic lava emplacement into the valley along its entire length of approximately 300 km as a single, channeled lava flow in mid-Miocene time and therefore prior to rifting. By modeling the slope angle of the underlying topography that the phonolitic lava required to achieve its present geometry, I was able to quantify the maximal elevation of the East African Plateau at that time. That slope angle was at least 0.18-0.2°, suggesting a minimum plateau elevation of 1,400 m. With these results I was capable to reconstruct the topographic history by a two-step uplift evolution in the realm of the East African Plateau. The pre-syn-rift uplift phase was related to plume-lithosphere interaction and thermal expansion. Its surface expression formed the areally expansive 1,400 m high East African Plateau until at least ~13.5 Ma. Additionally, concurrent volcanic activity since the early Miocene led to accumulations of volcanic rocks, especially in the present Kenya Rift region, and finally formed the Kenya Dome. Subsequently, the post-rift uplift phase induced pronounced relief contrasts due to isostatic relaxation and rift shoulder uplift since ~6 Ma. This two-step topographic evolution coincides with progressive aridification recorded by the first appearance of C4 plants in Kenya (~14 Ma) and finally dominating the entire environment (~8 Ma) as response

to the global decrease in pCO_2. Furthermore, the onset of expanding (~16 Ma) to widespread (~8 Ma) savannah type-vegetation in tropical Africa and successive connection-isolation events between the Guineo-Congolian rainforest at ~16 Ma and ~8 Ma, supporting my interpretation of two-tiered environmental change due to plateau uplift prior to 13.5 Ma and suggesting a causal link.

Contemporaneously to the elaboration of the topographic history of the East African Plateau, I developed a new method to model long, channeled lava flows, incorporating the calculations for the required slope angle of the Yatta lava flow (see above). The lava-flow model is an improved, composition and temperature dependent method to model the flow of lava along a channel with a rectangular cross section. The essential growth pattern is described by a one-dimensional model in which Newtonian rheological flow advance is governed by the development of viscosity and/or velocity in the lava interior, close to the flow front. The modeling of long, channeled lava flows is difficult because each individual parameter has the potential to substantially change the length of lava flow. Of particular importance are the H_2O content, the mean thickness, and the slope angle. The emplacement style of a phonolitic lava flow with low viscosity shows some correlations with two earlier end-member models, favoring the formation of long lava flows either in a channel with high effusion rates or in cooling efficient tubes. It is therefore tempting to speculate that my approach may provide a missing link between both models and thus represent a new method for assessing length-dominated lava flows characterized by high effusion rates, laminar flow, and rapid emplacement under approximately isothermal conditions. Although further refinement of the model may be required, its agreement with the actual observations for the Yatta lava flow may imply that it is possible to predict the physical properties and compositions of existing terrestrial, as well as length-dominated extraterrestrial lava flows that show similar characteristics and morphologies.

BIBLIOGRAPHY

Ablay, G. J., et al. The ~2 ka Subplinian Eruption of Montana Blanca, Tenerife. *Bulletin of Volcanology*, 57, 337-355, 1995.

Achauer, U., et al. New ideas on the Kenya rift based on the inversion of the combined dataset of the 1985 and 1989/90 seismic tomography experiments. *Tectonophysics*, 236, 305-329, 1994.

Baker, B. H. and Wohlenberg, J. Structure and Evolution of the Kenya Rift Valley. *Nature*, 229, 538-542, 1971.

Baker, B. H., et al. Geology of the the Eastern Rift System of Africa. *Geological Society of America*, *Special Paper*, 136, 1972.

Baloga, S. M., et al. Influence of volatile loss on thickness and density profiles of active basaltic flow lobes. *Journal of Geophysical Research*, 106, 13395-13405, 2001.

Benoit, M. H., et al. Crustal thinning between the Ethiopian and East African plateaus from modeling Rayleigh wave dispersion. *Geophysical Research Letters*, 33, 2006.

Bergner, A. G. N., et al. Tectonic and Climatic Controls on Evolution of Rift Lakes in the Central Kenya Rift, East Africa. *Quaternary Science Reviews*, 28, 2804-2816, 2009.

Bondre, N. R., et al. Morphology and emplacement of flows from the Deccan Volcanic Province, India. *Bulletin of Volcanology*, 66, 29-45, 2004.

Booth, B. and Self, S. Rheological features of the 1971 Mount Etna lavas. *Philosophical Transactions of the Royal Society of London*, 274, 99-106, 1973.

Bosworth, W. Off-axis volcanism in the Gregory Rift, east Africa: implications for models of continental rifting. *Geology*, 15, 397-400, 1987.

Bottinga, Y. and Weill, D. F. The viscosity of magmatic silicate liquids: a model for calculation. *American Journal of Science*, 272, 438-475, 1972.

Braun, J. and Beaumont, C. A physical explanation of the relation between flank uplifts and the breakup unconformity at rifted continental margins. *Geology*, 17, 760-764, 1989.

Bryan, W. B. Systemantics of Modal Phenocrysts Assemblages in Submarin Basalts: Petrologic Implications. *Contributions to Mineralogy and Petrology*, 83, 62-74, 1983.

Burke, K. and Whiteman, A. J. Uplift, rifting, and the break-up of Africa. *In*: Tarling, D. H. (ed.) *Implications of Continental Drift to the Earth Sciences.* Academic Press, London, 735-755, 1973.

Burke, K. The African Plate. *South African Journal of Geology*, 99, 341-409, 1996.

Burke, K. and Gunnel, Y. A Continental-Scale Synthesis of Geomorphology, Tectonics, and Environmental Change over the Past 180 Million Years. *Geological Society of America*, Memoir 201, 2008.

Burov, E. and Cloetingh, S. Controls of Mantle Plumes and Lithospheric Folding on Modes of Intraplate Continental Tectonics: Differences and Similarities. *Geophysical Journal International*, 178, 1691-1722, 2009.

Calvari, S. and Pinkerton, H. Lava tube morphology on Etna and evidence for lava flow emplacement mechanism. *Journal of Volcanology and Geothermal Research*, 90, 263-280, 1999.

Carrasco-Núñez, G. Lava Flow Growth Inferred from Morphometric Parameters: A Case Study of Citlaltépetl Volcano, Mexico. *Geological Magazine*, 134, 151-162, 1997.

Cashman, K., et al. Introduction to special section: long lava flows. *Journal of Geophysical Research*, 103, 27281-27289, 1998.

Cerling, T. E., et al. Global Vegetation Change Through the Miocene/Pliocene Boundary. *Nature*, 389, 153-158, 1997.

Chorowicz, J. The East African Rift System. *Journal of African Earth Sciences*, 43, 379-410, 2005.

Clague, D. A., et al. Kilauea Summit overflows: their ages and distribution in the Puna District, Hawai'i. *Bulletin of Volcanology*, 61, 363-381, 1999.

Class, C., et al. Geochemistry of Pliocene to Quaternary alkali basalts from the Huri Hills, northern Kenya. *Chemical Geology*, 113, 1-22, 1994.

Cohen, A. S., et al. Estimating the Age of Formation of Lakes: An Example of Lake Tanganyika, East African Rift. *Geology*, 21, 511-514, 1993.

Couch, S., et al. Mineral disequilibrium in lavas explained by convective self-mixing in open magma chambers. *Nature*, 441, 1037-1039, 2001.

Courtillot, V., et al. On causal links between flood basalts and continental breakup. *Earth and Planetary Science Letters*, 166, 177-195, 1999.

Couvreur, T. L. P., et al. Molecular Phylogenetics Reveal Multiple Tertiary Vicariance Origins of the African Rain Forest Trees. *Bio Med Central Biology*, 6, 54-63, 2008.

Crisp, J. and Baloga, S. A Method for Estimating Eruption Rates of Planetary Lava Flows. *Icarus*, 85, 512-515, 1990.

Crisp, J., et al. Crystallization history of the 1984 Mauna Loa flow. *Journal of Geophysical Research*, 99, 7177-7198, 1994.

Del Negro, C., et al. Simulations of the 2004 Lava Flow at Etna Volcano Using the Magflow Cellular Automata Model. *Bulletin of Volcanology*, 70, 805-812, 2007.

Dixey, F. The East African Rift System. *Colonial Geological Mining Research Bulletin*, 1, 71-72, 1956.

Dragoni, M. Modelling the rheology and cooling of lava flows. *In*: Kilburn, C. R. J., Luongo, G. (eds.) *Active Lavas: Monitoring and Modelling*. UCL Press, London, p. 374, 1993.

Dragoni, M. and Tallarico, A. The effect of crystallization on the rheology and dynamics of lava flows. *Journal of Volcanology and Geothermal Research*, 59, 241-252, 1994.

Ebinger, C. J. Tectonic development of the western branch of the East African rift system. *Geological Society of American Bulletin*, 101, 885-903, 1989.

Ebinger, C. J., et al. Effective elastic plate thickness beneath the East African and Afar plateaus and dynamic compensation of the uplifts. *Journal of Geophysical Research*, 94, 2883-2901, 1989.

Ebinger, C. J., et al. Late Eocene-Recent Volcanism and Faulting in the Southern Main Ethiopian Rift System. *Journal of the Geological Society*, 150, 99-108, 1993.

Ebinger, C. J. and Sleep, N. H. Cenozoic Magmatism Throughout East Africa Resulting From Impact of a Single Plume. *Nature*, 395, 788-791, 1998.

Ebinger, C. J. Continental break-up: The East African perspective. *Astronomy and Geophysics*, 46, 16-21, 2005.

Fairburn, W. A. Geology of the North Machakos-Thika area. *Geological Survey of Kenya*, Report 59, 1963.

Foster, A. and Gleadow, A. J. W. Structural framework and denudation history of the flanks of the Kenya and Anza Rifts, East Africa. *Tectonics*, 15, 258-271, 1996.

Fuchs, K., et al. Structure and Dynamic Processes in the Lithosphere of the Afro-Arabian Rift System. *Tectonophysics*, 278, 1-352, 1997.

Fujita, M. Geology of the Yatta Plateau, Kenya. *2nd Prelimary Report African Studies*, Nagoya University, Earth Sciences 2, 161-164, 1977.

Garcin, Y., et al. Late Pleistocene-Holocene rise and collapse of the Lake Suguta, northern Kenya Rift. *Quaternary Science Reviews*, 28, 911-925, 2009.

George, R., et al. Earliest magmatism in Ethiopia: Evidence for two mantle plumes in one flood basalt province. *Geology*, 26, 923-926, 1998.

Giordano, D., et al. Viscosity of a Teide phonolite in the welding interval. *Journal of Volcanology and Geothermal Research*, 103, 239-245, 2000.

Giordano, D. and Dingwell, D. B. Non-Arrhenian multicomponent melt viscosity: a model. *Earth and Planetary Science Letters*, 208, 337-349, 2003.

Giordano, D., et al. The viscosity of trachytes, and comparison with basalts, phonolites, and rhyolites. *Chemical Geology*, 213, 49-61, 2004.

Giresse, P. Mesozoic-Cenozoic history of the Congo Basin. *Journal of African Earth Sciences*, 43, 301-315, 2005.

Glaze, L. M. and Baloga, S. M. Rheologic inferences from the levees of lava flows on Mars. *Journal of Geophysical Research*, 111, 2006.

Glaze, L. M. and Baloga, S. M. Topographic variability on Mars: Implications for lava flow modeling. *Journal of Geophysical Research*, 112, 2007.

Greeley R., et al. Erosion by flowing lava: Field evidence. *Journal of Geophysical Research*, 103, 27325-27334, 1998.

Gregg, T. K. P. and Fink, J. Quantification of extraterrestrial lava flow effusion rates through laboratory simulation. *Journal of Geophysical Research*, 101, 16891-16900, 1996.

Griffith, R. W. The Dynamics of Lava Flows. *Annual Review of Fluid Mechanics*, 32, 477-518, 2000.

Gueydan, F., et al. Continental rifting as a function of lithosphere mantle strength. *Tectonophysics*, 460, 83-93, 2008.

Harris, A. J. L. and Rowland, S. K. FLOWGO: a kinematic thermo-rheological model for lava flowing in a channel. *Bulletin of Volcanology*, 63, 20-44, 2001.

Harris, A. J. L., et al. Best-Fit Results from Application of a Thermo-Rheological Model for Channelized Lava Flow to High Spatial Resolution Morphological Data. *Geophysical Research Letters*, 34, 2007.

Harris, A. J. L. and Rowland, S. K. Effusion rate controls on lava flow length and the role of heat loss: a review. *In*: Thordarson, T., Self, S., Larsen, G., Rowland, S. K., Hoskuldsson, A. (eds.) *Studies in Volcanology: The Legacy of George Walker*. Geological Society, London, 2, 33-51, 2009.

Hay, D. E., et al. Origin of Kenya Rift Plateau-type flood phonolites: Integrated petrologic and geophysical constraints on the evolution of the crust and upper mantle beneath the Kenya Rift. *Journal of Geophysical Research*, 100, 10549-10557, 1995.

Hetzel, R. and Strecker, M. R. Late Mozambique Belt structures in western Kenya and their influence on the Evolution of the Cenozoic Kenya Rift. *Journal of Structural Geology*, 16, 189-201, 1994.

Ho, A. and Cashman, K. V. Temperature constraints on the Ginkgo flow of the Columbia River Basalt Group. *Geology*, 25, 403-406, 1997.

Hoskuldsson, A. and Sparks, R. S. J. Thermodynamics and fluid dynamics of effusive subglacial eruptions. *Bulletin of Volcanology*, 59, 219-230, 1997.

Huerta, A. D., et al. Mantle transition zone structure beneath Kenya and Tanzania: more evidence for deep-seated thermal upwelling in the mantle. *Geophysical Journal International*, 177, 1249-1255, 2009.

Hui, H. and Zhang, Y. Toward a General Viscosity Equation for Natural Anhydrous And Hydrous Silicate Melts. *Geochimica et Cosmochimica Acta*, 71, 403-416, 2007.

Hulme, G. The Interpretation of Lava Flow Morphology. *Geophysical Journal of the Royal Astronomical Society*, 39, 361-383, 1974.

Hulme, G. The Determination of the Rheological Properties and Effusion Rate of an Olympus Mons Lava. *Icarus*, 27, 207-213, 1976.

Hulme, G. and Fielder, G. Effusion Rates and Rheology of Lunar Lavas. *Philosophical Transactions of the Royal Society of London*, 285, 227-234, 1976.

Jacobs, B. F. Palaeobotanical Studies from Tropical Africa: Relevance to the Evolution of Forest, Woodland and Savannah Biomes. *Philosophical Transactions of the Royal Society of London*, 359, 1573-1583, 2004.

Jeffreys, H. J. The Flow of Water in an Inclined Channel of Rectangular Section. *Philosophical Magazine*, 49, 793-807, 1925.

Joubert, P. Geology of the Loperot area. *Geological Survey of Kenya*, Report 74, 1966.

Kauahikaua, J., et al. Observations on basaltic lava streams in tubes from Kilauea Volcanic, Island of Hawaii. *Journal of Geophysical Research*, 103, 27303-27323, 1998.

Keszthelyi, L. A preliminary thermal budget for lava tubes on the earth and planets. *Journal of Geophysical Research*, 100, 20411-20420, 1995.

Keszthelyi, L. and Self, S. Some physical requirements for the emplacement of long basaltic lava flows. *Journal of Geophysical Research*, 103, 27447-27464, 1998.

Kilburn, C. R. J. and Lopes, R. M. C. General Patterns of Flow Field Growth: Aa and Blocky Lavas. *Journal of Geophysical Research*, 96, 19721-19732, 1991.

King, B. C. Volcanicity and Rift Tectonics in East Africa. *In*: Clifford, T. N., Gass, I. G. (eds.) *African Magmatism and Tectonics*. Oliver and Boyd, Edinburgh, 263-283, 1970.

King, B. C., et al. The history of the alkaline volcanoes and intrusive complexes of eastern Uganda and western Kenya. *Journal of the Geological Society of London*, 128, 173-205, 1972.

King, B. C., Structural and volcanic evolution of the Gregory rift valley. *In*: Bishop, W. W. (ed.) *Geological Backround to Fossil Man*. Scottish Academic Press, Edinburgh, 29-54, 1978.

Kingston, J. D., et al. Isotopic Evidence for Neogene Hominid Paleoenvironments in the Kenya Rift Valley. *Science*, 264, 955-959, 1994.

Koehn, D., et al. Rift nucleation, rift propagation and the creation of basement micro-plates within active rifts. *Tectonophysics*, 458, 105-116, 2008.

Kohn, B. P., et al. Visualizing Thermotectonic and Denudation Histories Using Apatite Fission Track Thermochronology. *Reviews in Mineralogy and Geochemistry*, 58, 527-565, 2005.

Kushiro, I., et al. Viscosities of basalt and andesite melts at high pressures. *Journal of Geophysical Research*, 81, 6351-6356, 1976.

Lange, R. A. and Carmichael, I. S. E. Hydrous Basaltic Andesites Associated with Minette and Related Lavas in Western Mexico. *Journal of Petrology*, 31, 1225-1259, 1990.

Le Bas, M. J. Per-alkaline volcanism, crustal swelling, and rifting. *Nature: Physical Science*, 230, 85-87, 1971.

Le Gall, B., et al. Rift Propagation at Craton Margin. Distribution of Faulting and Volcanism in the North Tanzanian Divergence (East Africa) During Neogene Times. *Tectonophysics*, 448, 1-19, 2008.

Liebske, C., et al. The influence of pressure and composition on the viscosity of andesitic melts. *Geochimica et Cosmochimica Acta*, 67, 473-485, 2003.

Lippard, S. J. The petrology of phonolites from the Kenya Rift. *Lithos*, 6, 217-234, 1973.

Lopes, R. M. C. and Kilburn, C. R. J. Emplacement of Lava Flow Fields: Application of Terrestrial Studies to Alba Patera, Mars. *Journal of Geophysical Research*, 95, 14383–14379, 1990.

Maguire, P. K. H. and Aftab Khan, M. The deep structure and dynamics of the East African Plateau, the Kenya Dome and the Gregory Rift. *Proceedings of the Geologists' Association*, 91, 25-31, 1980.

Marsh, B. On the crystallinity, probability of occurrence and rheology of lava and magma. *Contributions to Mineralogy and Petrology*, 78, 85-98, 1981.

Martin, U. and White, J. D. L. Melting and Mingling of Phonolitic Pumice Deposits with Intruding Dykes: An Example from the Otago Peninsula, New Zealand. *Journal of Volcanology and Geothermal Research*, 114, 129-149, 2002.

Miyamoto, H. and Sasaki, S. Simulating lava flows by an improved cellular automata method. *Computers and Geosciences*, 23, 283-292, 1997.

Miyamoto, H. and Sasaki, S. Numerical simulations of flood basalt lava flows: Roles of parameters on lava flow morphologies. *Journal of Geophysical Research*, 103, 27489-27502, 1998.

Moore, W. B., et al. The Role of Rheology in Lithospheric Thinning by Mantle Plumes. *Geophysical Research Letters*, 26, 1073-1076, 1999.

Morgan, M. E., et al. Carbon Isotopic Evidence for the Emergence of C_4 Plants in the Neogene from Pakistan and Kenya. *Nature*, 367, 162-165, 1994.

Morley, C. K., et al. Tectonic evolution of the Northern Kenyan rift. *Journal of the Geological Society of London*, 149, 333-348, 1992.

Nyblade, A. A. and Brazier, R. A. Precambrain lithospheric controls on the development of the East African rift system. *Geology*, 30, 755-758, 2002.

Persikov, E. S. Viscosities of model and magmatic melts at the pressures and temperatures of the Earth's crust and upper mantle. *Russian Geology and Geophysics*, 39, 1780-1792, 1998.

Pik, R., et al. Timing of East African Rift Development in Southern Ethiopia: Implication for Mantle Plume Activity and Evolution of Topography. *Geology*, 36, 167-170, 2008.

Pinkerton, H. and Sparks, R. S. J. The 1975 Subterminal Lavas, Mount Etna: A Case History of the Formation of a Compound Flow Field. *Journal of Volcanology and Geothermal Research*, 1, 167-182, 1976.

Pinkerton, H. and Stevenson, R. J. Methods of determining the rheological properties of magmas at sub-liquidus temperature. *Journal of Volcanology and Geothermal Research*, 53, 47-66, 1992.

Pinkerton, H. and Wilson, L. Factors effecting the lengths of channel-fed lava flows. *Bulletin of Volcanology*, 56, 108-120, 1994.

Pohl, W. and Horkel, A. Notes on the Geology and Mineral Resources of the Mtito Andei-Taita Area (Southern Kenya). *Mitteilungen der Österreichischen Geologischen Gesellschaft*, 73, 135-152, 1980.

Prodehl, C., et al. Crustal and upper mantle structure of the Kenya Rift. *Tectonophysics*, 236, 1-466, 1994.

Reidel, S. P. Emplacement of Columbia River Flood Basalt. *Journal of Geophysical Research*, 103, 27393-27410, 1998.

Retallack, G. J., et al. Fossil Soils and Grasses of a Middle Miocene East African Grassland. *Science*, 247, 1325-1328, 1990.

Richmond, B. G. and Jungers, W. L. Orrorin Tugenensis Femoral Morphology and the Evolution of Hominin Bipedalism. *Science*, 319, 1662-1665, 2008.

Riker, J. M., et al. The length of channelized lava flows: Insight from the 1859 eruption of Mauna Loa Volcano, Hawai'i. *Journal of Volcanology and Geothermal Research*, 183, 139-156, 2009.

Roberts, G. G. and White, N. Estimating uplift rate histories from river profiles using African examples. *Journal of Geophysical Research*, 115, 2010.

Romano, C., et al. The dry and hydrous viscosities of alkaline melts from Vesuvius and Phlegrean Fields. *Chemical Geology*, 202, 23-38, 2003.

Rosendahl, B. R. Architecture of continental rifts with special reference to East Africa. *Annual Reviews of Earth and Planetary Sciences*, 15, 445-503, 1987.

Rowland, S. K. and Walker, G. P. L. Pahoehoe and aa in Hawaii: volumetric flow rate controls the lava structure. *Bulletin of Volcanology*, 61, 615-628, 1990.

Saggerson, E. P. Geology of the Simba-Kibwezi Area. *Geological Survey of Kenya*, Report 58, 1963.

Sandwell, D. T. and Smith, W. H. F. Marine Gravity from Geosat and ERS 1 Satellite Altimetry. *Journal of Geophysical Research*, 102, 10039-10054, 1997.

Sakimoto, S., et al. Eruption constraints on tube-fed planetary lava flows. *Journal of Geophysical Research*, 102, 6597-6613, 1997.

Ségalen, L., et al. Timing of C4 Grass Expansion Across Sub-Saharan Africa. *Journal of Human Evolution*, 53, 549-559, 2007.

Self, S., et al. A new model for the emplacement of Columbia River basalts as large, inflated pahoehoe lava flow fields. *Geophysical Research Letters*, 23, 2689-2692, 1996.

Sepulchre, P., et al. Tectonic Uplift and Eastern Africa Aridification. *Science*, 313, 1419-1423, 2006.

Shakleton, R. M. Geology of the Nyeri Area. *Mineralogical and Geological Department of Kenya*, Report 12, 1945.

Shaw, H. R. and Swanson, D. A. Eruption and flow rates of flood basalts. *In*: Gilmore, E. H., Stradling, D. F. (eds.) *Proceedings of the Second Columbia River Basalt Symposium*. East. Wash. State Coll. Press, Cheney, pp. 271-299, 1970.

Simiyu, S. M. and Keller, G. R. An Integrated Analysis of Lithospheric Structure Across the East African Plateau Based on Gravity Anomalies and Recent Seismic Studies. *Tectonophysics*, 278, 291-313, 1997.

Smith, J. V. Structural analysis of flow-related textures in lavas. *Earth-Science Reviews*, 57, 279-297, 2002.

Smith, M. and Mosley, P. Crustal Heterogeneity and Basement Influence on the Development of the Kenya Rift, East Africa. *Tectonics*, 12, 591-606, 1993.

Smith, M. Stratigraphic and structural constraints on meachnism of active rifting in the Gregory Rift, Kenya. *Tectonophysics*, 236, 3-22, 1994.

Spiegel, C., et al. Morphotectonic Evolution of the Central Kenya Rift Flanks: Implications for Late Cenozoic Environmental Change in East Africa. *Geology*, 35, 427-430, 2007.

Stevenson, R. J., et al. Rheological estimates of rhyolite lava flows from the Okataina Volcanic Centre, New Zealand. *New Zealand Journal of Geology and Geophysics*, 37, 211-221, 1994.

Stevenson, R. J., et al. The influence of trace amounts of water on the viscosity of rhyolites. *Bulletin of Volcanology*, 60, 89-97, 1998.

Strecker, M. R., et al. Rotation of Extension Direction in the Central Kenya Rift. *Geology*, 18, 299-302, 1990.

Tallarico, A. and Dragoni, M. Viscous Newtonian Laminar Flow in a Rectangular Channel, Application to Etna Lava Flows. *Bulletin of Volcanology*, 61, 40-47, 1999.

Tolan, T., et al. Revision to the estimates of areal extent and volume of the Grande Ronde Basalt Group. *Geological Society of America, Special Paper*, 239, 1-20, 1989.

Tommasi, A. and Vauchez, A. Continental rifting parallel to ancient collisional belts: an effect of the mechanical anisotropy of the lithospheric mantle. *Earth and Planetary Science Letters*, 185, 199-210, 2001.

Trauth, M. H., et al. East African climate change and orbital forcing during the last 175 kyr BP. *Earth and Planetary Science Letters*, 206, 297-313, 2003.

Trauth, M. H., et al. Late Cenozoic Moisture History of East Africa. *Science*, 309, 2051-2053, 2005.

Veldkamp, A., et al. Late Cenozoic Fluvial Dynamics of the River Tana, Kenya, an Uplift Dominated Record. *Quaternary Science Reviews*, 26, 2897-2912, 2007.

Wadge, G. Effusion rate and the shape of aa lava flow fields on Mount Etna. *Geology*, 6, 503-506, 1978.

Wagner, M., et al. Apatite fission-track analysis of Kenyan basement rocks: constraints on the thermotectonic evolution of the Kenya dome. A reconnaissance study. *Tectonophysics*, 204, 93-110, 1992.

Walker, A., et al. Fossil mammal locality on Mount Elgon, eastern Uganda. *Nature*, 223, 591-596, 1969.

Walker, G. P. L. Lengths of lava flows. *Philosophical Transactions of the Royal Society of London*, 274, 107-118, 1973.

Walsh, L. E. Geology of the Ikutha Area. *Geological Survey of Kenya*, Report 56, 1963.

Wheildon, J., et al. Heat flow in the Kenya rift zone. *Tectonophysics*, 236, 131-149, 1994.

White, F. M. Viscous Fluid Flow. McGraw-Hill, New York, pp. 1-614, 1991.

White, R. S. and McKenzie, D. P. Magmatism at rift zones: The Generation of continental margins and flood basalts. *Journal of Geophysical Research*, 94, 7685-7729, 1989.

Whittington, A., et al. Water and the viscosity of depolymerized aluminosilicate melts. *Geochimica et Cosmochimica Acta*, 64, 3725-3736, 2000.

Wichura, H., et al. Evidence for middle Miocene uplift of the East African Plateau. *Geology*, 38, 543-546, 2010.

Williams, H. and McBirney, A. R. *Volcanology*. Freeman, Cooper and Co., San Francisco, 1979.

Williams, L. A. J. Physical aspects of magmatism in continental rifts. *In*: Palmáson, G. (ed.) *Continental and Oceanic Rifts.* American Geophysical Union, Washington D. C., 193-222, 1982.

Williams, L. A. J. and Chapman, G. R. Relationships between major structures, salic volcanism and sedimentation in the Kenya rift from the equator northwards to Lake Turkana. *In*: Frostick, L. E, Renaut, R. W., Reid, I., and Tiercelin, J. J. (eds.) *Sedimentation in the African Rifts.* Geological Society of London, Special Publications, 25, 59-74, 1986.

Wilson, L. and Head, J. W. Ascent and eruption of basaltic magma on the Earth and Moon. *Journal of Geophysical Research*, 86, 2987-3001, 1981.

Woldetinsae, G. The Lithosphere of the East African Rift and Plateau (Afar-Ethiopia-Turkana): Insights from Integrated 3-D Density Modelling, PhD thesis, 2005.

APPENDIX

I applied the empirical viscosity equation for anhydrous and hydrous natural silicate melts developed by *Hui and Zhang* (2007) to model the Yatta lava flow. This equation is given by:

$$\log\eta = A + \frac{B}{T} + \exp\left(C + \frac{D}{T}\right), \tag{A-1}$$

where η is the viscosity, T is the temperature in K, and A, B, C, and D are linear functions of mole fractions of oxide components except for H_2O (*Hui and Zhang,* 2007). The equation (A-1) incorporates 37 fitting parameters, which are all statistically significant, and is able to reproduce existent viscosity data with a 2σ deviation of 0.61 $\log\eta$ units in the available temperature and compositional range of natural silicate melts (*Hui and Zhang*, 2007). The final fit delivers the following linear functions:

$$\begin{aligned} A = [&-6.83X_{SiO_2} - 170.79X_{TiO_2} - 14.71X_{Al_2O_{3ex}} - 18.01X_{MgO} - 19.76X_{CaO} \\ &+ 34.31X_{(Na,K)_2O_{ex}} - 140.38Z + 159.26X_{H_2O} - 8.43X_{(Na,K)AlO_2}] \end{aligned} \tag{A-2}$$

$$\begin{aligned} B = [&18.14X_{SiO_2} + 248.93X_{TiO_2} + 32.61X_{Al_2O_{3ex}} + 25.96X_{MgO} + 22.64X_{CaO} \\ &- 68.29X_{(Na,K)_2O_{ex}} + 38.84Z - 48.55X_{H_2O} + 16.12X_{(Na,K)AlO_2}]1000/T \end{aligned} \tag{A-3}$$

$$\begin{aligned} C = [&21.73X_{Al_2O_{3ex}} - 61.98X_{(Fe,Mn)O} - 105.53X_{MgO} - 69.92X_{CaO} \\ &- 85.67X_{(Na,K)_2O_{ex}} + 332.01Z - 432.22X_{H_2O} - 3.16X_{(Na,K)AlO_2}] \end{aligned} \tag{A-4}$$

$$\begin{aligned} D = [&2.16X_{SiO_2} - 143.05X_{TiO_2} - 22.10X_{Al_2O_{3ex}} + 38.56X_{(Fe,Mn)O} + 110.83X_{MgO} \\ &+ 67.12X_{CaO} + 58.01X_{(Na,K)AlO_2} + 384.77X_{P_2O_5} - 404.97Z + 513.75X_{H_2O}]1000/T \end{aligned} \tag{A-5}$$

$$Z = (X_{H_2O})^{1/[1+(185.797/T)]}, \tag{A-6}$$

where X_i means mole fraction of oxide component i. Furthermore, Al_2O_{3ex} or $(Na,K)_2O_{ex}$ means, that excess aluminium or excess alkali are left as a component in the melts after forming $(Na,K)AlO_2$ (*Hui and Zhang,* 2007).